

Trace Element Geochemistry of Armenian Obsidian Sources and the Provenance of Archaeological Obsidian Artefacts

*Khachatur Meliksetian¹ – Ernst Pernicka² – Ruben Badalyan³ –
Thorsten Schifer⁴ – Jörg Keller⁵ – Boris Gasparyan⁶ –
Ruben Jrbashyan⁷ – Gevorg Navasardyan⁸ – René Kunze⁹*

Abstract: Since the mid-1990s we have been involved in the study and analysis of obsidian in Armenia, first only intermittently, then between 2002 and 2006 intensively with several field seasons to collect geological samples from all known obsidian sources in Armenia. Later a few samples from the Chikiani source in Georgia were included. For several reasons, this large dataset was only used as background information for various publications and reports but never published in total. Herewith we present neutron activation analyses of 153 obsidian samples together with detailed information on their geological setting and with some outlook on the distribution of obsidian in the Near East, with an emphasis on periods from the Neolithic to the Bronze Age. It is possible to discriminate all sources based on diagrams of a few geochemically significant trace elements that could be determined with high sensitivity and precision.

Keywords: Trace elements, obsidian, Armenia

Introduction

Obsidian represents an important and widely used material in prehistoric times for the regions of the Caucasus, the Near East and the Mediterranean. In many cases, obsidian artefacts are found quite far away from their original geological sources. The geochemical characteristics of obsidian allow the provenance of artefacts to be traced to their parent sources and thus represent a unique opportunity to outline prehistoric exchange, trade routes and contacts. Furthermore, the regional utilization of obsidian sources can be studied from the analyses of archaeological artefacts. Several noteworthy features make obsidian an almost ideal material for provenance studies using geochemical fingerprinting: first of all, there is no change in composition during the production of artefacts (in contrast to e.g. metals produced from ores); geological sources of obsidian are usually geochemically more

¹ Institute of Geological Sciences, National Academy of Sciences of the Republic of Armenia, Yerevan, Republic of Armenia; khachatur.meliksetian@geology.am.

² Institut für Ur- und Frühgeschichte und Archäologie des Mittelalters der Universität Tübingen; Curt-Engelhorn-Zentrum Archäometrie gGmbH, Mannheim, Germany; ernst.pernicka@ceza.de.

³ Institute of Archaeology and Ethnography, National Academy of Sciences of the Republic of Armenia, Yerevan, Republic of Armenia.

⁴ Institut für Ur- und Frühgeschichte und Archäologie des Mittelalters der Universität Tübingen; Curt-Engelhorn-Zentrum Archäometrie gGmbH, Mannheim, Germany.

⁵ Institute of Mineralogy, Petrology und Geochemistry, Albert Ludwig University of Freiburg, Germany.

⁶ Institute of Archaeology and Ethnography, National Academy of Sciences of the Republic of Armenia, Yerevan, Republic of Armenia.

⁷ Institute of Geological Sciences, National Academy of Sciences of the Republic of Armenia, Yerevan, Republic of Armenia.

⁸ Institute of Geological Sciences, National Academy of Sciences of the Republic of Armenia, Yerevan, Republic of Armenia.

⁹ Seminar for Oriental Archaeology and Art History, Institute of Archaeology, Martin-Luther-University Halle-Wittenberg, Germany.

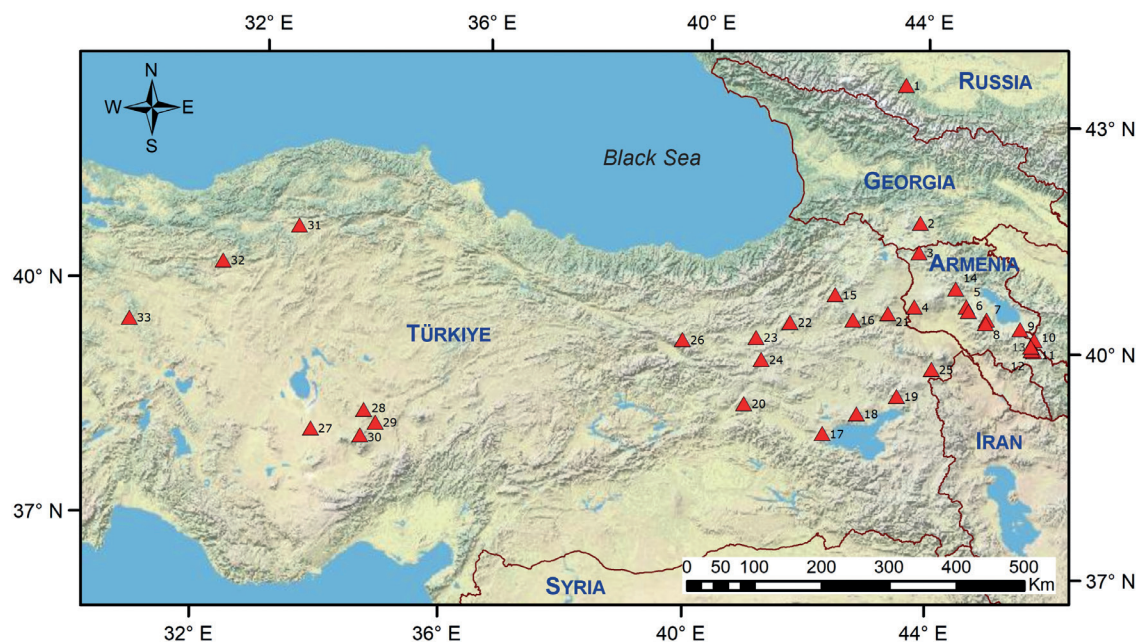


Fig. 1 Distribution of major obsidian sources (red triangles) of Anatolia, the Armenian Highlands and the Caucasus (after Karapetian 1972; Keller et al. 1996; Chataigner et al. 1998; Chataigner – Gratuzze 2014a). Sources indicated on the map: 1. Baksan; 2. Chikiani; 3. Kechut; 4. Arteni; 5. Gutansar; 6. Hatis; 7. Spitaksar; 8. Geghasar; 9. Khorapor; 10. Kecheldag; 11. Satanakar; 12. Sevkar; 13. Bazenk; 14. Sources on the Tsaghkunyats ridge (Damlik, Kamakar, Ttvarkar); 15. Sarıkamış North (Kızıl Kilisa); 16. Sarıkamış South (Mescitli); 17. Nemrut; 18. Suphan (Sipan); 19. Meydan Dağ; 20. Bingöl; 21. Yağlıca Dağ (Digor); 22. Pasinler; 23. West Erzurum; 24. South Erzurum; 25. Tondrak (Tendürek, Dogubayazit); 26. Erzincan; 27. Hasan Dağ; 28. Acıgöl; 29. Nenezi Dağ; 30. Göllü Dağ; 31. Sakaeli-Orta; 32. Yağlar; 33. Kütahya (graphics: K. Meliksetian)

or less homogenous; and finally, in most cases the geochemical variability between diverse sources of obsidian is absolutely sufficient to clearly discriminate them. The aims of this paper are: 1) to provide geological descriptions of the obsidian sources with updated geological maps and a complete geochemical characterization of South Caucasian obsidian together with an innovative geochemical fingerprinting method of Armenian obsidian sources, based on new analyses of 153 geological samples from almost all Armenian obsidian sources; 2) to compare the geochemical fingerprints of Armenian obsidian sources to those known in the South Caucasus region and in the territory of Türkiye, including previously published data; and 3) to study the provenance of 534 obsidian artefacts from Armenia and other regions (Dagestan, Georgia, Azerbaijan, Iran, Anatolia) covering a long time interval of prehistoric periods – from the Palaeolithic to the Early Iron Age.

Geological Samples

The Armenian Highlands and the territory of Armenia are among the areas of intense Pliocene-Quaternary volcanism. About 40% of the territory of Armenia is covered by young volcanic rocks.¹⁰ Among them, many acid volcanoes and their products (rhyolites, pumice, obsidians, perlites) are known. Obsidian in Armenia is of a very high quality and occurs in five volcanic provinces. Most of the sources are accessible and show archaeological evidence of prehistoric utilization.¹¹

¹⁰ Karapetian et al. 2001 and references therein.

¹¹ Badalyan et al. 2004.

	Source	Subsources	Age, by K-Ar, or $^{40}\text{Ar}/^{39}\text{Ar}$, Ma	Age by fission tracks, Ma	Region, volcanic province	Country	Coordinates (WGS-84, decimal degrees)		Number of samples
							Lat.	Long.	
1	Kechut	Agvorik	K-Ar 2.17–2.25 ^e	1.13±0.11 ^c 1.07±0.10 ^c 1.13±0.11 ^c	Javakheti volcanic ridge	Armenia	41.079	43.767	5
		Sizavet	–	1.04±0.10 ^c			41.108	43.855	3
2	Chikiani (Parvana, Paravani, Koyun-Dag)	–	K-Ar 2.70 ± 0.15 ⁱ $^{40}\text{Ar}/^{39}\text{Ar}$ 2.41 ± 0.05 ^k 2.83 ± 0.06 ^k 2.79±0.06 ^k	2.24 ^a 2.34 ± 0.10 ^g 2.63 ± 0.10 ^g	Javakheti volcanic ridge, Lake Paravani	Georgia	41.477	43.868	11
3	Tsaghkunyats	Hankavan	K-Ar, 5.4±0.4 ^m	4.49 ± 0.21 ^d 4.49 ± 0.21 ^d 4.26 ± 0.20 ^d 4.46 ± 0.27 ^d 4.56 ± 0.20 ^d 4.30±0.23 ^c 4.16±0.22 ^c	Tsaghkunyats ridge	Armenia	40.606	44.478	10
4		Damlik	K-Ar, 5.8 ^m				40.633	44.413	
5		Arkayasar	K-Ar, 4.8 ^m				40.552	44.542	
6	Arteni	Pokr Arteni	K-Ar 1.26 ± 0.05 ^j 1.60±0.15 ^f	1.23 ^a 1.27±0.09 ^c 1.17±0.11 ^d 1.31±0.08 ^d 1.29±0.08 ^d 1.20±0.10 ^c 0.76±0.06 ^c 1.27±0.09 ^c 0.75±0.06 ^c 1.20±0.10 ^c	Arteni volcanic complex, Aragats volcanic province	Armenia	40.359	43.785	20
7		Mets Arteni	K-Ar 1.45±0.15 ^f	1.22±0.08 ^d 1.38±0.09 ^d 1.35±0.08 ^d			40.375	43.786	
8	Gutansar	Jraber	K-Ar 1.2 ± 0.5 ^l	0.32±0.03 ^c 0.35±0.03 ^d 0.25±0.03 ^d 0.31±0.03 ^d	Gegham Plateau, Hrazdan-Abovyan group	Armenia	40.367	44.687	25
		Fantan	K-Ar 0.48 ± 0.05 ^l	0.32±0.02 ^d 0.30±0.02 ^d					
		Alapars	–	0.23±0.02 ^c 0.21±0.02 ^c 0.20±0.03 ^c 0.28±0.03 ^d 0.31±0.02 ^d					
		Gyumush	–	0.22±0.02 ^c 0.24±0.03 ^c 0.23±0.02 ^c					
		Gutansar volcano	K-Ar 0.9 ± 0.3 ^l 0.38 ± 0.06 ^l 0.47 ± 0.03 ^l 0.55 ^m	0.25±0.03 ^d 0.31±0.03 ^d					
9	Hatis	–	K-Ar 0.65 ^a 0.48±0.04 ^b 0.66 ± 0.04 ^l 0.74 ± 0.25 ^l 0.70 ± 0.03 ^l 0.48 ± 0.05 ^l	0.33 ^a 0.21±0.03 ^d 0.34±0.03 ^d 0.40±0.03 ^d	Gegham volcanic upland, Hrazdan-Abovyan group	Armenia	40.309	44.725	14
10	Geghasar	–	K-Ar 0.13 ± 0.08 ^l 0.10 ± 0.02 ^l	0.042±0.004 ^d 0.062±0.006 ^d 0.065±0.005 ^d 0.082±0.007 ^d 0.052±0.005 ^d	Gegham volcanic upland, Martuni group	Armenia	40.176	45.023	18
11	Spitaksar	–	K-Ar 0.20 ± 0.02 ^l	0.12±0.01 ^d			40.122	45.014	5

	Source	Subsources	Age, by K-Ar, or $^{40}\text{Ar}/^{39}\text{Ar}$, Ma	Age by fission tracks, Ma	Region, volcanic province	Country	Coordinates (WGS-84, decimal degrees)		Number of samples
							Lat.	Long.	
12	Khorapor	–	K-Ar 1.75 ^m	1.53±0.09 ^d	Vardenis volcanic upland	Armenia	40.056	45.638	6
13	Syunik	Mets Satanakar	K-Ar 0.9 ^a	0.43 ± 0.03 ^d 0.56 ± 0.05 ^d	Syunik volcanic upland	Armenia	39.826	45.827	10
14		Sevkar		0.54 ± 0.03 ^d 0.61 ± 0.04 ^d 0.53 ± 0.03 ^d			39.776	45.857	23
15		Bazenk		0.56 ± 0.04 ^d			39.796	45.844	3
Total									153

Notes: Ages of obsidian and associated rhyolite flows are given according to: ^a Komarov et al. 1972; ^b Bigazzi et al. 1994; ^c Oddone et al. 2000; ^d Badalian et al. 2001; ^e Karapetian et al. 2001; ^f Chernyshev et al. 2002; ^g Chataigner et al. 2003; ^h Arutyunyan et al. 2007; ⁱ Lebedev et al. 2008; ^j Lebedev et al. 2011; ^k Le Bourdonnec et al. 2012; ^l Lebedev et al. 2013, ^m Baghdasaryan – Ghukasyan 1985.

Table 1 Geological source samples of obsidian with their locations and geological ages

153 geological samples representing almost all occurrences of obsidian in Armenia and Georgia were thoroughly sampled during field campaigns in 2002–2003 and in 2010. Samples from the Chikiani source, southern Georgia, were provided by Sergey Karapetyan, (two samples) and Christine Chataigner (five samples). The geological sources and the number of samples studied are summarized in Table 1.

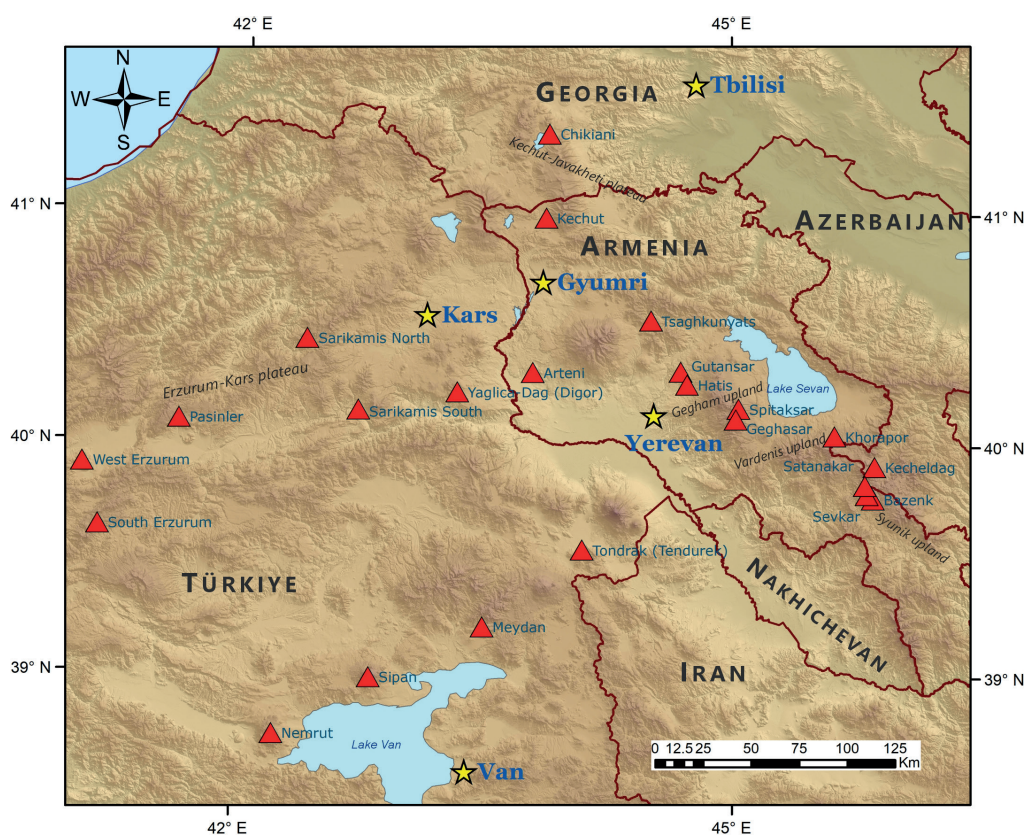


Fig. 2 Distribution of obsidian sources (red triangles) of the Lesser Caucasus and adjacent regions and volcanic provinces, the Erzurum-Kars and Kechut-Javakheti (Akhalkalaki) volcanic plateaus, the Aragats stratovolcano, the Tsaghkunyats ridge and the Gegham, Vardenis and Syunik volcanic uplands (graphics: K. Meliksetian)



Fig. 3 Distribution of archaeological obsidian artefacts (blue diamonds) analysed in this study (graphics: K. Meliksetian)

To utilize a wider database and enhance the consistency of geochemical fingerprinting of sources and the reliability of tracing the provenance of artefacts, we also attempted to use previously published geochemical data characterizing Armenian obsidian sources by XRF and INAA.¹² However, these authors studied only a limited number of geological samples, while James Blackman and co-workers¹³ analysed more than 100 geological samples, but provided only average compositions, which limits the usage of these analyses for comparison and geochemical fingerprinting. Recently published data on obsidian occurrences of northeastern Türkiye (Kars-Erzurum Plateau)¹⁴ were also used, since many artefacts from archaeological sites in Armenia originate from sources on the Kars-Erzurum Plateau.

Information on the geological samples, including geographical locations, coordinates and age determinations using K-Ar, $^{40}\text{Ar}/^{39}\text{Ar}$, and fission tracks of samples analysed in this study are summarized in Table 1. The locations of regional obsidian sources are shown in Fig. 1; the geographical distribution of obsidian sources in the South Caucasus and neighbouring areas is shown on the map in Fig. 2. Fig. 3 shows the geographical distribution of archaeological artefacts analysed in this study.

¹² Keller et al. 1996; Blackman et al. 1998; Oddone et al. 2000; Cherry et al. 2010.

¹³ Blackman et al. 1998.

¹⁴ Chataigner et al. 2014.

Element	Radioisotope	Half-life	Energy [keV]	Run	$\sigma\%$
Na	²⁴ Na	15.0 h	1368.5	1	2
K	⁴² K	12.4 h	1524.7	1	5
Sc	⁶⁴ Sc	83.8 d	889.2	2	1.5
Cr	⁵¹ Cr	27.8 d	320.1	2	13
Fe	⁵⁹ Fe	44.6 d	1099.3; 1291.5	2	2
Co	⁶⁰ Co	5.27 a	1173.2; 1332.5	2	10
Zn	⁶⁵ Zn	243.7 d	1115.5	2	11
As	⁷⁶ As	23.3 h	559.3	1	15
Rb	⁸⁶ Rb	18.6 d	1078.8	1	4
Zr	⁹⁵ Zr	64.02 d	756.7; 724.2	1	10–20
Sb	¹²² Sb	2.7 d	564.1	1	14
Sb	¹²⁴ Sb	60.2 d	1691.0	2	16
Cs	¹³⁴ Cs	2.1 a	795.8	2	3.5
Ba	¹³¹ Ba	11.7 d	496.3	1; 2	7
La	¹⁴⁰ La	40.2 h	487.0; 1596.2	1	2
Ce	¹⁴¹ Ce	32.5 d	145.1	2	5
Nd	¹⁴⁷ Nd	11.1 d	531.0	2	25
Sm	¹⁵⁴ Sm	46.5 h	103.2	1	2
Eu	¹⁵² Eu	12.7 a	1407.2	2	7
Tb	¹⁶⁰ Tb	72.3 d	86.8; 879.3	2	8
Yb	¹⁷⁵ Yb	4.2 d	396.1	1	9
Lu	¹⁷⁷ Lu	6.7 d	208.3	2	8
Hf	¹⁸¹ Hf	42.4 d	482.2	2	4
Ta	¹⁸² Ta	115 d	67.8; 1221.3	2	6
Th	²³³ Th	27 d	311.9	2	2
U	²³⁹ U	2.35 d	228.2; 277.6	1	7

Table 2 Measurement parameters for INAA of obsidian. $\sigma\%$ is the average standard deviation due to counting statistics, systematic and random errors

Analytical Techniques

Instrumental neutron activation analysis is a well-suited and commonly used method for provenance studies of archaeological obsidian findings. The method is a non-destructive multi-element analytical technique used for quantitative analysis of major, minor and trace elements. Compared with other analytical techniques, sample preparation is inexpensive and a great number of elements can be determined simultaneously with high sensitivity. The main objective of the analyses is the identification of the sources of archaeological artefacts by chemical ‘fingerprinting’.

The method of INAA is based on the irradiation of samples with thermal neutrons. Atomic nuclei capturing a neutron assume an unstable state and are converted to radioactive isotopes. The gamma rays emitted by radioactive decay have characteristic energies for the corresponding elements. The count rates of identified decays are used for quantification using standard reference materials that are irradiated simultaneously together with the samples.¹⁵ The method can also be applied for the analysis of obsidian.¹⁶

¹⁵ For the analysis of pottery, an instrumental procedure was developed by Perlman – Asaro 1969.

¹⁶ Further information about techniques and methods are published by Kuleff – Djingova 1999.

At the Curt-Engelhorn-Centre of Archaeometry (Mannheim, Germany) measurements were performed with three high-purity germanium detectors (HPGe, Ortec), cooled with electric X-coolers. The detectors have a resolution of 1.8keV and a counting efficiency of 38% at the 1332.5keV peak of ^{60}Co . To minimize the environmental radiation, the detectors are shielded by cases of lead bricks. The measurements were carried out using the GammaVision (Ortec) software that is used as a multichannel analyser (MCA) emulator and a program for the analysis of gamma spectra. In principle, the method can be applied non-destructively, but the sample size is limited and the samples remain radioactive for a certain time. Thus it is not really non-destructive, but for geological samples this is not important. Archaeological specimens were analysed by taking small cleavage samples and not complete artefacts. About 150–200mg of sample material was encapsulated in high-purity polyethylene containers (Posthumus Plastics, NL) together with flux monitors. For the most part, NIST-SRM278 (obsidian rock, National Institute of Standards & Technology) was used as the reference material. The irradiation of the samples and standard materials was carried out in the TRIGA reactor at the Institute for Nuclear Chemistry at Mainz University for 12 hours at a neutron flux of $1 \times 10^{12} \text{n} \cdot \text{cm}^{-2} \cdot \text{s}^{-1}$. Two measurement runs were performed after cooling times of 6 days and 25–30 days, taking into account the different half-lives of the radioisotopes (for details, see Table 2). For elements determined by two energy peaks, the weighted average value is given. Corrections for fission products of ^{235}U are necessary for Ba, Ce and Zr. The influence factors and the corresponding corrections were calculated from the uranium concentration in the samples.¹⁷

Geological Settings of Rhyolite: Obsidian Volcanoes in the Southern Caucasus

The Armenian Highlands represents part of the intensely deformed central segment of the Alpine-Himalayan belt. The complex geological structure of the territory of Armenia (Lesser Caucasus, northeastern part of the Armenian Highlands) is formed by a collision geodynamic setting, resulting in a merged mosaic of different geotectonic units (blocks) combining fragments of island arcs, continental plates and oceanic crust within a quite small territory.

It is widely accepted that the current complex geological structure of the region under study is mainly formed by the convergence and interaction (continental collision) of the Afro-Arabian margin and the active margin of Eurasia, the wedging-in of the Arabian northern margin and the resulting shift to the sides of the Anatolian and Iranian blocks with the Lesser Caucasus and Armenian Highlands in the centre.¹⁸ The geological cross-section of the Lesser Caucasus shows evidence of widespread volcanic activity from the Jurassic to the Holocene era.

The intense Pliocene-Quaternary volcanism of the Armenian Highlands and the Lesser Caucasus is related to ongoing collision tectonics. About half of the territory of Armenia is covered by Pliocene-Quaternary volcanic eruption products such as lava flows, ignimbrites, rhyolite-obsidian domes, flows and extrusive bodies.¹⁹ Occurrences of acid volcanism with obsidian are known in all five Quaternary volcanic provinces of the Lesser Caucasus: the Javakheti volcanic plateau, the area of the Aragats volcano and within the Gegham, Vardenis, and Syunik volcanic uplands. Several geographically close obsidian sources of the Tsaghkunyats ridge in central Armenia are related to Pliocene acid volcanism.

Three distinct types of volcanism were identified for the Lesser Caucasus: fissures, areals and central vents.²⁰ Volcanism, issuing from riftogenic fissures, produced huge volumes of almost non-differentiated subalkaline and calc-alkaline flood basalts (dolerites) in the Upper Pliocene – Early

¹⁷ See also Pernicka et al. 1997.

¹⁸ Yilmaz et al. 2000; Philip et al. 2001.

¹⁹ Jrbashyan et al. 1996; Karapetian et al. 2001; Meliksetian 2013.

²⁰ Shirinyan 1975; Skhirtladze 1958; Jrbashyan et al. 1996.

Pleistocene, covering large areas in northern and central Armenia and southern Georgia, namely on the Javakheti, Lori, and Kotayk plateaus, as well as lengthy flows extending along the canyons of the Akhuryan, Debed, Hrazdan, and Mashavera rivers and the Lake Sevan basin. The ages of the fissure flood basalts of the Lesser Caucasus are based on geological structures and the stratigraphic sequence considered as Upper Pliocene.²¹ More recent K-Ar measurements confirm this relative dating and suggest a long-term activity of fissure volcanism – from 3.5Ma to 2.37Ma.²²

Areal volcanism formed huge volcanic uplands, such as Kechut-Javakheti, Syunik, Gegham and Vardenis in the southern Caucasus. More than 500 monogenic volcanic centres were identified within the territory of Armenia,²³ most of them cinder cones.

Several huge polygenic stratovolcanoes are well known in Armenia, namely Aragats (4090m), Arailer (2575.9m), Ishkhanasar (3550m), Tsghuk (3584m), and finally, the highest peak in the region, the Ararat volcano (altitude 5165m) in the territory of eastern Türkiye bordering on Armenia. The activity of these central-vent stratovolcanoes is considered to have lasted more than 1Ma²⁴ and up to 1.5Ma.²⁵

Geological maps of Armenian obsidian-bearing volcanoes have been prepared by Karapetyan in his monograph²⁶ dealing with the volcanology and petrography of the Pliocene-Quaternary acid volcanism of the Lesser Caucasus. These maps have since also been published several times.²⁷ In this contribution we present new, updated versions of these maps prepared in GIS format (Figs. 4–11). We will also touch briefly upon some noteworthy volcanological and geological features of the obsidian occurrences. The ages of the obsidian flows as determined by K-Ar and fission tracks are included in Table 1. For all rhyolitic domes of the Lesser Caucasus, high explosivity is typical in the early stages of eruptions; this and the mineral assemblage in equilibrium are indications of high pressure (up to 2kbar) of the fluid phase in the volcanic chamber and volcanic vents.²⁸ Usually, high pressure of volatiles in acid volcanic systems results in the hydration and frothing of acid volcanic glass and the formation of pumices, and further excessive and fast degassing with the formation of obsidian.

Javakheti Volcanic Ridge

Two sources of obsidian are related to this volcanic plateau: Sizavet and Aghvorik in the southern part of the ridge near Ashotsk (Sizavet and Aghvorik villages) in Armenia, and Chikiani in southern Georgia, near Lake Paravani (Parvana) in the northern part of the Javakheti ridge.

For the Sizavet and Aghvorik sources, the eruption centres of the rhyolitic lavas are not known (possibly eroded), but a relatively small amount of rhyolitic lavas and obsidians – black, striped, and spotted, with faded shine – are found near the villages of Aghvorik and Sizavet.²⁹ Within the northern extension of the plateau (Akhalkalaki Plateau, southern Georgia), we find the large rhyolitic dome-shaped volcanic edifice of Chikiani on the northeastern coast of Lake Parvana (Paravani). It is formed by flows of rhyolites, perlites and obsidians, extending from the Chikiani dome in an eastern direction for several hundred metres. Chikiani is one of the most important and widely utilized sources of the Lesser Caucasus region.³⁰ Obsidian from Chikiani is of a high quality and is usually

²¹ Aslanyan 1958; Kharazyan 1983.

²² Baghdasaryan – Ghukasyan 1985; Balog et al. 1990; Chernyshev et al. 2002; Neill et al. 2015.

²³ Shirinyan – Zadoyan 1990.

²⁴ Nadareishvili et al. 2002.

²⁵ Karakhanian et al. 2003.

²⁶ Karapetian 1972.

²⁷ Aslanyan et al. 1980; Keller et al. 1996; Blackman et al. 1998; Chataigner et al. 1998.

²⁸ Meliksetian – Karapetian 1981.

²⁹ Kharazyan 1968; Blackman et al. 1998.

³⁰ Blackman et al. 1998; Badalyan 2010.

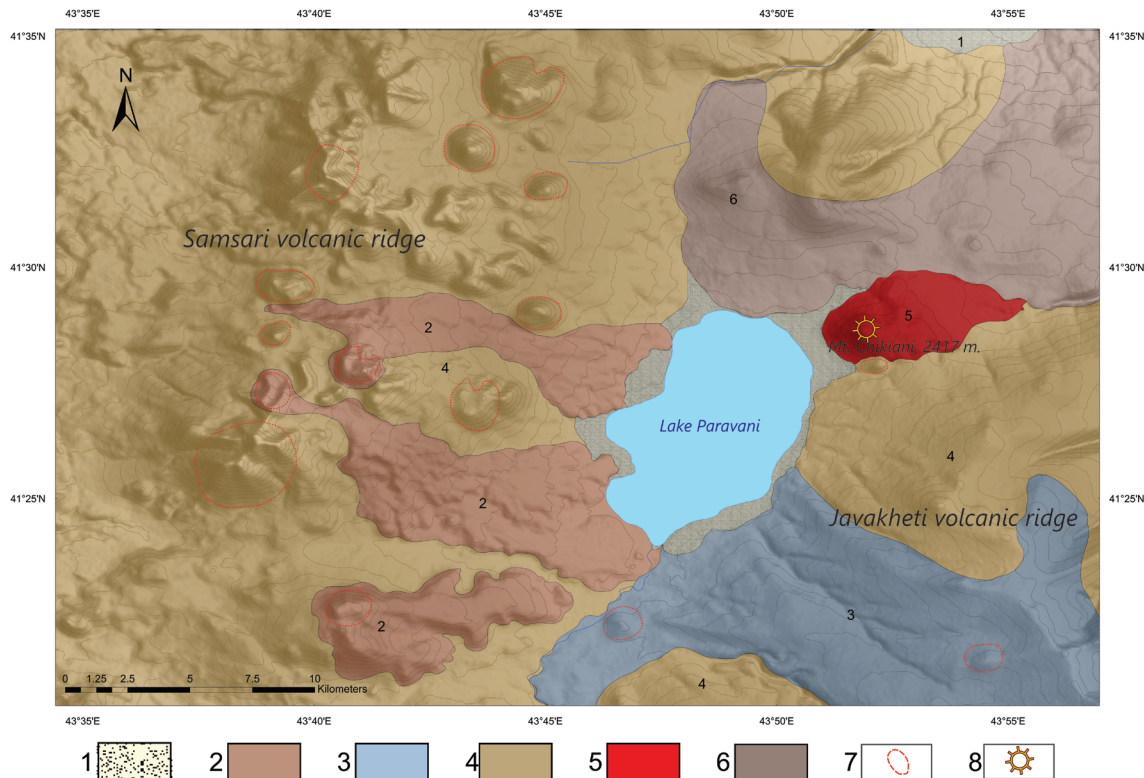


Fig. 4 Geological map of the Chikiani obsidian dome. Legend: Q_3 – Q_4 Upper Pleistocene – Holocene: 1. Alluvia, diluvia, eluvia, proluvia deposits; 2. Andesitic lava flows of volcanos Abouli, Godorebi. – Q_2 – Q_3 Middle – Upper Pleistocene: 3. Basaltic lavas. – Q_2 Middle Pleistocene: 4. Basaltic trachyandesites lava flow of volcano Inakdagh. – N_2 – Q_1 Upper Pliocene – Lower Pleistocene: 5. Rhyolitic perlite, obsidian lavas of the Chikiani volcano; 6. Doleritic basalts; 7. Cinder cones; 8. Rhyolitic domes (graphics: G. Navasardyan)

black to dark brown as well as translucent grey-brown.³¹ A geological map of the Chikiani source is shown in Fig. 4. Lebedev and co-workers report a K-Ar age of 2.70 ± 0.15 Ma,³² and Le Bourdonnec and co-workers, $^{40}\text{Ar}/^{39}\text{Ar}$ ages of 2.41 ± 0.05 Ma, 2.83 ± 0.06 Ma, and 2.79 ± 0.06 Ma.³³

The lowest flat topography of the region (Akhalkalaki Plateau) is covered by thick layers of mafic doleritic basaltic lava flows usually described as valley series of Upper Pliocene – Lower Pleistocene age.³⁴ The Javakheti volcanic ridge is composed of more evolved Quaternary volcanic series, mostly andesitic and also dacitic in composition, that originated as a result of fractional crystallization of basaltic melts with little crustal input.³⁵ Volcanism of the neighbouring Samsari ridge in southern Georgia is younger compared with the Javakheti ridge volcanism and continued to the Upper Pleistocene and Holocene.

Aragats Volcanic Province

The Aragats volcano (4090m) in Armenia is one of the largest polygenetic stratovolcanoes in the region. As a result of volcanic activity within the Aragats volcanic area (about 5000km²),

³¹ Badalyan et al. 2004.

³² Lebedev et al. 2008.

³³ Le Bourdonnec et al. 2012.

³⁴ Neill et al. 2103.

³⁵ Neill et al. 2013.

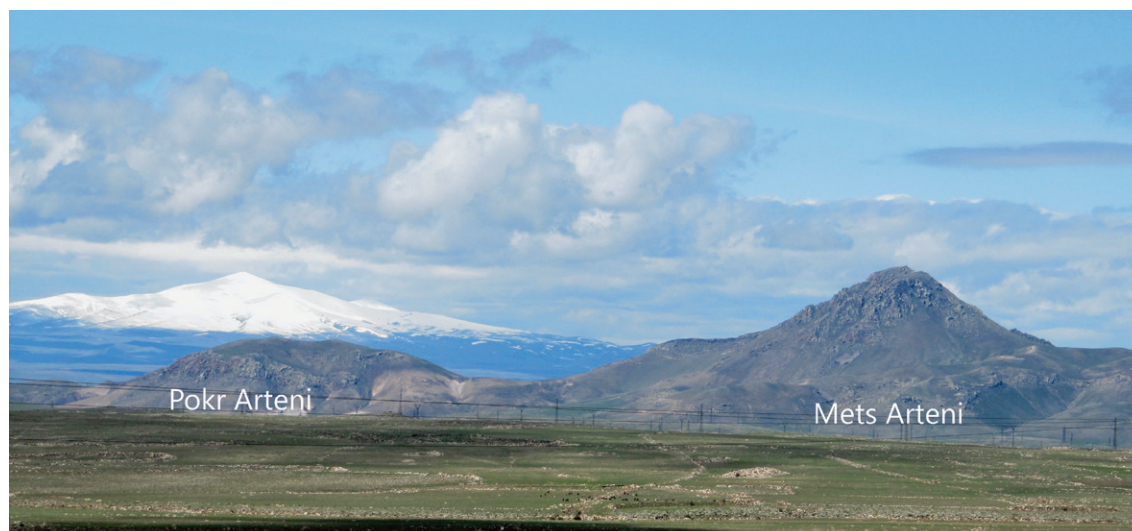


Fig. 5 The Arteni volcanic complex in Armenia, Aragats volcanic province, two geochemically distinct sources, with Pokr and Mets Arteni in the foreground and with snow-covered Yağlıca Dağ (Digor) across the border with Türkiye in the background (photo: K. Meliksetian)

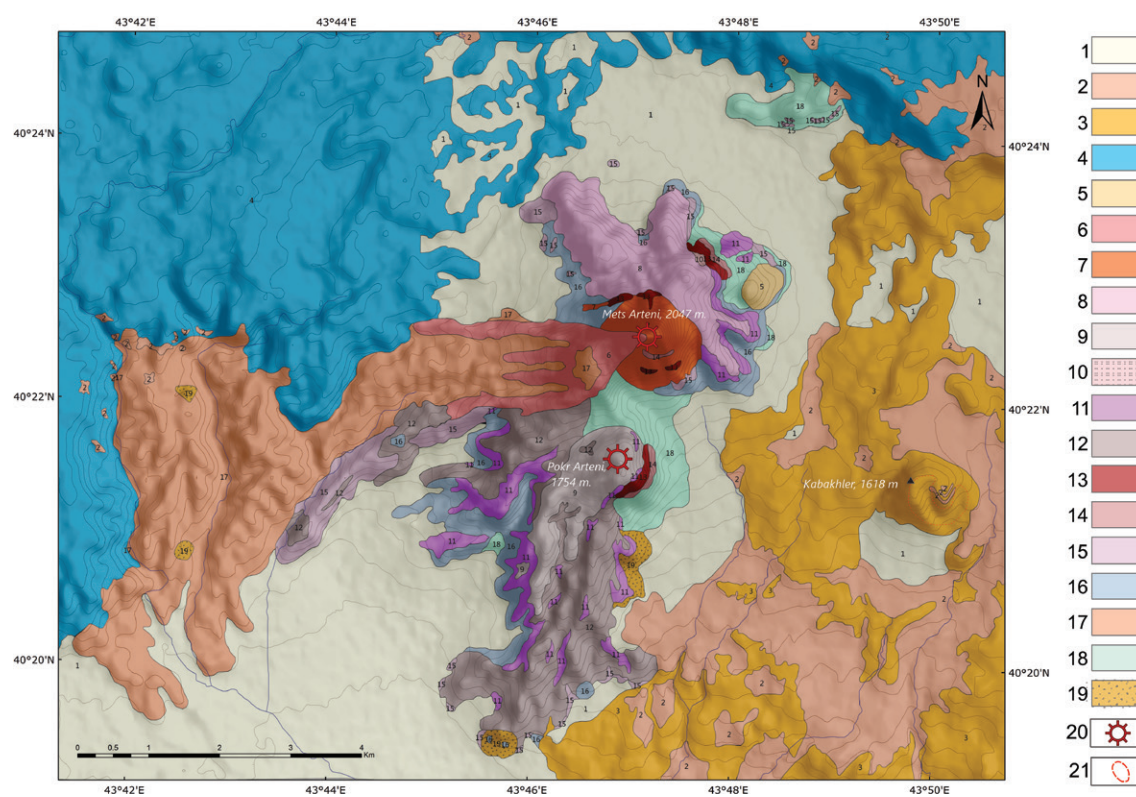


Fig. 6. Geological map of the Arteni volcanic complex. Legend: Holocene: 1. Alluvial, diluvia, proluvial deposits. – Q_2 Middle Pleistocene: 2. Tuffs of the Yerevan-Leninakan type, 3. Basaltic trachyandesites of the Ddmasar volcano. – Q_2-Q_1 Middle Pleistocene – Early Pleistocene: 4. Trachyandesite, trachydacite lavas. – Q_1 Early Pleistocene: Products of the Arteni volcano (5–19): 5. High silica dacites Tapak Blur dome; 6. Rhyolitic lavas, upper unit; 7. Rhyolites of the Khtsan dome; 8. Rhyolite lava flows and lavabreccia of the Mets Arteni volcano; 9. Rhyolite lavas of the Pokr Arteni volcano; 10. Rhyolite tuffs; 11. Rhyolite lavas, middle unit; 12. Perlite, obsidian lavas and lavabreccia of the Pokr Arteni volcano; 13. Perlite extrusions; 14. Perlite eruptive breccias; 15. Rhyolitic lavas, lower unit, glassy and crystallized; 16. Perlite-obsidian tuffs and tuff-breccias; 17. Perlite-pumice agglomerates of the Aragats flow; 18. Explosive perlite-pumice weak formation; 19. Obsidians; 20. Dome-shaped volcanic centers Mets and Pokr Arteni; 21. Cinder cones (graphics: G. Navasardyan)

two polygenic stratovolcanoes were formed: Aragats itself (Quaternary) and Arailer (Upper Pliocene – Lower Pleistocene), as well as 100 monogenic centres (cinder cones, domes). Huge fields of lava flows, ranging in composition from basaltic to dacitic as well as ignimbrite-forming Plinian eruptions, are related to the Aragats volcano.

The Arteni volcanic complex (Fig. 5) is located within the Aragats volcanic province. The age of the Arteni rhyolites is considered to be early Pleistocene. K-Ar ages yielded 1.45–1.5Ma for Mets Arteni,³⁶ fission tracks, 1.27Ma,³⁷ and 1.26Ma for Pokr Arteni.³⁸ These dates are also included in Table 1. Thus, the rhyolitic eruptions and formation of domes of the Arteni volcano correspond to the Early Pleistocene. The eruption products of the Arteni volcano are covered by more recent middle Pleistocene andesitic lava flows of the neighbouring Kabakhler cinder cone and by ignimbrites of the Aragats stratovolcano.

Arteni is the most complex rhyolite volcano in Armenia, and consists of two independent rhyolite volcanoes, namely Mets (Big) Arteni (2047m) and Pokr (Little) Arteni (1754m). The obsidian of the Arteni complex is of a high quality; ‘smoky quartz’-like translucent, reddish-brown and black varieties and dozens of subvarieties are known.³⁹ The geological map of the Arteni volcano is shown in Fig. 6. A significant feature of the Arteni volcanic complex is the ~7km-long Aragats flow that erupted from the Mets Arteni volcano. Obsidian is exposed in the lower part of the flow and appears mostly as translucent obsidian.

It is worthy of note that Arteni is one of the largest sources of obsidian in the region that was widely utilized in prehistoric times.⁴⁰ Eruption products consist of rhyolitic and perlitic lava flows, tuffs, and pyroclastic deposits with obsidian. A significant feature is the appearance of a rhyolite-obsidian flow of up to 7–8km in length extending from Arteni to the west, and a shorter one of about 3km in length to the south, which is an indication of a high temperature of the eruption material and a relatively low viscosity of the melts, enabling them to flow for such distances. Typically acidic lavas are too viscous, in contrast to basaltic and basaltic andesite lavas, to flow over such a long distance and usually form short flows (up to few hundred metres) or domes and extrusions as well as coulee-type flows, also called dome flow. Several eruption episodes were described: explosive eruptions of rhyolite pumice and perlitic pyroclastics (Fig. 7), eruptions of several generations of zoned rhyolite-obsidian and obsidian lava flows (Fig. 8), and emplacement of extrusives forming domes.⁴¹ The latest episodes of volcanic activity are marked by an emplacement of an extrusive named Khcan (Cork) plugged in the conduit of the Mets Arteni volcano and by the formation of a small extrusive named Tapak blur (Flat Hill). Earlier geochemical studies note that in spite of geographic proximity and similar ages, the obsidian samples from Mets and Pokr Arteni are geochemically different enough to be distinguished as separate sources.⁴² Our data confirms this conclusion; further below we will touch upon the geochemistry of the Arteni volcanic complex in more detail.

The *Gegham volcanic upland* in the eastern part of the Armenian Highlands, in central Armenia, is a typical example of laminar volcanism and presents itself morphologically as an elongated oval shield with dimensions of about 65 × 35km. The highest point of the Gegham upland with around 127 known monogenic volcanic centres is the Azhdahak volcano with an altitude of 3597m. Within the upland, intense Neogene-Quaternary volcanic activity is indicated by fissure flood basalts of subalkaline composition and differentiated volcanic products erupted from monogenic centres, varying in composition from trachybasalts, basaltic-trachyandesites and trachyandesites to trachytes, trachydacites and trachyrhyolites.

³⁶ Chernyshev et al. 2002.

³⁷ Oddone et al. 2000.

³⁸ Lebedev et al. 2011.

³⁹ Described in detail by Karapetian 1972.

⁴⁰ Badalyan et al. 2004.

⁴¹ Karapetian et al. 2001.

⁴² Meliksetian – Karapetian 1981; Keller et al. 1996; Blackman et al. 1998; Karapetian et al. 2001.



Fig. 7 Products of explosive eruptions of rhyolitic pumice and perlite pyroclastics from the Mets Arteni volcano (photo: K. Meliksetian)



Fig. 8 Obsidian cliff in a small modern quarry across a lava flow erupted from the Pokr Arteni volcano (photo: K. Meliksetian)



Fig. 9 Gutansar volcano, Gegham volcanic upland (photo: R. Badalyan)



Fig. 10 Jraber extrusive body related to the Gutansar volcanic complex. Obsidian outcrop on the Yerevan-Sevan highway (photo: R. Badalyan)

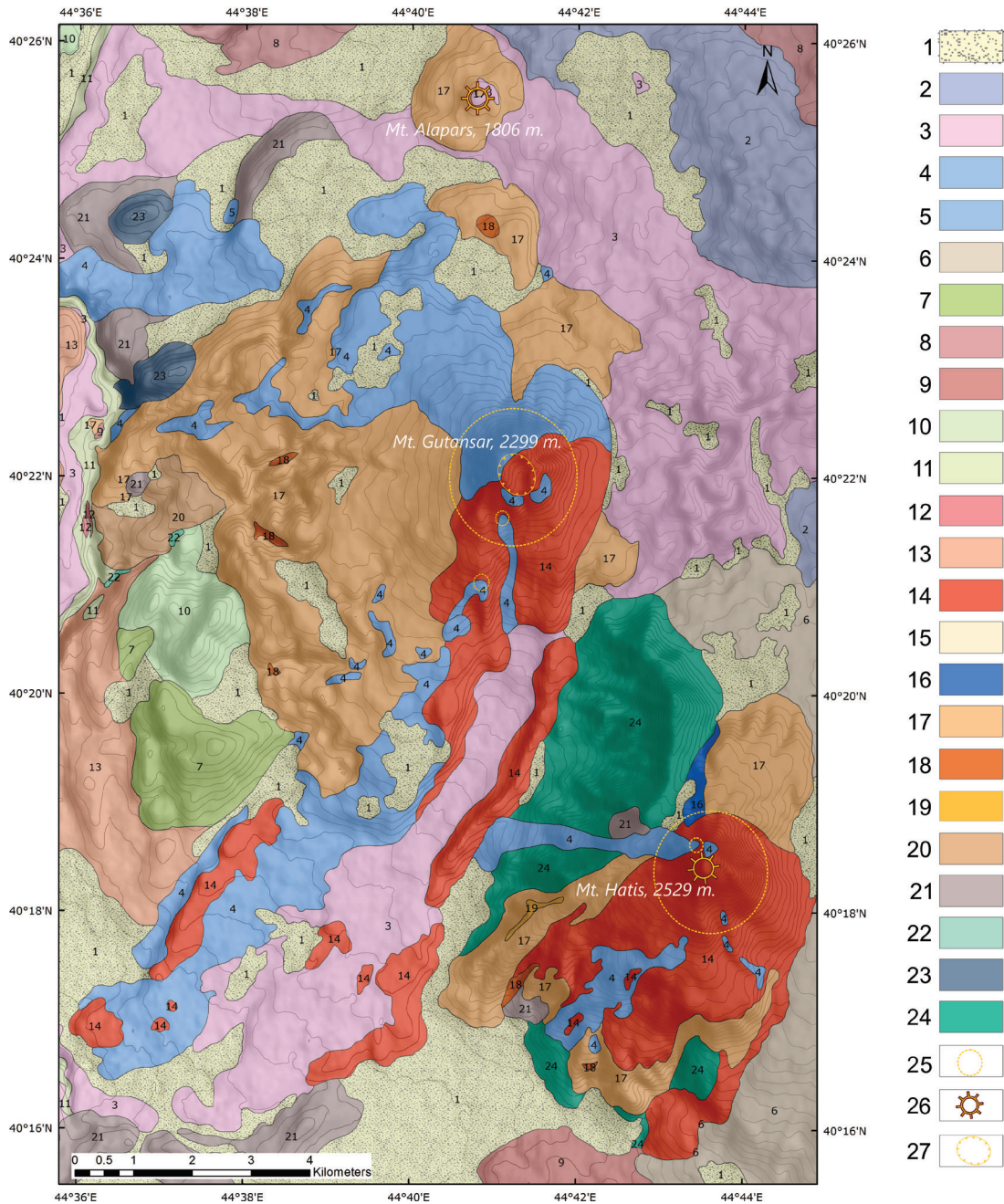


Fig. 11 Geological map of Hatis and the Gutansar volcanic complex. Legend: Q_3 – Q_4 Upper Pleistocene – Holocene: 1. Alluvial, and colluvial deposits; 2. Basaltic trachyandesite lava from the west slope of the Gegham ridge. – Q_3 Upper Pleistocene: 3. Thinly columnar quartz containing basaltic trachyandesites from the Hrazdan River canyon; 4. Basaltic trachyandesites, basaltic lavas of the Quaternary volcanic group Hatis and Gutansar. – Q_2 Middle Pleistocene: 5. Tuff of Yerevan-Leninakan type; 6. Basaltic trachyandesite lava region, Zovashen, Hatis, Zar villages; 7. Olivine basaltic trachyandesite lavas. – Q_1 Lower Pleistocene: 8. Basaltic trachyandesites and andesite-dacite lavas of the Merksar volcano; 9. Basaltic trachyandesite lava region, Zar and Akunk villages; 10. Hornblende trachyandesites and andesite-dacites of the Nurnus and Karashamb villages region; 11. Large columnar quartz containing basaltic trachyandesites from the Hrazdan River canyon; 12. Small olivine basaltic trachyandesites from the Razdan River canyon; 13. Basaltic trachyandesites, basaltic (doleritic, avgitic) lavas, acidic volcanic complex products of the Hatis and Gutansar volcanoes; 14. Rhyolite and dacite lavas from the Hatis and Gutansar volcanoes; 15. Pumice quartz feldspar sands, Abovyan city region; 16. Explosive perlite-pumice rocks from the Hatis volcano; 17. Perlite-pumice lava and agglomerate formation with relic obsidian bodies; 18. Rhyolite lavas, lower suite; 19. Obsidian flow and interlayers. – N_2^2 Upper Pliocene: 20. Nurnus basaltic lavas; 21. Dolerite basalts; 22. Diatomite and diatomaceous clay. – N_2^1 Lower Pliocene: 23. Rhyolite, rhyodacite lavas of extrusive dome-shaped Gyumush and Avazan; 24. Kaputan volcanic clastic complex (trachyandesites, andesite-dacites, basaltic trachyandesites, basalts; 25. Bimodal volcanoes, Hatis and Gutansar; 26. Dome of Hatis volcano; 27. Crater of Gutansar volcano (graphics: G. Navasardyan)

The obsidian in the Gegham volcanic province occurs in the western part of the upland (Gutansar and Hatis, Hrazdan-Abovyan group) and in the southeastern part (Spitaksar and Geghasar, Martuni group).

The *Gutansar volcanic complex* is a huge extrusion known in the literature as the Jraber extrusion. It consists of several outcrops and volcanic domes named Gutansar (2229m, Figs. 9–10), Alapars and Fantan, identified as independent volcanoes.⁴³ The total area of extrusion is about 70km².

The Yerevan-Sevan highway runs across the extrusion, and spectacular obsidian and perlite outcrops can be seen on both sides along the road (Figs. 9–10). A single sample from Armenia analysed in the seminal work by Colin Renfrew,⁴⁴ mentioned as ‘Yerevan obsidian’, actually belongs to the Gutansar complex.⁴⁵ Samples from the Gutansar volcanic complex were previously analysed by many authors. Optical emission spectrography was used for samples ‘north of Yerevan’ from the collection of the British Museum⁴⁶. According to John Dixon,⁴⁷ they are certainly related to Gutansar or Hatis. Ten samples collected along the Yerevan-Tsakghakdsor road were analysed by WDXRF by Mario Fornaseri et al.⁴⁸ According to Chataigner,⁴⁹ this corresponds to the section near Jraber. Jörg Keller et al.⁵⁰ also link those samples to Gutansar, which is the same. Blackman⁵¹ used NAA to analyse six samples from ‘the source between Hrazdan and the north-western part of Lake Sevan’ and most of the samples were attributed to the homogeneous group named ‘Sevan I’, and only one sample was classified as ‘Sevan II’. Later, 18 samples from Jraber were analysed by Vincenzo Francaviglia.⁵²

A geological map of the eastern part of the Gegham volcanic upland is shown in Fig. 11. The activity of Gutansar began with eruptions of rhyolitic pyroclastic material followed by rhyolitic flows and obsidians, and ended with quite lengthy flows of rhyolitic and dacitic lava, the final portions of which plugged the volcano channels and formed typical dome-shaped structures. In the Upper Pleistocene, the volcano was cut by other volcanoes of andesite and basaltic andesite composition, which erupted lengthy lava flows. A large crater (600m in diameter, 5–8m deep) formed on the Gutansar summit during the Middle Pleistocene. The Large Extrusion (Jraber extrusion) occupies an area between the villages of Fantan, Gyumush (Karenis), Jraber, and the city of Charentsavan. Considering its geochemical homogeneity, geological structure and widely accepted volcanological conceptions, it can be assumed that the activity of the Gutansar volcanic complex is related to the formation of a huge rhyolite extrusion, and acid lava reached the surface by forming the Gutansar volcano and smaller domes at Alapars and Fantan.

The geological history of the Hatis volcano (2529m., Figs. 12–13) is very similar to Gutansar: eruptions of rhyolitic pyroclastics followed by rhyolitic obsidian and dacitic lava flows. Final viscous portions of lava plugged the conduit of the volcano and formed a dome-shaped structure (or volcanic neck).⁵³ In the Middle Pleistocene, Hatis was cut by younger volcanoes of andesite and basaltic andesite composition. Geochemically, Hatis is very close to Gutansar but can still be distinguished. Recent age determinations of Hatis and Gutansar⁵⁴ yielded the following results: 1.2 ± 0.5 Ma for Jraber obsidian; 0.9 ± 0.3 Ma for Gutansar rhyolite, and younger ages for some rhyolite lava flows; 0.38 ± 0.06 Ma, and $0.66 \pm 0.04/0.48 \pm 0.04$ Ma for Hatis. Although the

⁴³ Karapetian 1972.

⁴⁴ Renfrew et al. 1966.

⁴⁵ Keller et al. 1996.

⁴⁶ Cann – Renfrew 1964, 127.

⁴⁷ Dixon 1977.

⁴⁸ Fornaseri et al. 1977.

⁴⁹ Chataigner 1995.

⁵⁰ Keller et al. 1996.

⁵¹ Blackman 1984.

⁵² Francaviglia 1994.

⁵³ Karapetian et al. 2001.

⁵⁴ Lebedev et al. 2013.



Fig. 12 Hatis volcano, Gegham volcanic upland (photo: R. Badalyan)



Fig. 13 Outcrop of obsidian on the northwestern slopes of the Hatis volcano (photo: K. Meliksetian)

geological relationship does not suggest such a long time interval,⁵⁵ the large uncertainties of the first two ‘older’ determinations still leave open the question of the exact volcanostratigraphy of Gutansar and Hatis.

Further to the southeastern part of the Gegham volcanic upland are two rhyolitic volcanoes, namely Spitaksar (‘White Mountain’, 3560m, Fig. 14) and Geghasar (‘Beautiful Mountain’ 3446m, Figs. 15–16), located about 5km from each other. The activity of these volcanoes followed a similar scheme: explosive eruptions formed pyroclastic deposits and tuffs of rhyolitic composition, followed by lava flows. According to recent age determinations, Spitaksar obsidian formed 0.20 ± 0.02 Ma ago, while Geghasar yielded somewhat younger ages of 0.13 ± 0.08 Ma

⁵⁵ Karapetian et al. 2001.



Fig. 14 Spitaksar volcano, Gegham volcanic upland (photo: G. Navasardyan)



Fig. 15 View of the Geghasar volcano taken from the slopes of Spitaksar. Dark linear cliffs on the slopes indicate the presence of obsidian (photo: K. Meliksetian)



Fig. 16 Thick coulee-type lava flow at Geghasar. Dark cliffs represent obsidian in the middle and upper parts of the flow (photo: K. Meliksetian)

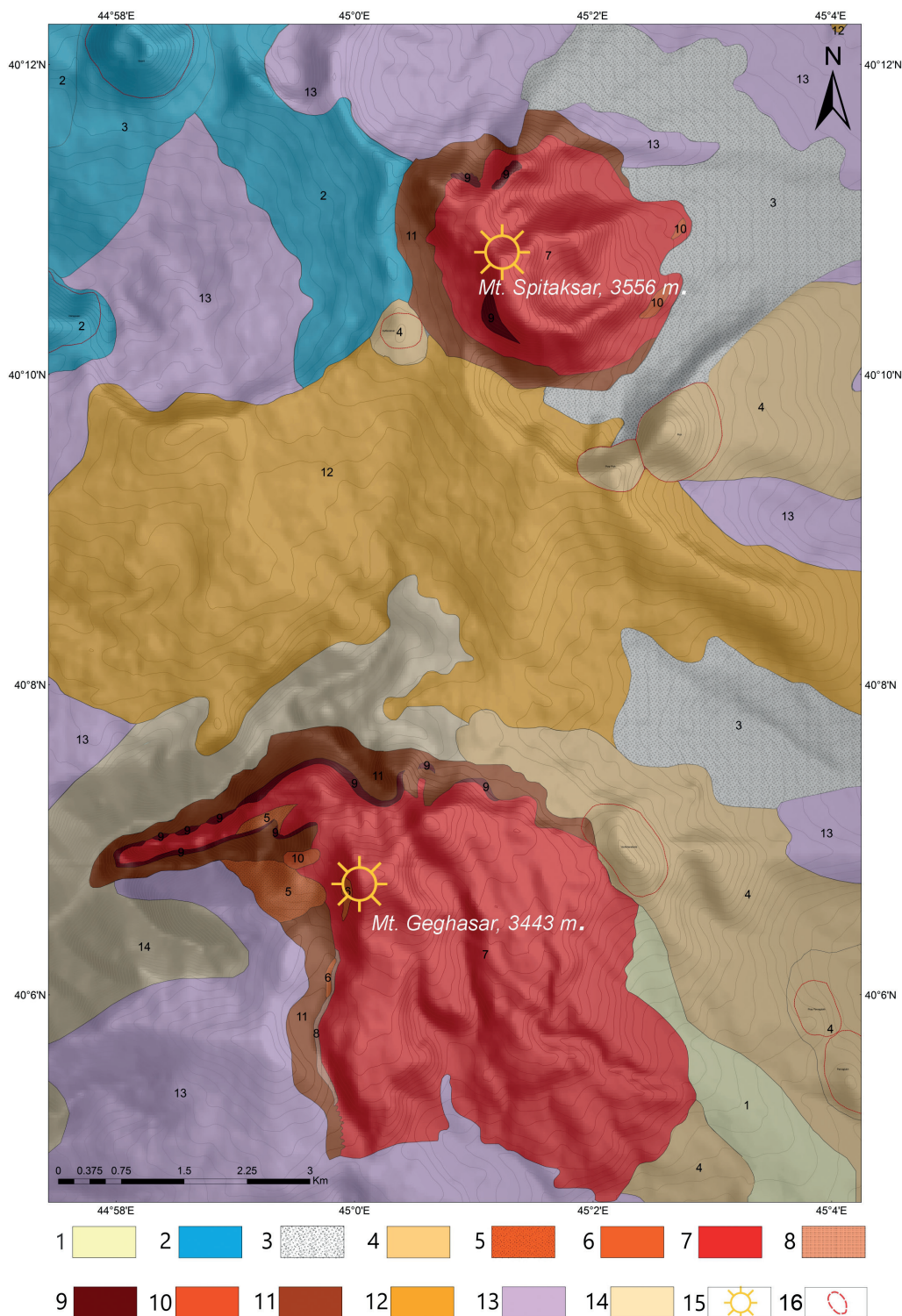


Fig. 17 Geological map of the Spitaksar and Geghasar volcanic complexes (Gegham volcanic upland). Legend: Q_3 – Q_4 Upper Pleistocene – Holocene: 1. Alluvia, diluvia, eluvia, proluvia deposits, pebble, sand, sandy-loam, loam, rubble; 2. Trachyandesites, andesites from the Nazeli, Vishapasar and Azhdahak volcanoes. – Q_3 Upper Pleistocene: 3. Glacial and fluvioglacial deposits. – Q_1 – Q_2 Lower – Middle Pleistocene: 4. Basaltic trachyandesites, trachyandesites from the Vochkharatum, Mets and Poqr Pich and Ashtarakner volcanoes. – Q_1 – Lower Pleistocene: Products of the Spitaksar and Geghasar volcanoes (11–17): 5. Hornblending rhyolite and dacites; 6. Rhyolites apical area of the Geghasar volcano; 7. Perlite lavas and breccias; 8. Perlite tuffs and breccias; 9. Zonal rhyolite flow with obsidian bottom and top; 10. Obsidians; 11. Perlite-pumice explosive and agglomerate products. – N_2^2 Upper Pliocene: 12. Basaltic trachyandesites, trachyandesites of Manichar lava flow. – N_2^1 Lower Pliocene: 13. Basaltic trachyandesites, trachyandesites, trachytes (Gegham suite). – Lower Pliocene – Upper Miocene: 14. Volcanoclastic deposits (Vokhchaberd suite); 15. Domes of Spitaksar and Geghasar volcanoes; 16. Scoria cones (graphics: G. Navasardyan)



Fig. 18 Obsidian with large plagioclase phenocrysts, Khorapor volcano (photo: K. Meliksetian)

(groundmass) and $0.08 \pm 0.02\text{Ma}$ (feldspar).⁵⁶ The obsidian is related to the basal parts of the flows that erupted from these domes. Obsidian from Geghasar and Spitaksar is of a high quality⁵⁷ and is characterized by a wide variety of colours from opaque white and translucent light grey to reddish brown and black. As will be shown below, both Geghasar and Spitaksar are geochemically identical and clearly different from all other obsidian sources.

The *Vardenis volcanic upland* is another area of intense Pliocene-Quaternary volcanic activity in Armenia, where the activity continued into the Holocene, namely at the Porak, Smbatar and Vayots-Sar volcanoes (Fig. 17).⁵⁸ Grey- to black-coloured obsidian is known only at the Khorapor volcano (2906m). However, the obsidian is of a low quality as it contains abundant plagioclase phenocrysts ranging up to 5mm in diameter (Fig. 18).

Further south is the huge *Syunik volcanic upland*. The southwestern slopes of the Syunik upland are in Armenia (Figs. 19 and 24) and the northeastern part extends into the region of Nagorno-Karabakh or Artsakh (the former Nagorno-Karabakh autonomous region of the Azerbaijan SSR in Soviet times).

The Syunik volcanic upland represents one of the most interesting young volcanic areas in Armenia considering the integrity of the volcanic centres and the compositions of the eruption products. The highest points of the Syunik upland are the peaks of the polygenic stratovolcanoes Tsghuk (3581m) and Ishkhanasar (3550m). The number of known volcanic centres amounts to 163; most of them are lava and cinder cones as well as rhyolitic domes. The distribution of volcanic centres along the fault lines noted for the Gegham upland is also clearly evident for the Syunik volcanic upland.⁵⁹ The composition of the volcanic series of Syunik differs sharply from the Gegham and Aragats series in the high alkaline composition, resulting in mafic alkaline series: olivine basalts, trachybasalts, tephrites and basanites; intermediate and acid series consist

⁵⁶ Lebedev et al. 2013.

⁵⁷ Badalyan et al. 2004.

⁵⁸ Karakhanian et al. 2003 and references therein.

⁵⁹ Karakhanian et al. 2003.

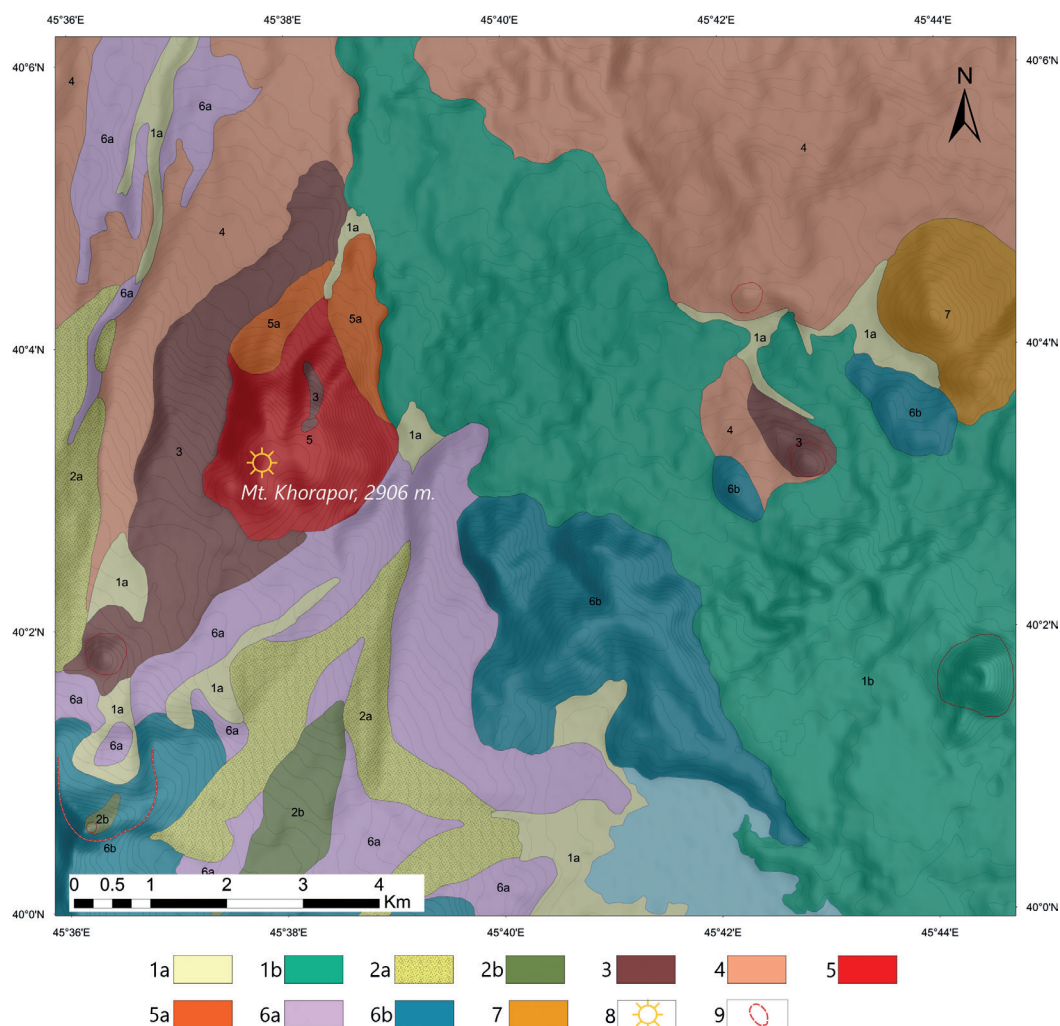


Fig. 19 Geological map of the Khorapor volcanic complex (Vardenis volcanic upland). Legend: Q_4 Holocene: 1a. Alluvia, diluvia, eluvia, proluvia deposits; 1b. Basaltic trachyandesites, trachyandesites lava flow from the Porak volcano. – Q_3 Upper Pleistocene: 2a. Glacial and fluvio-glacial deposits; 2b. Basalts lava flow from the Sandukhqasar volcano. – Q_2 Middle Pleistocene: 3. Basaltic trachyandesite lava flow of volcano Sarigagat (Spandaramet) and Kanachsar (Argiler). – Q_1 Lower Pleistocene: 4. Basalts and basaltic trachyandesite lava flow N slope of the Vardenis range. – N_2^2 – Q_1 Upper Pliocene – Lower Pleistocene: 5. Rhyolites of the dome-shaped Khorapor volcano; 5a. Obsidians of the northwest and northeast parts of the dome-shaped Khorapor volcano. – N_2^1 Lower Pliocene: 6a. Volcanogenic, volcano-sedimentary formation; 6b. Rhyolites of the dome-shaped Maralsar, Gizhsar, Charokh and foot of the Sandukhqasar volcanoes. – Middle Eocene: 7. Andesites of Dalisar; 8. Dome of Khorapor volcano; 9. Volcanoes (graphics: G. Navasardyan)

of trachyandesites, trachydacites, trachytes, dacites and rhyolites. Several large and huge rhyolitic volcanoes are known at Syunik, namely Bazenk (3221m), Sevkar (3233m, Figs. 20–21), Mets Satanakar (3169m, Figs. 22–23), Pokr Satanakar (3162m), Mijnek Satanakar (2788m) and Kecheldag (Merkasar, 3171m). Another source of obsidian is Miocene Bartsratumb on the Zangezour ridge near the border of Armenia with Nakhichevan (Azerbaijan). No new analyses of obsidian are available from Bartsratumb and Kecheldag, but for Kecheldag several analyses are available in the literature.⁶⁰ The ‘Kelbadzhar’ source mentioned by Blackman⁶¹ is actually an obsidian outcrop of the lava flow from the Kecheldag volcano, located further north.

⁶⁰ Keller et al. 1996; Blackman et al. 1998.

⁶¹ Blackman et al. 1998.



Fig. 20 Obsidian outcrop at the Pokr Sevkar volcano (Syunik volcanic upland) (photo: R. Badalyan)



Fig. 21 Obsidian flow on the slopes of the Sevkar volcano (Syunik volcanic upland) (photo: R. Badalyan)



Fig. 22 Obsidian flow at the Mets Satanakar volcano (Syunik volcanic upland) (photo: R. Badalyan)



Fig. 23 A large block of obsidian, Mets Satanakar volcano (photo: R. Badalyan)

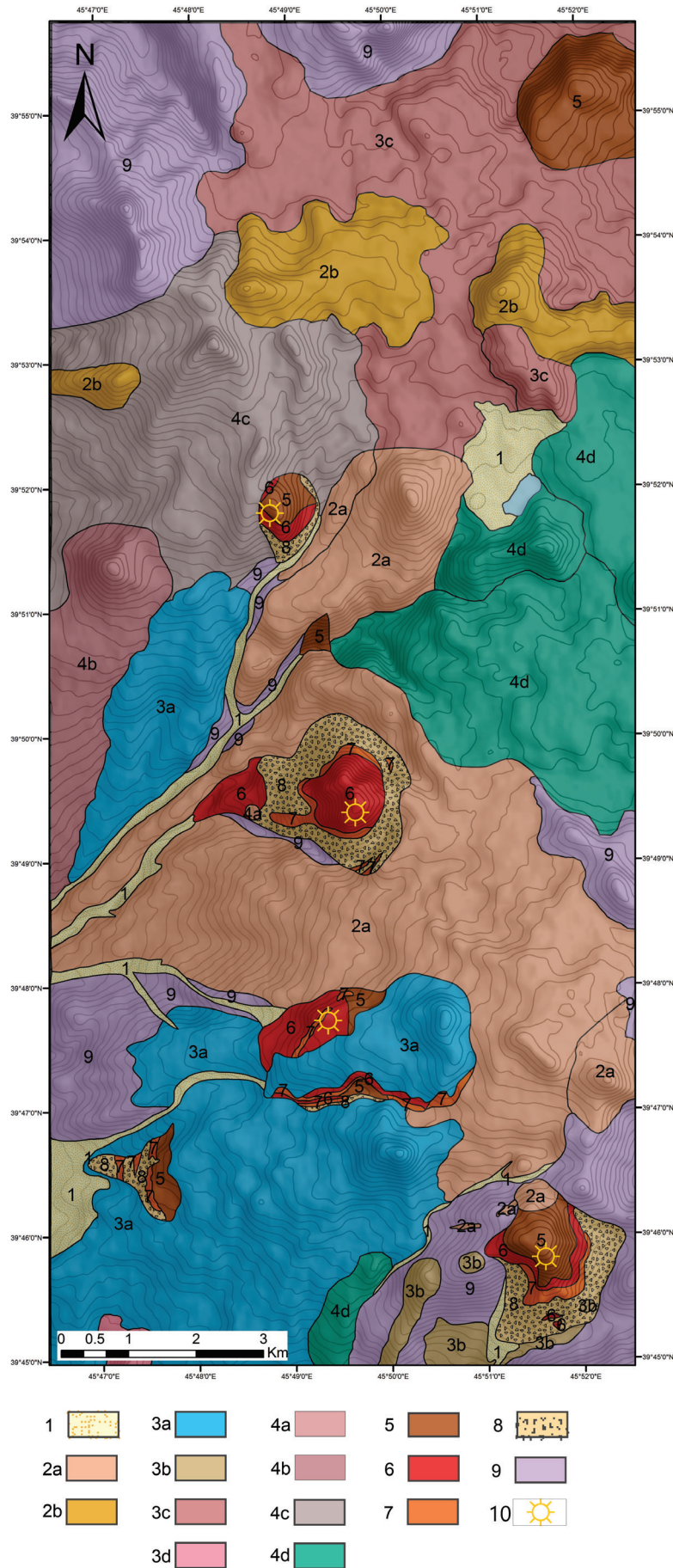


Fig. 24 Geological map of obsidian volcanoes of Syunik volcanic upland. Legend: Q_3 –H Upper Pleistocene – Holocene: 1. Alluvia, diluvia deposits. – Q_3 Upper Pleistocene: 2a. Basaltic trachyandesites lava from the Erkvoryakner and Gomayr volcanoes; 2b. Lava flows of the north part of the Syunik ridge. – Q_2 Middle Pleistocene: 3a. Hornblende, hornblende-pyroxene basaltic trachyandesites from the Mets Sevkhach and Sevkhach volcanoes; 3b. Basaltic trachyandesitic and trachyandesitic lava from the Berd, Kentronakan and SW foot of the Bazenk volcanoes; 3c. Lava flows of the north part of the Syunik ridge; 3d. Trachyandesitic lava flow from the Vorotan volcano. – Q_1 Lower Pleistocene: 4a. Hornblende trachyandesites from the Koracblur volcano; 4b. Trachyandesites and basaltic trachyandesite lavas from the volcanoes Karmirsar, Kisvats and others; 4c. Biotite-hornblende trachyandesite, trachydacite neighbourhoods of the Mets Satanakar volcano; 4d. Lava flows of the E, EN part of the Syunik ridge. – N_2 – Q_1 Upper Pliocene – Lower Pleistocene: Products of the volcanoes Bazenk, Mets Satanakar and others: 5. Perlite-obsidian lavas and breccia; 6. Rhyolites; 7. Black and grey obsidians with spherical segregations; 8. Perlites and pumice. – Pre-upper Pliocene: 9. Volcanogenic, volcano-sedimentary formation, trachyandesites, trachydacites, tuff, tuff breccias; 10. Domes of rhyolitic volcanoes (graphics: G. Navasardyan)

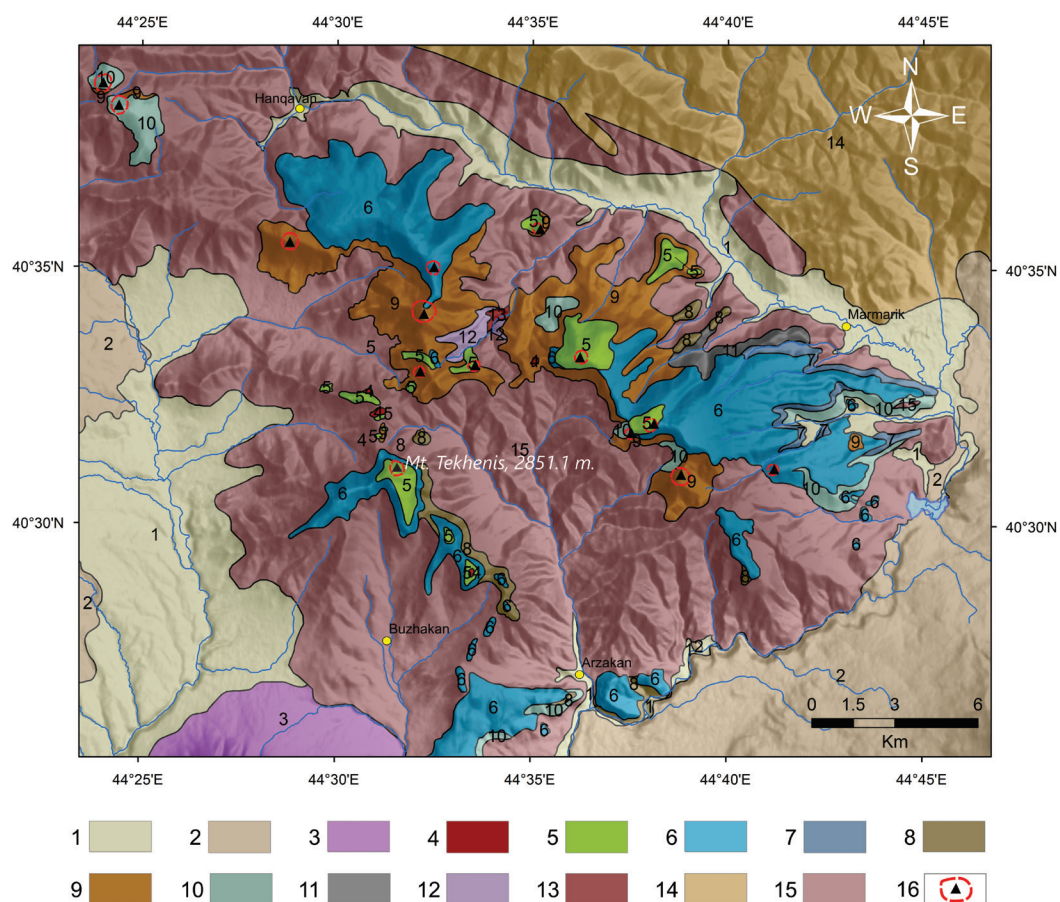


Fig. 25 Geological map of the Tsaghkunyats ridge. Legend: Q_3 – Q_4 Upper Pleistocene – Holocene: 1. Alluvia, diluvia, eluvia, proluvia deposits. – Q_1 – Q_2 Middle – Lower Pleistocene: 2. Quaternary basaltic trachyandesites, trachyandesites, trachydacites lavas of Gegham ridge and Aragats volcano. – N_2^2 Upper Pliocene: 3. Lavas of Arailer polygenetic volcano. – N_2^1 Lower Pliocene: 4. Biotitic rhyolite dacites; 5. Upper olivine basaltic trachyandesites and pyroxene trachyandesites; 6. Upper hornblende trachyandesites, andesitic dacites; 7. Lower olivine basaltic trachyandesites and pyroxene trachyandesites; 8. Volcano-clastic products of intermediate and acid composition (Buzhakan type); 9. Upper rhyolitic and rhyolitic dacite: obsidian-perlite rocks and clastic-breccia; 10. Perlite-obsidian pyroclastic, interlaced with lake and river sediments and volcanic ash. – N_2^1 – N_1^3 Lower Pliocene – Upper Miocene: 11. Lower hornblende andesitic dacites; 12. Volcano-clastic products of andesitic composition. – N_1^3 Upper Miocene: 13. Rhyolitic pyroclastics; 14. Paleogene volcanic and intrusive units; 15. Proterozoic metamorphic basement, Jurassic and Cretaceous volcanic, sedimentary and intrusive units; 16. Volcanic centres (graphics: G. Navasardyan)

The *Tsaghkunyats ridge* in central Armenia (Fig. 25) is formed by metamorphic rocks of the Proterozoic basement. Volcanic activity occurred in the Late Miocene and Pliocene, mostly of basaltic-andesite and andesite composition, with several rhyolitic volcanic centres and domes of Pliocene age. The largest eruption centres are Tekhenis, Arkayasar, Damlik, and Kamakar.⁶² Grey-, black-, red- and brown-coloured opaque obsidian is related to the Damlik (2781m) and Kamakar (2565m) volcanoes. In many cases, rhyolitic lavas and pyroclastic rocks are covered by younger basalt-andesites. Available age determinations are summarized in Table 1 and suggest a formation of rhyolites and obsidians in the Late Miocene – Early Pliocene, in the range of 3.9–5.8Ma.

⁶² Karapetian et al. 2001.

Geochemistry of Obsidian Sources in the Southern Caucasus

The geological features of obsidian were already studied in Soviet times and summarized in numerous papers and monographs published in Russian.⁶³ Geochemical and petrological features were first studied with AES, INAA and flame photometry⁶⁴ as well as the composition of accessory minerals in obsidians. More recently, initiated by the interest generated by archaeological investigations and attempts to trace the provenance of archaeological obsidian artefacts, several studies of the geology and geochemistry of Armenian obsidian occurrences were performed. Below we provide a brief overview of these works.

As discussed previously, several samples from Armenia named ‘Yerevan source’ or ‘Sevan source’ were analysed. The geochemistry of Armenian (and southern Caucasian) obsidian in connection with provenance studies of archaeological artefacts was first reported in the pioneering work by Jörg Keller and Ernst Pernicka in collaboration with the Armenian volcanologists Sergey Karapetyan and Ruben Jrbashyan.⁶⁵ This work provided XRF analyses of the major elements and Rb, Sr, Ba, Y, Nb, Zr and INAA data for Sc, Cr, Co, Zn, As, Sb, Cs, Hf, Ta, Th, U and the REE of the major obsidian sources in Armenia and the southern Caucasus altogether, as well as a reliable fingerprinting approach through use of both major and minor element geochemistry.

A big step forward in the studies of the geochemistry of Armenian obsidian sources was accomplished by Blackman together with the archaeologists Ruben Badalyan, Zaal Kikodze and Philip Kohl.⁶⁶ In addition to 118 INAA analyses of geological samples, this paper also provided analyses of more than 500 archaeological artefacts collected in the region, and also outlined seven geochemical groups of unidentified artefacts (Transcaucasian Unknown, TCUNK). Detailed geological descriptions of the rhyolite and obsidian occurrences were provided,⁶⁷ as well as their trace element geochemistry and petrology based on already published geochemical data.⁶⁸ These authors also discussed Sr isotope ratios of obsidians analysed in the isotope laboratory of the Institute of Geological Sciences of the National Academy of Sciences of Armenia.⁶⁹ A series of papers by Chataigner and co-workers⁷⁰ provided geochemical characterizations of obsidian sources in the South Caucasus region and neighbouring northeastern Türkiye based on LA-ICP-MS. We summarize this recent data and compare it with our results to enlarge the geochemical database. Particularly important are the results by Chataigner et al. on obsidian occurrences in northeastern Türkiye that so far have not been characterized in detail by other authors.⁷¹

Frahm and co-workers proposed a method for rapid analysis of hundreds of artefacts in the field using a portable XRF instrument.⁷² Portable XRF was also used in recent works by Kristine Martirosyan-Olshansky⁷³ and Aleksan Juharyan.⁷⁴ Such a ‘ten-second analysis’ is certainly useful for screening a large number of samples as a first step in order to find out if obsidian from different sources or only from a single one was used at an archaeological site. If the archaeological site is located near a geological source, then it may be possible to relate the archaeological material to this source. This was demonstrated for the Palaeolithic sites Lusakert-1 and Nor Geghi-1 near Gutansar, where 93% of the obsidian artefacts derived from this single source.⁷⁵ It is, however,

⁶³ Karapetian 1972; Nasedkin 1981 and others.

⁶⁴ Meliksetian – Karapetian 1981.

⁶⁵ Keller et al. 1996.

⁶⁶ Blackman et al. 1998.

⁶⁷ Karapetian et al. 2001.

⁶⁸ Meliksetian – Karapetian 1981; Keller et al. 1996.

⁶⁹ Karapetian et al. 2001.

⁷⁰ Chataigner et al. 2014; Chataigner – Gratuze 2014a; Chataigner – Gratuze 2014b.

⁷¹ Chataigner et al. 2014.

⁷² Frahm – Feinberg 2013.

⁷³ Martirosyan-Olshansky 2018.

⁷⁴ Juharyan 2018.

⁷⁵ Frahm et al. 2014.

less precise and accurate than the traditionally employed methods, and its power to discriminate is markedly inferior to true multi-element analyses and is thus less useful for provenance analysis. Therefore, this method will not replace precise geochemical investigations and a good geochemical database with accurate analyses of obsidian sources. In another paper, the application of multiscalar magnetic variations in the Gutansar obsidian complex was tested⁷⁶ and allowed to change the scale of archaeological sourcing if the geological source comprises several geochemically identical bodies of obsidian. It was suggested that variations in the magnetic properties may be helpful to identify possible workshop locations and distinguish between geochemically identical lava flows.⁷⁷ Another study of Armenian obsidian was accomplished by Chataigner et al.⁷⁸ based on the analysis of 73 geological samples.

In this paper we attempt to provide a complete geochemical characterization of the geological obsidian sources of the southern Caucasus based on 153 new analyses of geological samples carefully selected from almost all obsidian occurrences in Armenia. Samples from Chikiani (Georgia) were provided by Chataigner and Karapetyan. Together with the geochemical fingerprinting of sources, we attempt to identify the provenance of 534 archaeological samples, mainly from Armenian archaeological sites, but also from Georgia, Azerbaijan, Dagestan (Russia), Iran and the Troad. All analyses of the geological samples and of obsidian artefacts from outside the territory of the Republic of Armenia are summarized in the Appendix.⁷⁹

The current study also includes a comparison of South Caucasian and Anatolian sources, as well as the results of interlaboratory comparisons of analyses of Armenian obsidians analysed by different methods.⁸⁰

Jörg Keller and Carola Seifried used major elements for a basic grouping of Anatolian and Armenian obsidians and demonstrated that in some cases major element concentrations can be sufficient for identifying the provenance of artefacts.⁸¹ They proposed the CaO-Fe₂O₃ relationship as a basic discriminator for Anatolian and Armenian-Caucasian sources but they also suggested that additional characterization can be provided by detailed trace element and REE data analysed with neutron activation analysis (INAA). For fingerprinting, an enlarged database for the comparison of Anatolian sources with Armenian obsidians was used.⁸² Th-La diagrams were particularly effective for expressing these chemical differences, and as a final step, the element-by-element comparison was suggested. Thus, it was suggested that direct use of the analytical data is preferred to the use of more complex parameters like ratios, factors, functions, dendrograms, etc.

On the other hand, Blackman and co-workers used hierarchical aggregative clustering analysis to build a dendrogram, plotted as a function of dissimilarity.⁸³ Nevertheless, further discriminations are based on La-Th and Ta-Sc binary plots.

In the following we use the approach suggested by Keller and co-workers,⁸⁴ which is simple and easy to understand for everyone. A difficulty arises in that major element concentrations are not always available, as most of them cannot be determined by INAA, and additional analyses such as XRF or ICP-MS would be required. A general problem is also evident: with an increasing number of analyses of individual sources, more inhomogeneities in some sources are recognized, which often results in a widening of the compositional fields in many diagrams.

⁷⁶ Frahm et al. 2016.

⁷⁷ Frahm – Feinberg 2013; Frahm et al. 2014.

⁷⁸ Chataigner et al. 1998.

⁷⁹ Analyses of archaeological samples are available on request from the first author. However, they will also be published in another publication.

⁸⁰ This work; Keller et al. 1996; Blackman et al. 1998; Cherry et al. 2010; Chataigner et al. 2014; Chataigner – Gratuze 2014a; Chataigner – Gratuze 2014b.

⁸¹ Keller – Seifried 1990.

⁸² Keller et al. 1996.

⁸³ Blackman et al. 1998.

⁸⁴ Keller et al. 1996.

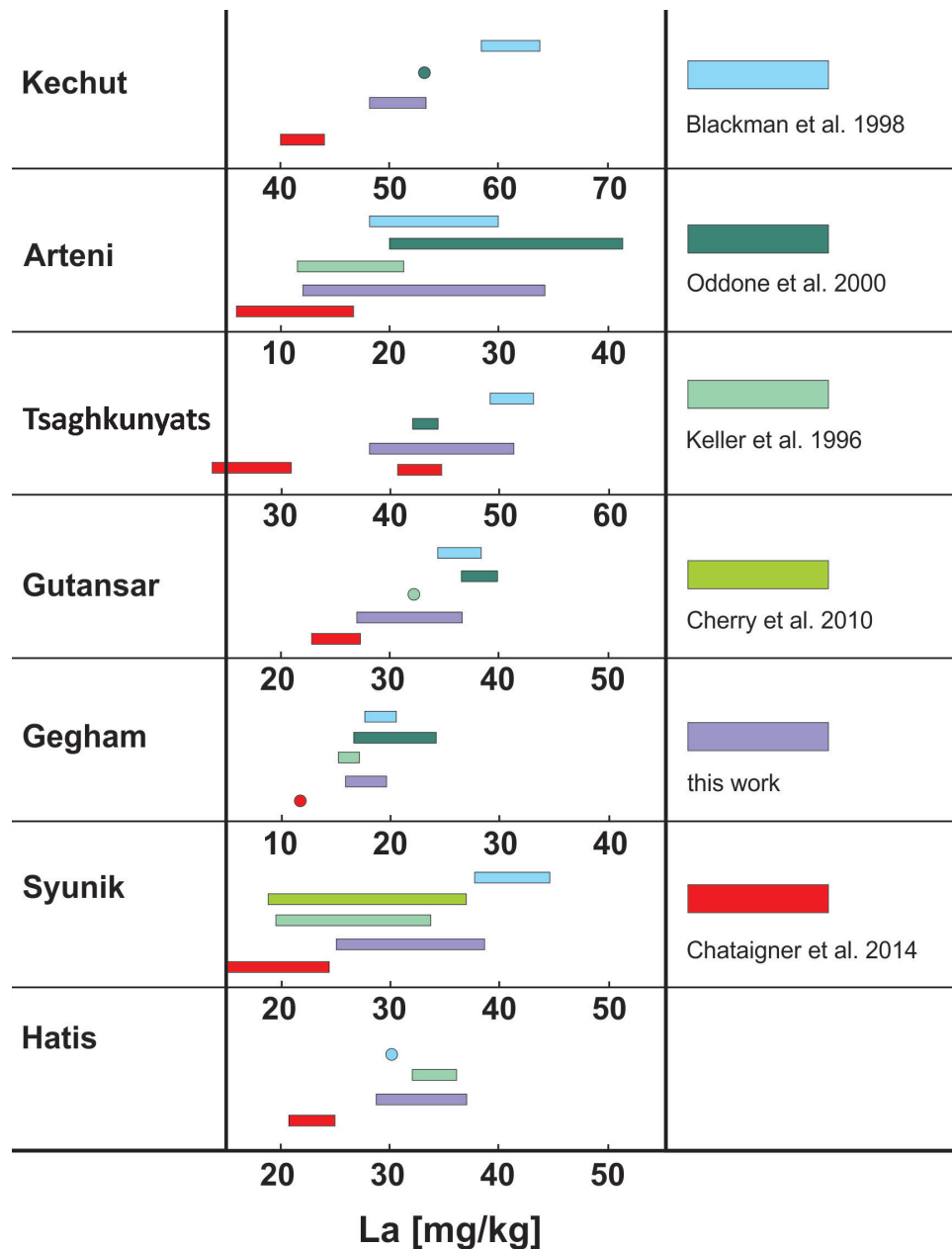


Fig. 26 Comparison of lanthanum concentrations in obsidian samples from seven Armenian sources for which data have been reported. Chataigner et al. 2014 report two compositionally different types of obsidian from Tsaghkunyats, which is indicated by two red bars. Nevertheless, the data obtained with LA-ICP-MS are systematically lower than the data obtained by INAA (graphics: E. Pernicka)

This, in fact, makes the process for reliably tracing the provenance of the artefacts through element-by-element comparison even more complicated, but on the other hand, this provides a chance to solve the problem of the origin of many artefacts that have remained unidentified until now.

Another difficulty is related to analyses from different laboratories using different methods. Besides possible problems with precision and accuracy, different sets of elements are often reported and used for fingerprinting. This is especially problematic for the comparison of datasets obtained with most widely applied XRF methods and neutron activation analysis (INAA). While XRF yields high precision for the concentrations of the major (rock-forming) elements but has a relatively low sensitivity for most trace elements, most INAA datasets contain only

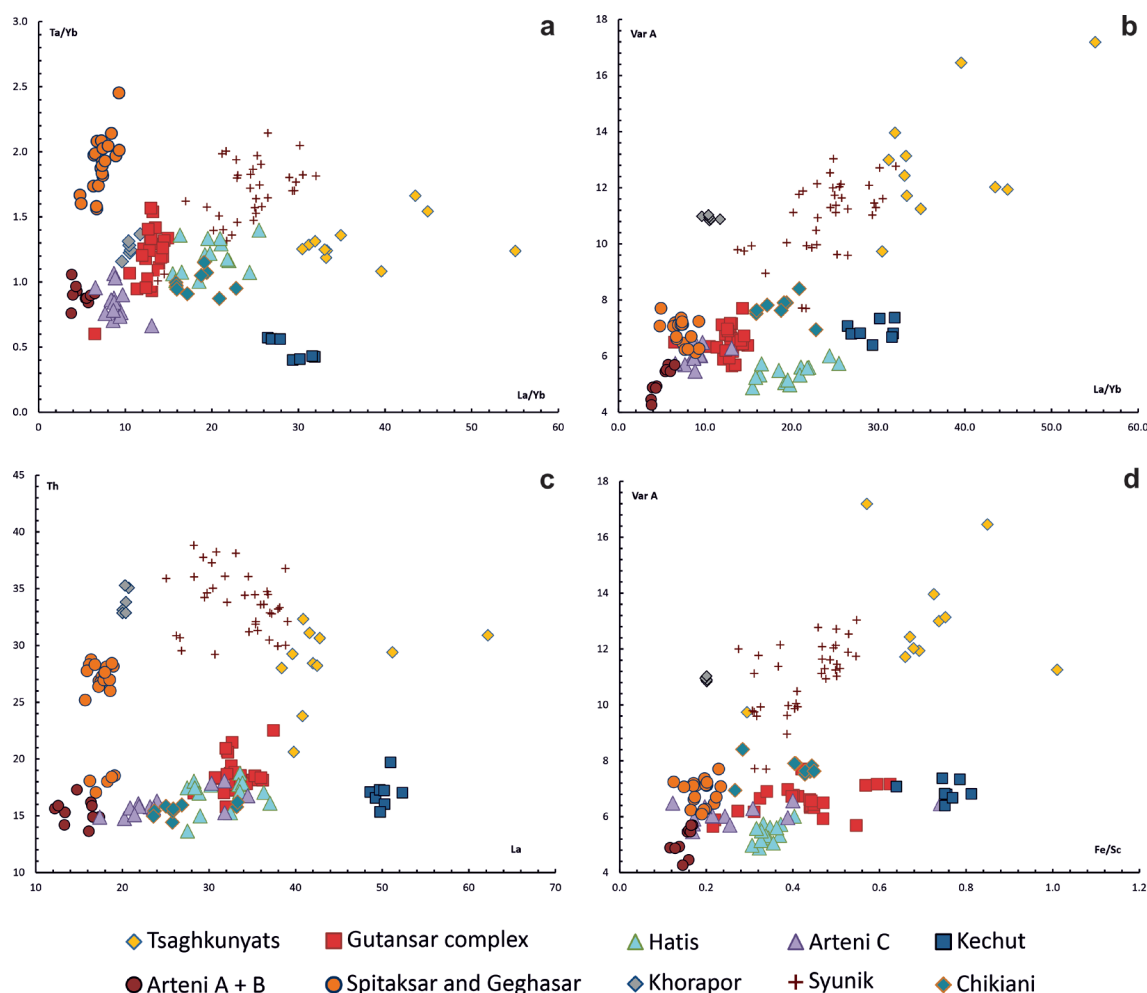


Fig. 27 Discrimination of the obsidian sources analysed in this study. a. La/Yb ratio versus Ta/Yb ratio; b. La/Yb ratio versus Var A; c. La versus Th; d. Fe/Sc ratio versus Var A (graphics: K. Meliksetian)

Na, K, and Fe as major elements and element concentrations of some 20 or more trace elements. But even the range of trace elements is not congruent for both methods. A new approach became popular with the advent of portable XRF instruments, which make it possible to analyse many samples directly in the field or in collections non-destructively, albeit with limited sensitivity and precision. Accordingly, sometimes no concentration values are reported at all⁸⁵ or only for a limited set of elements like Rb, Sr, Y, Zr and Nb,⁸⁶ as these are the trace elements that can be determined with the highest sensitivity. Of these, only Rb, Sr, and Zr can be compared with INAA data. However, even the best obtainable precision with any of these methods is about 1% relative, so that it is certainly unrealistic to report concentrations with up to four significant digits, especially if analyses were performed with a portable XRF instrument, in which case one would expect precisions in the order of 5% relative.⁸⁷ A new method that was introduced two decades ago is proving very promising, namely mass-spectrometry coupled with laser ablation (LA-ICP-MS). This method has been extensively applied to glass and obsidian by Bernard Gratuze's group and they have recently published a series of articles on obsidian sources

⁸⁵ E.g. Frahm et al. 2014.

⁸⁶ E.g. Frahm et al. 2016; Abedi et al. 2018.

⁸⁷ E.g. Abedi et al. 2018.

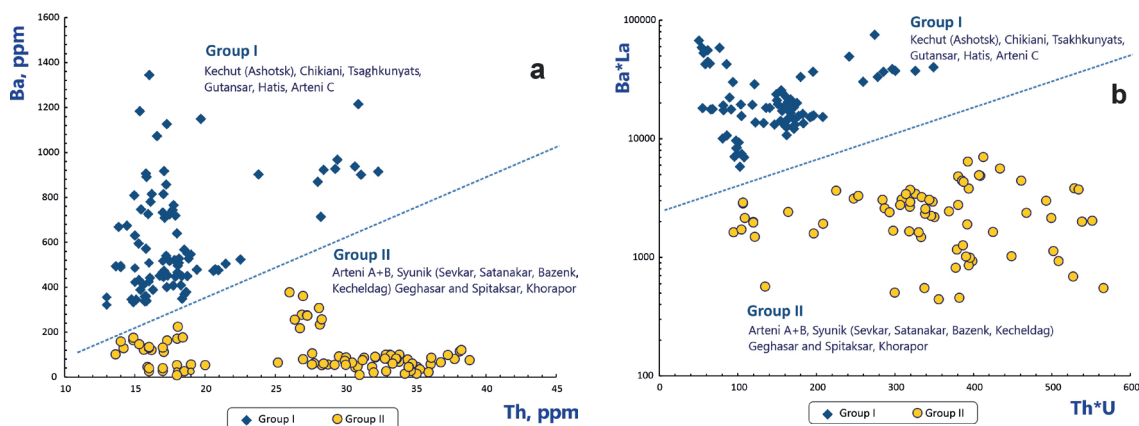


Fig. 28 a. Diagram of Th versus Ba to distinguish two major groups of Armenian obsidian sources; b. Multiplicative coefficients Ba*La versus Th*U for obsidian from Caucasian and NE Anatolian occurrences. All obsidian sources are clearly separated into two distinct geochemical groups (graphics: K. Meliksetian)

in the southern Caucasus and eastern Anatolia.⁸⁸ However, it seems that there are small but systematic differences between most analyses obtained with INAA and the data from this group (Fig. 26).⁸⁹ These differences have been observed not only for lanthanum but also for cerium, hafnium, tantalum and thorium, all of which are important elements for the discrimination of obsidian sources.

As useful discriminating factors Fe/Sc versus a compound variable A (abbreviated as Var A), was introduced by Arnold Aspinall et al.,⁹⁰ while La versus Th and others was used in earlier works. For this study we first tried to use some new diagrams for a primary division of obsidian sources such as Ta/Yb versus La/Yb (Fig. 27.a), widely used in petrology for volcanic and intrusive rocks.

Relatively good discrimination is also provided by a La/Yb versus Var A diagram (Fig. 27.b) together with commonly used diagrams such as La versus Th (Fig. 27.c). Together with a diagram of Var A versus Fe/Sc (Fig. 27.d), these old and new plots provide relatively good discrimination of Armenian (and Caucasian) obsidian, but with an increasing number of analyses, many sources turn out to be actually overlapping (Arteni with Gutansar and Spitaksar, Chikiani with Hatis and Gutansar etc., see Fig. 27), and it is not possible to use these plots for reliable assignment of some of the artefacts. There are several reasons for this: besides the increase in the total number of analyses, which expands the range of the source fields, it is important to remember that the absolute values of the elements could be different for various reasons, but the elemental ratios may be similar. In the case of binary plots, such as La-Th, the concentrations of these elements could be very close for diverse sources, but other elements may exhibit largely variable values. It is suggested that one of the possible solutions for these difficulties could be a breakdown of all sources into smaller geochemical groups using geochemical indicators that are clearly linked to petrology and then using the above-mentioned diagrams for each group separately.

A division of Armenian obsidian sources into two geochemically reasonable groups, namely Ba-rich on the one hand and Rb-rich on the other, based on absolute concentrations of Ba, Rb and other geochemically related elements, was suggested earlier.⁹¹ Ba-rich (Ba-, Sr-, Zr-, Hf-, LREE-rich) sources – with the exception of the Mets Arteni volcano – are typical for obsidian of the western volcanic zone of Armenia, and Rb-rich (Rb, Cs, Th, U, Ta, Nb) obsidian sources are characteristic for the eastern zone as well as for the Mets Arteni volcano, except for the Aragats flow.

⁸⁸ Chataigner et al. 2014; Chataigner – Gratuze 2014a; Chataigner – Gratuze 2014b.

⁸⁹ See Nedelcheva et al. this volume.

⁹⁰ Variable A = [Cs+Ta+Rb/100+(Th+La+Ce)/10]/Sc, Aspinall et al. 1972.

⁹¹ Karapetian et al. 2001.

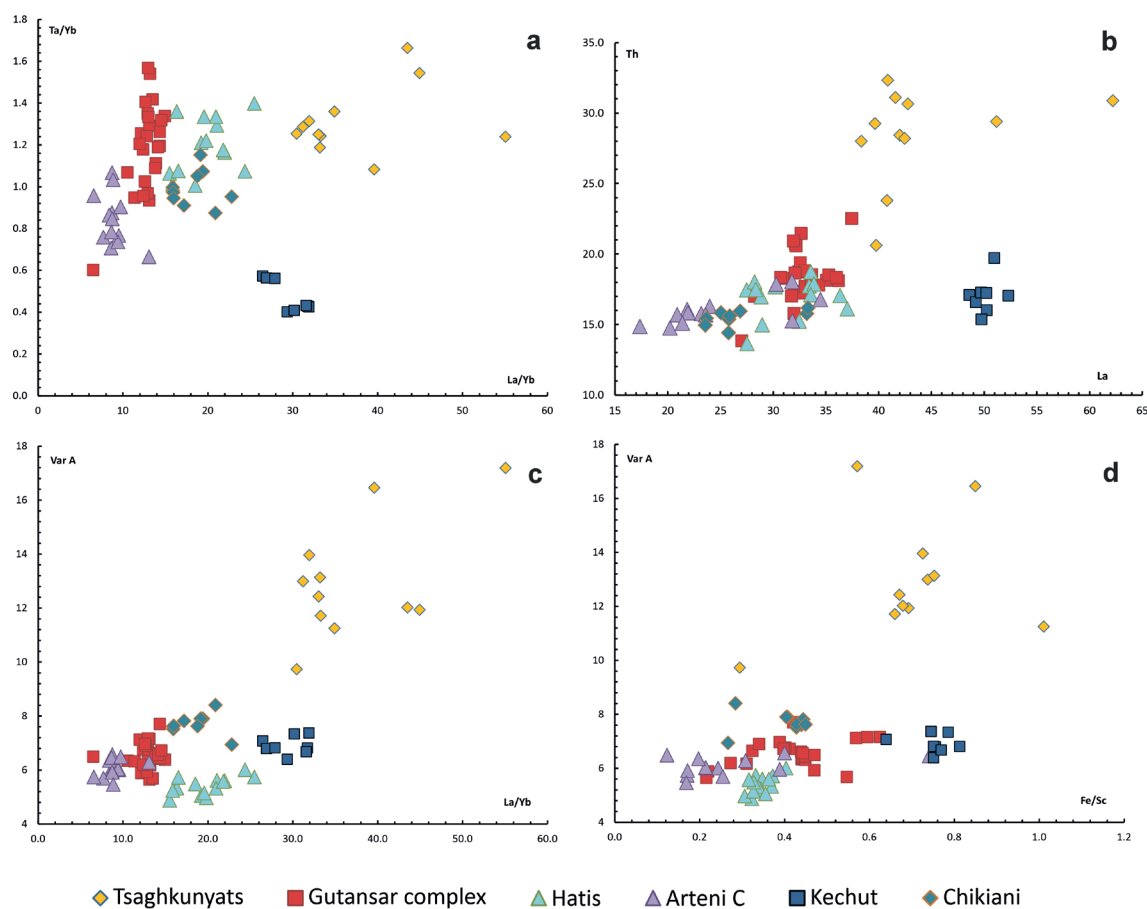


Fig. 29 Further diagrams for the discrimination of Group I obsidian sources analysed in this study. a. La/Yb ratio versus Ta/Yb ratio; b. La versus Th; c. La/Yb ratio versus Var A; d. Fe/Sc ratio versus Var A (graphics: K. Meliksetian)

Generally, these two groups can be related to S-type granites (Ba-, Sr-rich) and I-type granites (Rb-, Ta-rich), which generally characterize granitic rocks by their genesis, as rhyolites (obsidians) are volcanic analogues of granitic rocks. Accordingly, such a general approach to geochemical differentiation could be applied for obsidian sources as well.

We tried to develop this classification in the form of several binary plots, and it turned out that a clear separation of these two geochemical groups could be best obtained in a diagram of Ba versus Th (Fig. 28.a). An even better discrimination of these two geochemical groups could be obtained by multiplication of geochemically related indicator elements like Ba*La versus Th*U (Fig. 28.b). Multiplication of the concentration values of related elements enhances the effect by an order of magnitude. Such coefficients were first used in mathematical models for the interpretation of geochemical prospecting data to increase the contrast range of geochemical features and clearly identify anomalies⁹² and they prove to be useful for the discrimination of major geochemical groups of obsidian as well.

Thus, Fig. 28 clearly shows that all obsidian sources of the South Caucasus can be separated unequivocally into two geochemical groups. As a first step, any artefact analysis can be easily attributed to one of these groups, and further steps may include diagrams such as La/Yb versus Ta/Yb, La/Yb versus Var A, La versus Th, Fe/Sc versus Var A and others for each group separately. As is observed in Fig. 29 (for Group I) and Fig. 30 (for Group II), there is almost no overlap

⁹² Ovchinnikov – Grigoryan 1970.

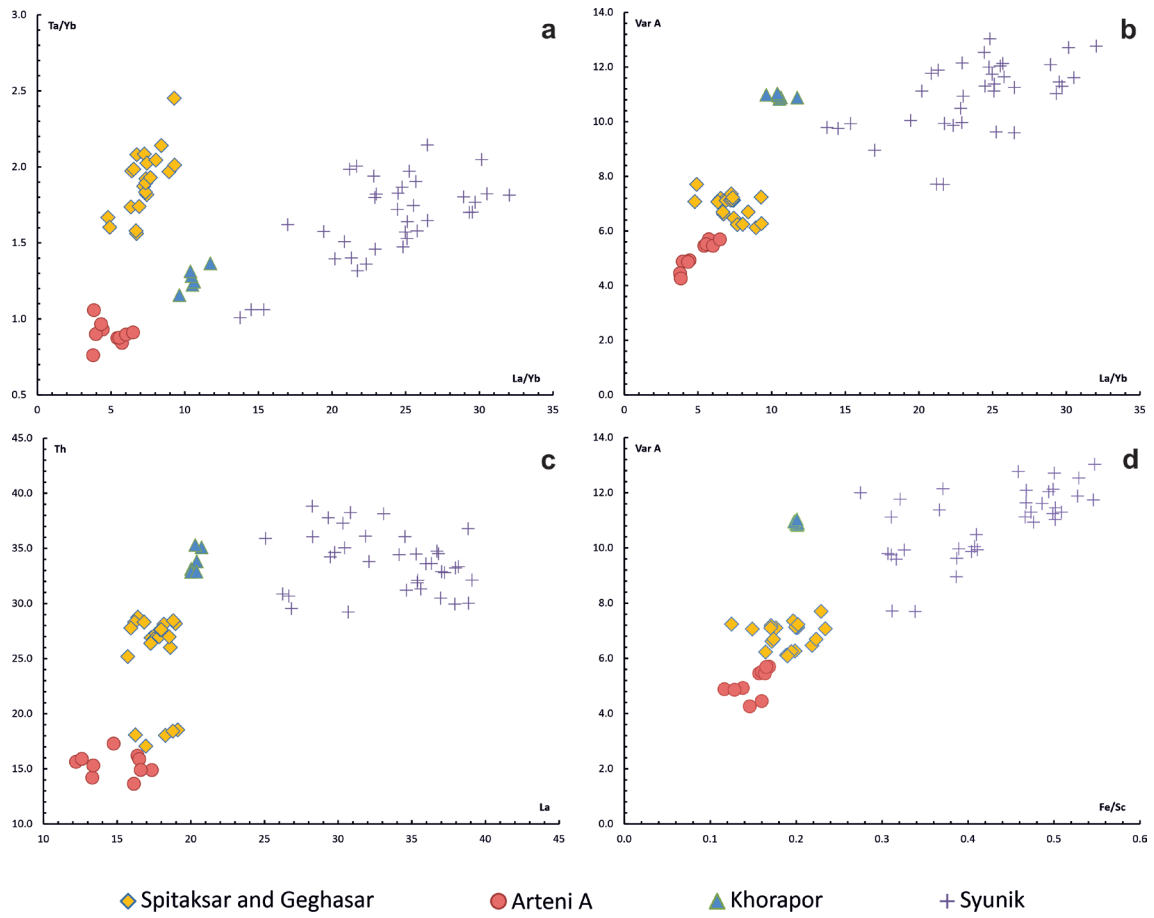


Fig. 30 Further diagrams for the discrimination of Group II obsidian sources analysed in this study. a. La/Yb ratio versus Ta/Yb ratio; b. La/Yb ratio versus Var A; c. La versus Th; d. Fe/Sc ratio versus Var A (graphics: K. Meliksetian)

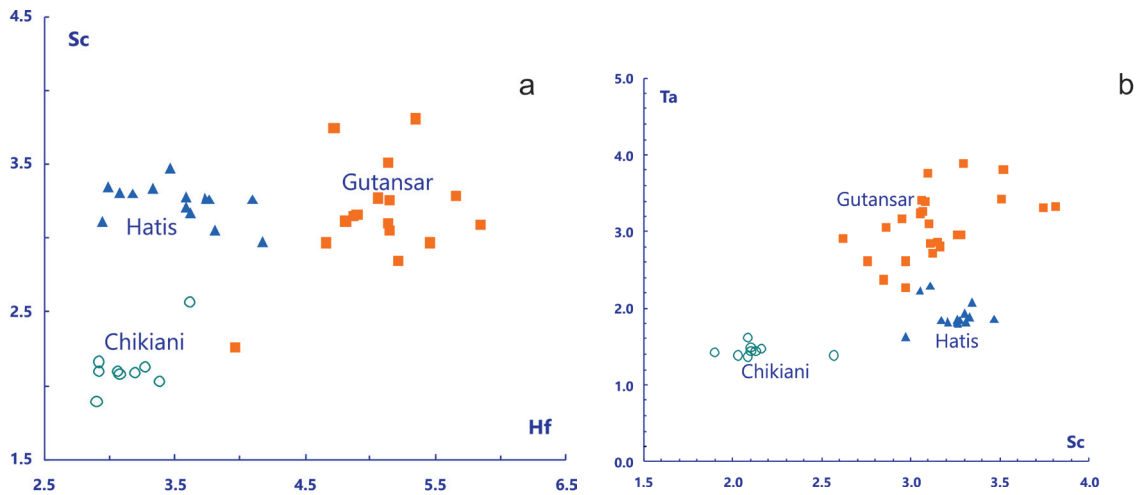


Fig. 31 Diagrams for the discrimination of the Hatis, Gutansar and Chikiani sources. a. Hf versus Sc; b. Sc versus Ta (graphics: K. Meliksetian)

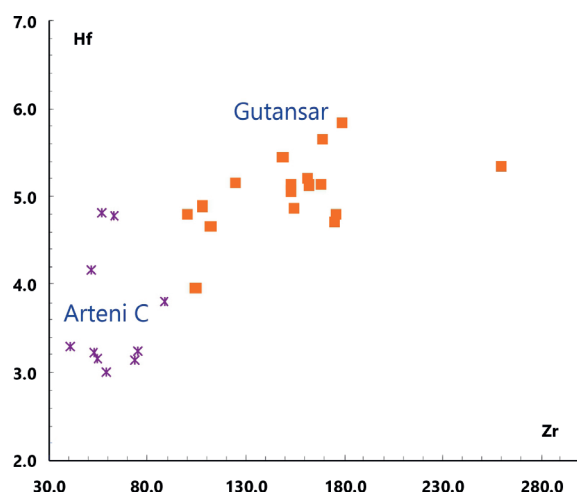


Fig. 32 Zr versus Hf diagram for the discrimination of the Gutansar and Arteni C sources (graphics: K. Meliksetian)

on diagrams if data points of the two source groups are plotted separately rather than a large number of data of all sources on the same diagram.

For sources still overlapping or showing close geochemical characteristics on the previous diagrams, other diagrams, such as, for instance, Hf versus Sc (Fig. 31.a) and Sc versus Ta (Fig. 31.b) provide clear separation of the Chikiani, Gutansar and Hatis sources, and Zr versus Hf clearly separates Arteni C and Gutansar, as is observed in Fig. 32.

It is suggested that such an approach is helpful in most cases to set up a fingerprinting method to establish the origin of obsidian artefacts deriving from the different South Caucasian sources.

Geochemical Comparison of Obsidian Sources in the Lesser Caucasus, the Northeastern Part of the Armenian Volcanic Highlands and Northeastern Türkiye

Before the recent work of Chataigner and co-workers,⁹³ the abundant obsidian sources of northeastern Türkiye were not thoroughly studied and their geochemical characteristics were not well known or only sporadically characterized. Some major element XRF and INAA data were provided earlier.⁹⁴ Some volcanological and petrological publications⁹⁵ provided some analyses of northeastern Anatolian rhyolites, but these data are difficult to use for provenance studies due to unclear geographical localization, especially if one considers the fact that obsidian is an aphyric glassy rhyolite but not vice versa.

In any case, a large number of obsidian artefacts from Armenia that were analysed within this study, particularly from sites in the northwestern part of Armenia neighbouring the Kars Plateau in northeastern Türkiye were of unknown origin, as mentioned earlier.⁹⁶

Some of the artefacts from the southern Caucasus discussed in the study by Blackman and co-workers⁹⁷ also remain unidentified and were combined into six groups designated as Transcaucasian unknown (TCUNK). In this chapter we will attempt to compare the compositions of northeastern Turkish sources⁹⁸ with our data and with the compositions of unidentified artefacts (TCUNK groups 1 to 6).⁹⁹

The data provided by Chataigner et al.¹⁰⁰ and Chataigner and Gratuze¹⁰¹ for obsidian occurrences in northeastern Türkiye were classified into seven chemical (and geological) groups of obsidians and, in addition, some samples from the southeastern part of Türkiye, such as Sipan (Süphan Dağ), Muş, Tondrak (Tendürek) were also analysed and used in their discussion.

⁹³ Chataigner et al. 2014; Chataigner – Gratuze 2014a; Chataigner – Gratuze 2014b.

⁹⁴ Keller – Seifried 1990.

⁹⁵ Pearce et al. 1990; Keskin et al. 1998; Keskin 2003.

⁹⁶ Badalyan et al. 2004; Badalyan 2010.

⁹⁷ Blackman et al. 1998.

⁹⁸ Chataigner et al. 2014.

⁹⁹ Blackman et al. 1998.

¹⁰⁰ Chataigner et al. 2014.

¹⁰¹ Chataigner – Gratuze 2014a; Chataigner – Gratuze 2014b.

LA-ICP-MS analysis¹⁰² provides a larger number of elemental concentrations (31 trace and 6 major elements) compared with INAA used in this study (22 trace and 3 major elements). In particular, with the LA-ICP-MS method, elements such as Nb, Sr, Y can be determined that are geochemically important in magmatic processes, but were not analysed in our study due to the limitations of the INAA method. On the other hand, with INAA it is possible to accurately determine Sc with very low ($\sigma=1.5\%$) uncertainty. This element is important in provenance studies of obsidians and is used in the famous Aspinall formula¹⁰³ and in our discrimination scheme for the separation of obsidians from Chikiani, Gutansar and Hatis using the diagrams Hf versus Sc (Fig. 31.a) and Sc versus Ta (Fig. 31.b).

The elements Nb, Sr, Y are used extensively by Chataigner's group for fingerprinting Anatolian and Caucasian obsidian sources, but for the sake of comparison of our dataset of Armenian and Georgian obsidians with those from northeastern Türkiye, we constrain the discussion to elements that are precisely determined by both LA-ICP-MS and INAA such as REE, Ta, Zr, Ba, Rb, Th and U.

A clear discrimination of Armenian obsidians by their Ba and Th contents (Fig. 28.a) and by using a diagram of multiplied concentrations of the geochemically related elements Ba*La versus Th*U (Fig. 28.b) was demonstrated earlier. After this initial grouping, further diagrams yielded further separations between individual sources.

It turned out that the seven sources of northeastern Türkiye analysed and discussed¹⁰⁴ fit into this scheme and exhibit generally similar geochemical trends, but it is worth noting that the Ba*La versus Th*U diagram provides a better division of the major geochemical groups and is used for further comparison of northeastern Anatolian and Armenian obsidians. (Fig. 33). In this semi-logarithmic diagram, the small but systematic differences mentioned above are not decisive, but nevertheless, the data obtained by LA-ICP-MS tend to lower values because lanthanum and thorium are on average about 30% lower than in our dataset for the same sources.

Thus, the West Erzurum 1, Yağlıca South and Yağlıca Summit (Digor), as well as the Sarıkamış South Mescitli sources belong to the high Ba type (Group I), while West Erzurum 2, South Erzurum, Pasinler, Sarıkamış Kizil Kilisa and Sarıkamış North Hamamlı match the low Ba type (Group II). It is noteworthy that the West Erzurum source can be clearly divided into two distinct groups based on this approach.

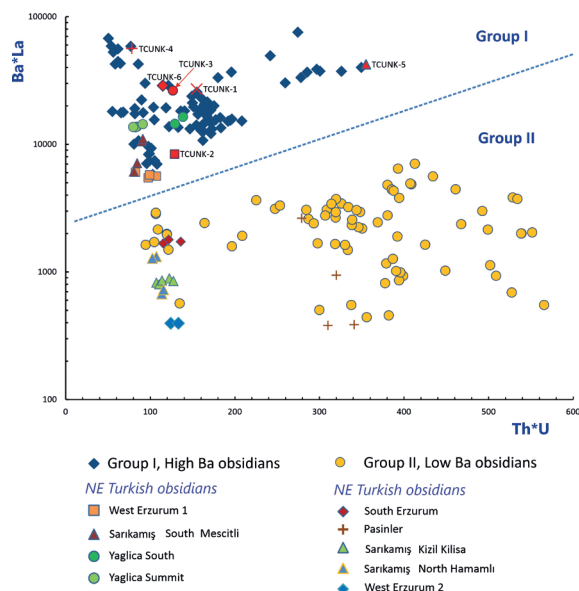


Fig. 33 Ba*La versus Th*U for obsidians of northeastern Türkiye and TCUNK groups compared with Group I and Group II Armenian obsidian sources and Chikiani. Red symbols annotated on the diagram represent TCUNK groups 1–6, all of which belong to Group I (graphics: K. Meliksetian)

¹⁰² Chataigner et al. 2014.

¹⁰³ Aspinall et al. 1972.

¹⁰⁴ Chataigner et al. 2014.

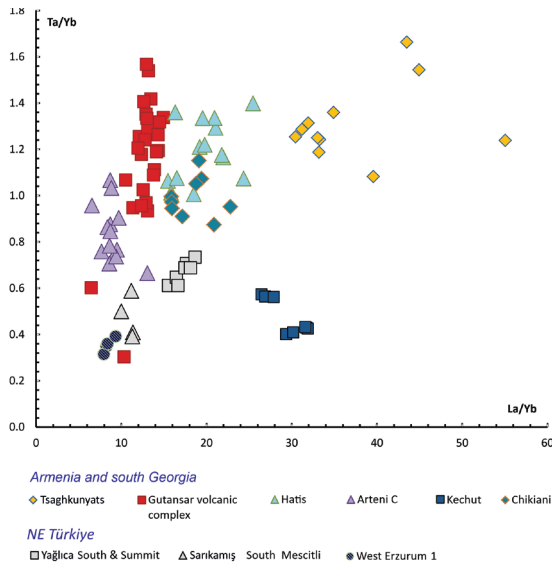


Fig. 34 La/Yb versus Ta/Yb diagram for the discrimination of obsidians of Group I of Armenia and northeastern Türkiye (graphics: K. Meliksetian)

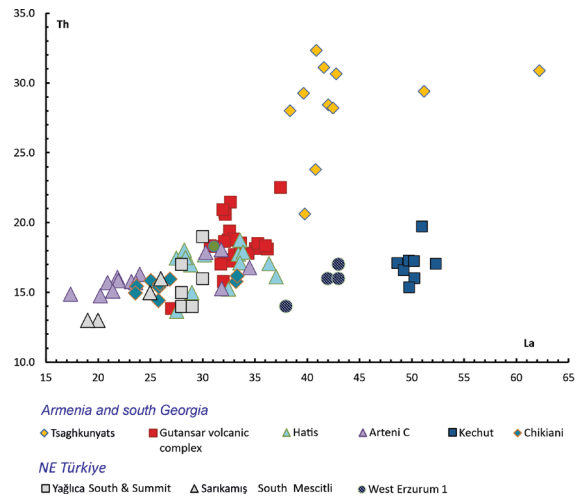


Fig. 35 La versus Th for Armenian and NE Anatolian Group I obsidian sources. Yağlıca South and Yağlıca Summit and Sarıkamış South Mescitli completely overlap with Hatis, Chikiani and Arteni C (graphics: K. Meliksetian)

Discrimination of Group I Armenian and Northeastern Anatolian Sources

After this initial grouping, we attempted to further fingerprint the obsidian sources of northeastern Türkiye using the same scheme developed for Armenian obsidians. The diagram La/Yb versus Ta/Yb (Fig. 34) provides relatively good discrimination from the Armenian and the Chikiani obsidians (Group I), but it turned out that on other diagrams such as La versus Th (Fig. 35), previously used for additional discrimination of Group I sources, these sources overlap. This holds particularly true for the Sarıkamış South Mescitli obsidians and also for the Yağlıca source, which is geochemically and geographically close to Arteni C, located in the western part of Armenia. But in the diagram Ta/Yb versus Zr/Ta, these northeastern Anatolian sources and the Armenian and Georgian Group I obsidians can be clearly separated (Fig. 36).

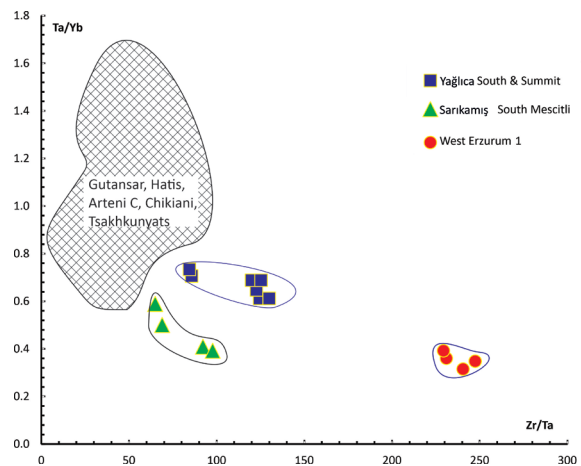


Fig. 36 Zr/Ta versus Ta/Yb diagram for the discrimination of Armenian and Georgian and NE Anatolian Group I obsidians (the Kechut source is not shown due to high, out of scale Zr/Ta ratios, but Kechut clearly exhibits a different geochemical pattern and is not overlapping in other diagrams) (graphics: K. Meliksetian)

Discrimination of Group II Armenian and Northeastern Anatolian Sources

As mentioned above, based on the discrimination with a Ba*La versus Th*U diagram (Fig. 33), the following obsidians of northeastern Anatolia plot with the Low Ba type (Group II): West Erzurum 2, South Erzurum, Pasinler, Sarıkamış Kizil Kilisa and Sarıkamış North Hamamlı. For further discrimination we use the La/Yb versus Ta/Yb diagram (Fig. 37), where Armenian

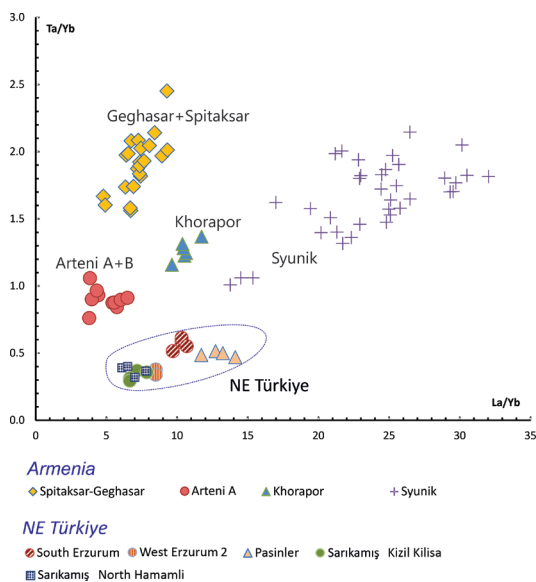


Fig. 37 La/Yb versus Ta/Yb diagram for Group II sources of Armenia and northeastern Türkiye (graphics: K. Meliksetian)

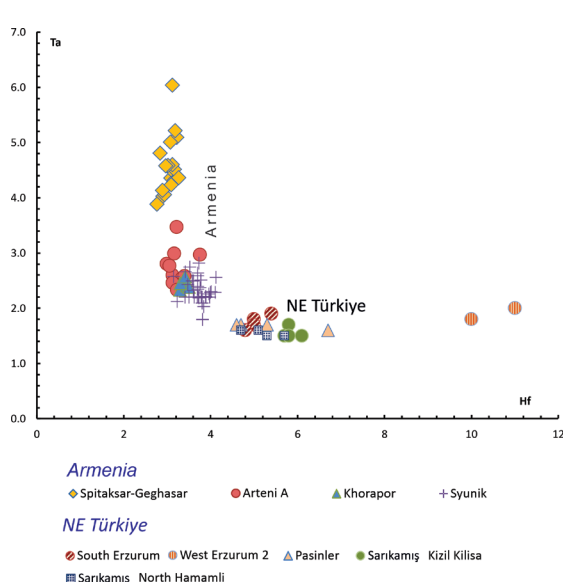


Fig. 38 Hf versus Ta diagram for the discrimination of obsidians of Group II of Armenia and northeastern Anatolia. Armenian and NE Anatolian obsidians are clearly separated (graphics: K. Meliksetian)

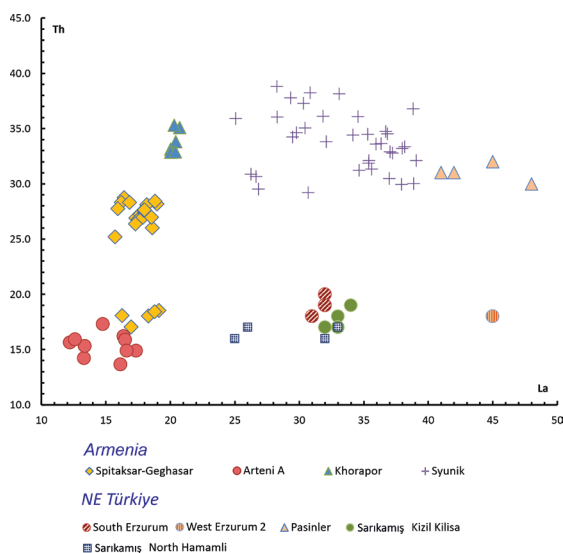


Fig. 39 La versus Th diagram for the discrimination of obsidians of Group II of Armenia and northeastern Türkiye. Armenian and NE Anatolian obsidians are separated. The diagram also provides discrimination of West Erzurum 2 and Pasinler from other Group II obsidians, while the data points of both Sarikamiş sources and south Erzurum still overlap (graphics: K. Meliksetian)

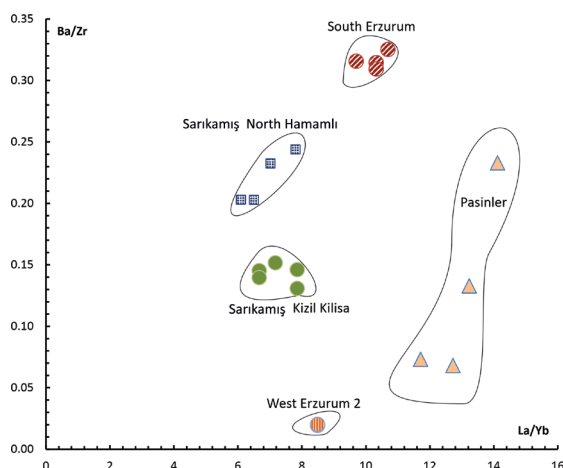


Fig. 40 La/Yb versus Ba/Zr diagram for the discrimination of geochemically similar obsidians of Group II of northeastern Türkiye, namely the South Erzurum, West Erzurum 2, Sarikamiş Kizil Kilisa, Sarikamiş North Hamamlı and Pasinler sources. Armenian obsidians of Group II are not shown due to greater variations of the ratios (graphics: K. Meliksetian)

obsidian sources of Group II are clearly separated from those of northeastern Anatolia. Good discrimination of Armenian and northeastern Anatolian obsidians is also provided by the Ta versus Hf diagram (Fig. 38). But none of these diagrams allow a discrimination of Anatolian Group II obsidians, since their data points group into a narrow field. The diagram La versus Th (Fig. 39) provides discrimination of Armenian and northeastern Anatolian obsidians and also a differentiation of West Erzurum 2 and Pasinler from other Group II obsidians, while the data points of both Sarikamiş sources and South Erzurum still overlap.

Finally, the La/Yb versus Ba/Zr diagram (Fig. 40) can be used for the discrimination of the geochemically similar obsidians of Group II of northeastern Türkiye, namely South Erzurum, Sarıkamış Kilzil Kilisa, and Sarıkamış North Hamamlı. This diagram also helps to distinguish the West Erzurum 2 and Pasinler sources from other Group II Anatolian sources.

New Data and Unknown Geochemical Groups

Previous studies¹⁰⁵ touched upon unknown sources identified among obsidian artefacts from Armenia. As mentioned above, six geochemical groups were identified and designated as TCUNK (Transcaucasian unknown)¹⁰⁶ and their average compositions determined by INAA were provided. It was suggested that the groups TCUNK 1–6 represent unsampled/unstudied obsidian sources in Armenia or further west in northeastern Anatolia. It was furthermore suggested that the possible localization of the sources TCUNK 1 and TCUNK 2 may be indicated by their geographical distribution in archaeological sites in the southern Caucasus,¹⁰⁷ mostly recorded in settlements of the Shirak Plain in northwestern Armenia. Since this region of Armenia borders with the Kars Plateau in Türkiye, it was concluded that TCUNK 1 and TCUNK 2 may be located near the Shirak Plain on the Kars Plateau in northeastern Türkiye. In this section

we discuss some geochemical features of the TCUNK 1–6 groups, attempting to relate them to our geochemical database and to the sources of northeastern Türkiye.¹⁰⁸

The first attempt to divide the TCUNK groups into Group I and Group II (Fig. 33) showed that all unknown geochemical groups belong to the high Ba type and can be assigned to Group I of the Armenian and northeastern Anatolian obsidians. Further comparison using La/Yb versus Ta/Yb diagram (Fig. 41) clearly demonstrates that TCUNK 1 belongs to the source named Yağlıca South.¹⁰⁹ Source TCUNK 2 geochemically clearly resembles the West Erzurum 1 source described by the same authors, if one considers the contents of REE, Ta, Rb, Cs, Th, U, with some notable differences in the concentrations of Ba, Zr and Hf, possibly related to an inhomogeneity of the source and/or different analytical methods.¹¹⁰ Thus, the hypothesis that TCUNK 1 and TCUNK 2 are located on the Kars-Erzurum Plateau in northeastern

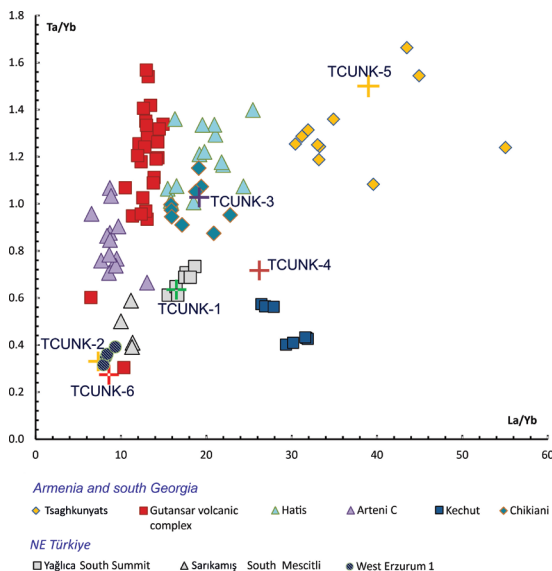


Fig. 41 La/Yb versus Ta/Yb diagram for Group I obsidian sources of Armenia, Georgia (Chikiani), obsidians of northeastern Türkiye, in comparison with TCUNK groups after Blackman et al. 1998 (graphics: K. Meliksetian)

¹⁰⁵ Blackman et al. 1998; Badalyan et al. 2004; Badalyan 2010.

¹⁰⁶ Blackman et al. 1998. Surprisingly, there is a mistake in Appendix E, page 231. TCUNK 1, 2, 3, 4, 6, and 7 are listed in the table (but not TCUNK 5!). However, in the text and the diagrams TCUNK 1–5 are discussed, and there is no indication of TCUNK 6 and 7! Detailed analysis of this table and the TCUNKs plotted in the diagrams lead us to the conclusion that TCUNK 6 /table is actually TCUNK 5, and we consider TCUNK 7/table as TCUNK 6, because the TCUNKs are numbered from 1 to 6 in the text.

¹⁰⁷ Badalyan 2010.

¹⁰⁸ Chataigner et al. 2014.

¹⁰⁹ Chataigner et al. 2014.

¹¹⁰ Blackman et al. 1998; Chataigner et al. 2014.

Türkiye¹¹¹ can now be confirmed and these sources can be identified as the Yağlıca South and West Erzurum 1 sources. It turned out that the average composition of TCUNK 3 matches geochemically the Hatis source, as can be concluded from the La/Yb versus Ta/Yb diagram (Fig. 41) and from Hf versus Sc (Fig. 42).

The trace element pattern of TCUNK 4 remains unidentified, although it shows some geochemical similarities with the Chikiani and Kechut sources, but is different with regard to the high concentrations of the light REE.

The geochemical characteristics of the TCUNK 5 source closely resemble those of our set of samples from the Tsaghkunyats ridge. Obsidians from this source have been found at several locations and are geochemically similar, although with some variations. Accordingly, we suggest identifying TCUNK 5 with the Tsaghkunyats source, taking into account specific geochemical features like the high content of Ba (920 µg/g in TCUNK 5 compared to 700–1200 µg/g in Tsaghkunyats obsidians), Th (31.7 µg/g in TCUNK 5 compared to 20–33 µg/g for Tsaghkunyats obsidians), and a well-pronounced enrichment of LREE over HREE (high La/Yb = 39, La/Yb ratios in Tsaghkunyats obsidians – 30–55, average La/Yb=37).

Artefacts identified as TCUNK 6 cannot be attributed to any of the characterized regional sources. Although some geochemical features are similar to Gutansar or West Erzurum, the concentrations of several important fingerprinting elements like La, Ta, Hf, and Zr are clearly different, so that TCUNK 6 still remains an unknown source.

Distribution of Obsidian from Armenian Sources at Archaeological Sites in the Near East

So far 534 obsidian artefacts from Armenia and other countries (Dagestan, Georgia, Azerbaijan, Iran, Türkiye) have also been analysed in order to study the distribution of obsidian from Armenian sources in different archaeological periods. The data of artefacts from Armenian sites were published in a recent monograph¹¹² and the data from sites outside the territory of the Republic of Armenia are given in the Appendix. The dates of the artefacts cover a wide range from the Palaeolithic to the Early Iron Age. The study is not yet completed and different periods are not adequately sampled, but it may still be worthwhile to present the general tendency of the usage of Armenian obsidian sources in prehistoric times. The same analytical method was applied as for the geological samples described above and the results will be published in due course.¹¹³

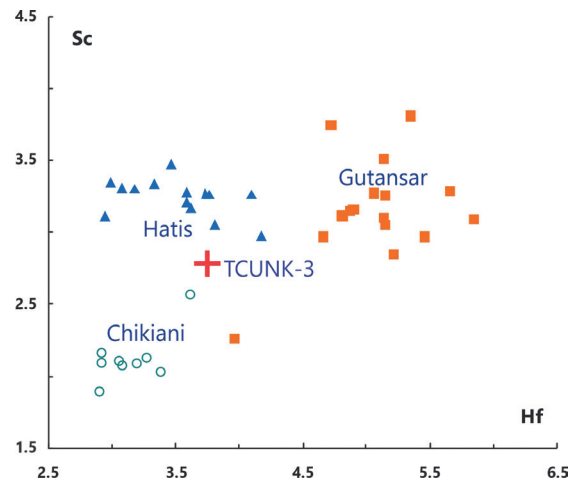


Fig. 42 Hf versus Sc diagram for the discrimination of Hatis, Gutansar, Chikiani and TCUNK 3, which partly overlap on other diagrams, discussed earlier (graphics: K. Meliksetian)

¹¹¹ Badalyan et al. 1996.

¹¹² Badalyan et al. in press.

¹¹³ These data would have extended the length of this article beyond limits, but they are also available on request from the first author.

Gegham Volcanic Upland

Gutansar Volcanic Complex

Obsidian from the Gutansar complex is among the most widely used varieties in the prehistory of the region. Of 534 artefacts analysed in this study, 106 originate from Gutansar. Artefacts that originated from Gutansar were widely used locally¹¹⁴ (Fig. 43), but also exported to distant sites like the Troad: in Troy and at Yenibademli Höyük on the island of Imbros/Gökçeada as well as at Laodicea in Phrygia north of the modern town of Denizli, all dated to the late Chalcolithic or the Early Bronze Age (Fig. 44). Blackman et al. reported two artefacts from Gutansar identified at Tal-i Malyan in Iran.¹¹⁵ Gutansar belongs to Group I; some additional geochemical features are shown in Figs. 29, 31, and 32. It is worth noting that several outcrops and extrusive domes clustered as the Gutansar volcanic complex can be grouped together as a single geochemical source. The typical geochemical features are: average enrichment of light REE over heavy REE (La/Yb ratios are in the range of 10–15); high contents of Ba (340–670µg/g), Zr (83–260µg/g) and Hf (4–5.8µg/g); as well as high average concentrations of Ta, Sc, and La and low concentrations of Th (13–22µg/g). The concentrations of uranium vary in a narrow range of 7–10µg/g in most of the samples. The geochemical indicator with the largest spread is Ba/Rb, which varies from 2 to 6, while in many other Armenian sources this ratio is less than 1.

Artefacts that can be related to Gutansar can easily be identified with the initial classification using the diagrams Th versus Ba and Th*U versus Ba*La (Fig. 28) and further by the diagrams Ta/Yb versus Th/Yb (Fig. 34), Th versus La (Fig. 36), La/Yb versus Var A (Fig. 29.c), Fe/Sc versus Var A, (Fig. 29.d) and additionally, if required to distinguish from Hatis and Chikiani, by Hf versus Sc (Fig. 31.a), Sc versus Ta (Fig. 31.b), and Zr versus Hf (Fig. 32). Table 3 provides a list of artefacts that could be related to the Gutansar volcanic source.

Site	Dating	Country	Number of artefacts
Norabats	EBA	Armenia	20
Aratashen	Late Neolithic	Armenia	16
Shengavit	EBA	Armenia	15
Aknashen	Late Neolithic	Armenia	12
Voskeblur	EBA	Armenia	10
Apnagyugh-8 / Kmlo-2 Cave	Mesolithic/Early Neolithic	Armenia	6
Metsamor	EBA	Armenia	5
Armavir	EBA	Armenia	4
Artashat	Chalcolithic	Armenia	3
Berdshen	MBA	Armenia	3
Troy	EBA	Türkiye	2
Verin Naver	MBA	Armenia	2
Dvin	EBA	Armenia	1
Fioletovo	EBA	Armenia	1
Gegharot	EBA	Armenia	1
Tsaghkassar	EBA	Armenia	1
Yenibademli Hoyuk	EBA	Troad, Türkiye	1
Padar	EBA	Azerbaijan	1
Norabak-1	EBA–MBA?	Armenia	1
Shavruk	EBA–MBA?	Armenia	1
Total			106

Table 3 List of obsidian artefacts originating from Gutansar (EBA = Early Bronze Age, MBA = Middle Bronze Age)

¹¹⁴ Badalyan et al. 2004.

¹¹⁵ Blackman et al. 1998.

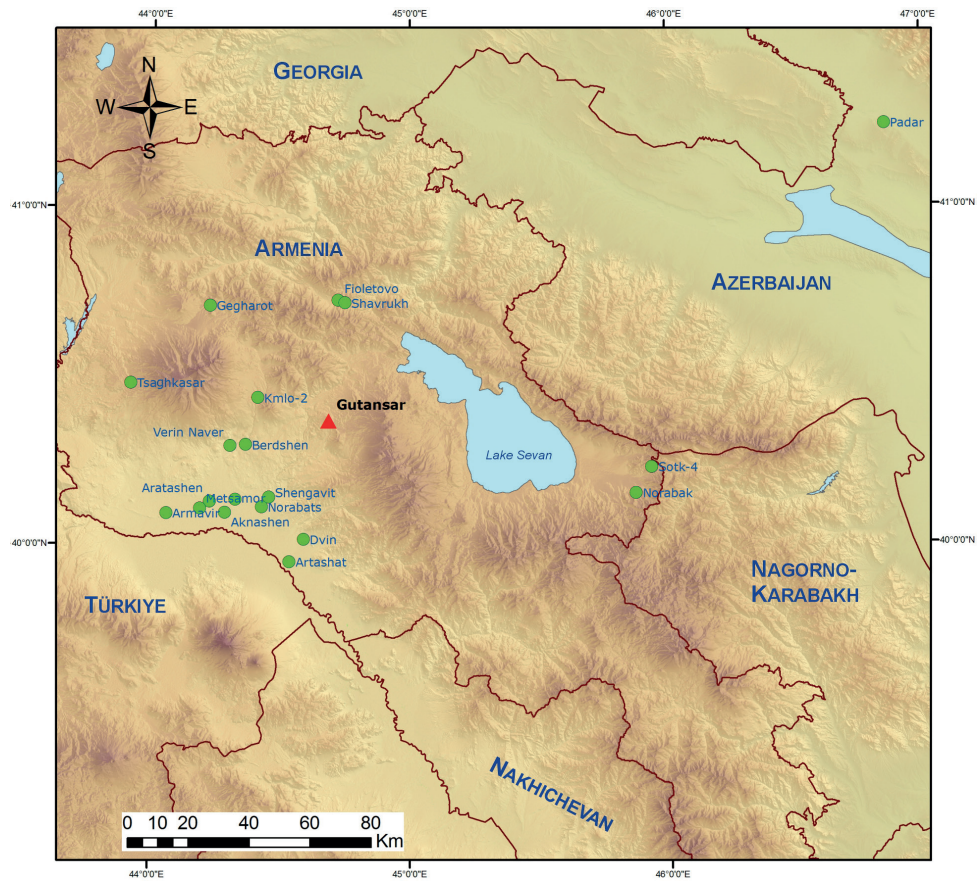


Fig. 43 Regional distribution of obsidian from Gutansar (red triangle) within archaeological sites (green circles) of the southern Caucasus (graphics: K. Meliksetian)



Fig. 44 The regional distribution of obsidian shows that obsidian from Gutansar is found at large distances from the source, namely in Troy and Yenibademli Höyük (the Troad, northeastern Aegean) and in Tal-i-Malyan, Iran (Tal-i-Malyan analysis after Blackman et al. 1998) (graphics: K. Meliksetian)

The geographical distribution of archaeological obsidian originating from Gutansar is displayed in Figs. 43 and 44.

Hatis

Obsidian from Hatis is classified in Group I and is geochemically very close to obsidian from the Gutansar volcanic complex, but can be distinguished by somewhat higher La/Yb ratios and lower Ta and Hf concentrations (see Figs. 27.a, 31.a, 31.b). Among the artefacts analysed in this study, we identified nine artefacts from Hatis within regional archaeological sites in the Ararat Valley.

Spitaksar and Geghasar

These two sources are geochemically very similar, and considering their geographical proximity, they can be combined and considered as one obsidian source. This viewpoint is also consistent with earlier data.¹¹⁶ The only notable distinction between Spitaksar (5 analyses) and Geghasar (18 analyses) is a somewhat lower content of Th in Spitaksar obsidian, but it is not known if this is a general characteristic of Spitaksar or only of the five samples analysed. Spitaksar and Geghasar belong to Group II and are clearly separated from all other Caucasian and Anatolian sources by high Ta (3.9–6 μ g/g). Similar or even higher concentrations of Ta are found only in the peralkaline sources of Nemrut in southeastern Anatolia. Another distinguishing geochemical feature is the relatively low enrichment of LREE over HREE (La/Yb=4.8–9.3). Obsidian from Spitaksar and Geghasar is easily distinguished from other sources in Group II by the clustering of artefacts in the following diagrams: Ta/Yb versus Th/Yb (Fig. 30.a), La versus Th (Fig. 30.c), Var A versus La/Yb (Fig. 30.b), Var A versus Fe/Sc (Fig. 30 d) and Sc versus Ta (Fig. 45). Artefacts from

Site	Dating	Country	Number of artefacts
Kanagegh	LBA	Armenia	6
Artashat	Chalcolithic	Armenia	5
Leila Tepe	Chalcolithic	Azerbaijan	4
Artefacts from Tehran National Museum	unknown	Iran	3
Chkalovka	EBA	Armenia	2
Fioletovo	EBA	Armenia	2
Norabats	EBA	Armenia	2
Kol Par	EBA–HL?	Armenia	2
Tsovak-1	EBA–HL?	Armenia	2
Aygevan	EBA	Armenia	1
Camay	EBA	Azerbaijan	1
Apnagyugh-8 / Kmlo-2 Cave	Mesolithic/Early Neolithic	Armenia	1
Metsamor	EBA	Armenia	1
Padar	EBA	Azerbaijan	1
Velikent	EBA	Dagestan, Russia	1
Norabak-3	EBA–MBA?	Armenia	1
Sotk1	EBA	Armenia	1
Norabak-1	EBA–MBA?	Armenia	1
Sotk4	EBA–LBA/EIA	Armenia	1
Total			31

Table 4 List of obsidian artefacts originating from Geghasar and Spitaksar (EBA = Early Bronze Age, MBA = Middle Bronze Age, LBA = Late Bronze Age, EIA = Early Iron Age, HL = Hellenistic)

¹¹⁶ Keller et al. 1996.

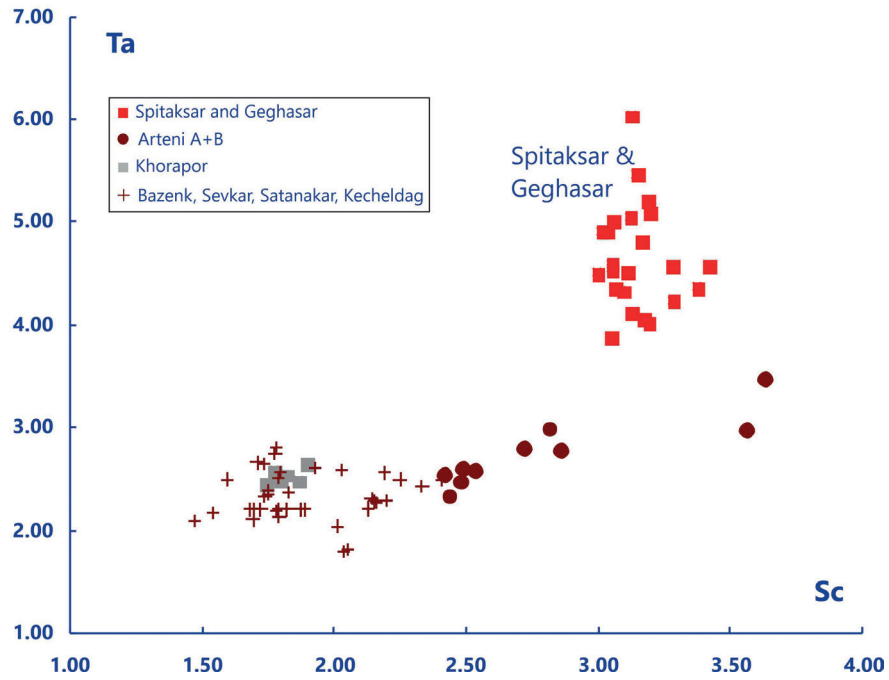


Fig. 45 Sc versus Ta diagram for the discrimination of Spitaqsar and Geghasar from other Group II obsidians (graphics: K. Meliksetian)

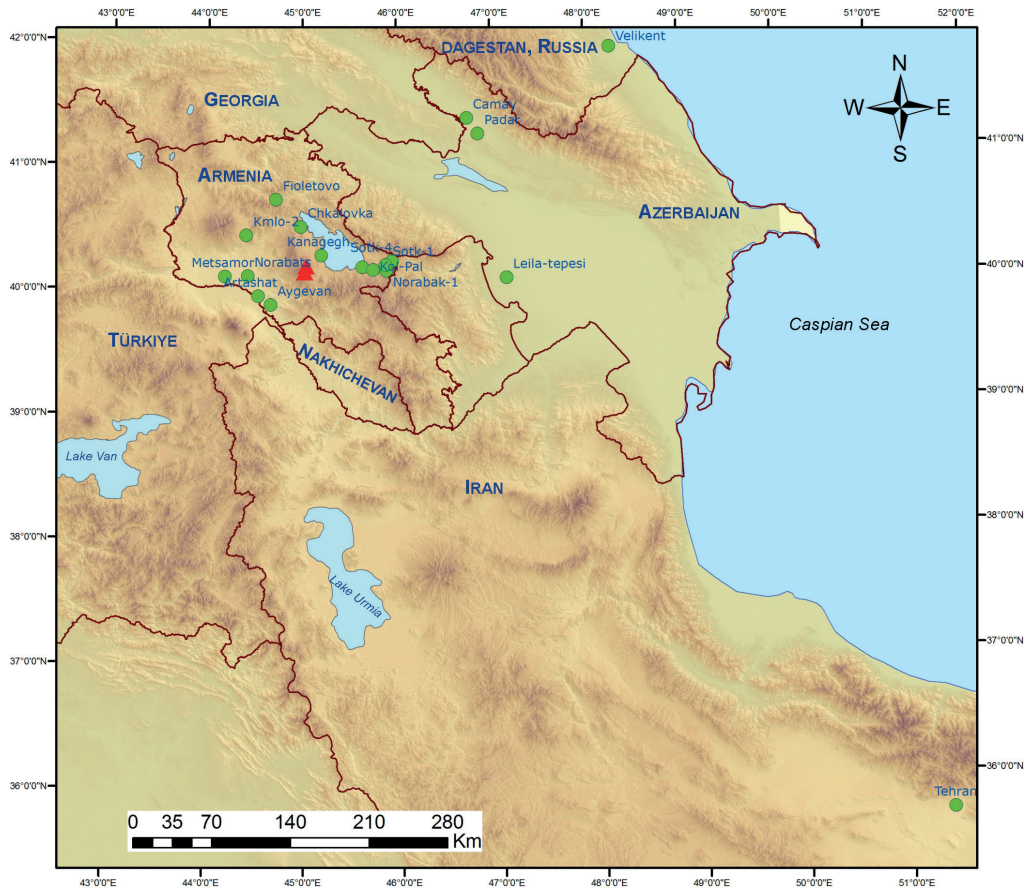


Fig. 46 Regional distribution of archaeological sites (green circles) with obsidian artefacts deriving from the Geghasar and Spitaqsar sources (red triangles) (graphics: K. Meliksetian)

Geghasar and Spitaksar were found to be used not only locally, but also quite far from the sources at sites in Iran and Dagestan, as indicated in Fig. 46 and in Table 4. A single sample deriving from Geghasar found in Velikent in Dagestan, Russia, was also previously identified by Blackman.¹¹⁷

Aragats Volcanic Province

As was mentioned above, the Arteni volcanic complex consists of two major volcanic domes, Mets Arteni and Pokr Arteni and lava flows related to them, as well as of a few smaller domes. Keller and co-workers distinguished three sources at Arteni, A, B and C, mentioning that Arteni A and Arteni B are quite similar.¹¹⁸ Our data confirm this division, and we consider Mets Arteni as Arteni (A+B) and Pokr Arteni as well as the Aragats flow as Arteni C.

In spite of their geographical proximity and similar geological structure, obsidians from Mets and Pokr Arteni exhibit significant differences in their geochemistries. The Pokr Arteni and Aragats flows belong to Group I and are characterized by relatively high Ba (330–500 µg/g) and La (17–34 µg/g), and a high level of LHREE enrichment over HREE (La/Yb = 6.6–13.1), while obsidian found on the slopes of the Mets Arteni volcano in the form of blocks and dykes is classified as Group II and is low in Ba, La and REE in general, but a little higher in Rb (120–170 µg/g) compared with the Pokr Arteni and Aragats flows. It is noteworthy that in spite of the fact that the Aragats flow erupted from Mets Arteni, it still belongs to Group I (samples MA-114713, MA-114715, MA-114714). The enrichment of LREE over HREE in Mets Arteni (La/Yb = 3.8–6.5) is much lower than in samples from Pokr Arteni and the Aragats flow (6.6–13.1). Most likely the geochemical variations indicate age relationships and demonstrate the evolution of the magma chamber, (or the presence of two different magma sources) rather than just a simple geographic division between Mets Arteni and Pokr Arteni. Unfortunately, a detailed geochemical and age mapping is missing, and it is not possible to link all usable obsidian outcrops to their geochemistries and ages.

Site	Dating	Country	Number of artefacts
Anushavan	EBA	Armenia	48
Aknashen	Late Neolithic	Armenia	20
Harich	EBA	Armenia	18
Metsamor	EBA	Armenia	10
Tsaghkasar	EBA	Armenia	8
Apnagyugh-8 / Kmlo-2 Cave	Mesolithic/Early Neolithic	Armenia	7
Lanjik	EBA	Armenia	7
Armavir	EBA	Armenia	6
Lusakhyur	EBA	Armenia	4
Aratashen	Late Neolithic	Armenia	3
Shengavit	EBA	Armenia	3
Shavrukh	EBA–MBA	Armenia	2
Karmrakar	EBA	Armenia	2
Teghut	Chalcolithic	Armenia	1
Verin Naver	MBA	Armenia	1
Velikent	EBA	Dagestan, Russia	1
Total			141

Table 5 Artefacts analysed in this study originating from the Mets and Pokr Arteni sources (EBA = Early Bronze Age, MBA = Middle Bronze Age)

¹¹⁷ Gadzhiev et al. 2000.

¹¹⁸ Keller et al. 1996.

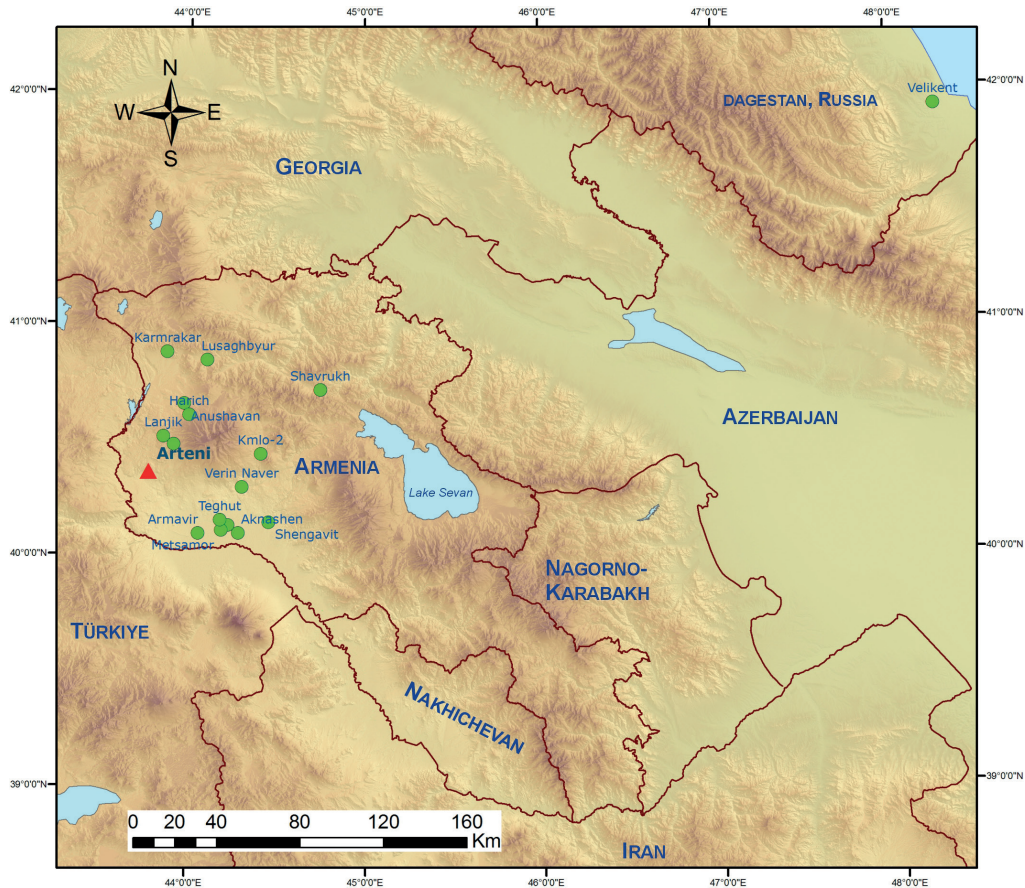


Fig. 47 Geographical distribution of archaeological sites (green circles) with obsidian artefacts deriving from the Arteni sources (red triangle) (graphics: K. Meliksetian)

After initial grouping into Group I (Arteni C) and Group II (Arteni A+B), artefacts originating from Arteni can be recognized and distinguished from other sources using the Ta/Yb versus Th/Yb diagram (Fig. 29.a for Group I and Fig. 30.a for Group II) and La/Yb versus Var A (Fig. 29.c for Group I and Fig. 30.b for Group II). As some Arteni C samples exhibit some overlap with Gutansar, we also refer to the Zr versus Hf diagram (Fig. 32) for their division. Obsidian from both Arteni sources was widely used at regional sites, but it was also recognized at quite distant sites in northern Azerbaijan and at Velikent in Dagestan, Russia. Previously, a single sample of obsidian from Velikent, Dagestan, was identified by Blackman¹¹⁹ as deriving from Arteni, as was another one at Tal-i Malyan in Iran.¹²⁰ Table 5 lists the archaeological sites and number of artefacts originating from both Arteni sources, and the map on Fig. 47 shows the geographical distribution of obsidian from the Arteni sources.

Kechut-Javakheti Volcanic Plateau

Obsidian from Kechut (Ashotsk), represented by two identical subsources, Sizavet and Agvorik in northwestern Armenia, close to the border with Türkiye and Georgia, exhibits some noteworthy geochemical characteristics and can easily be distinguished from all other sources: First of all, it

¹¹⁹ In Gadzhiev et al. 2000.

¹²⁰ Blackman et al. 1998.

Site	Dating	Country	Number of artefacts
Udabno	LBA	Georgia	18
Tsikhiagora	EBA	Georgia	8
Camay	EBA	Azerbaijan	7
Minberek	EBA	Azerbaijan	5
Kurdulu	MBA	Azerbaijan	3
Padar	EBA	Azerbaijan	3
Tachtiperda	LBA	Georgia	3
Berdshen	MBA	Armenia	1
Derbent	EBA	Dagestan, Russia	1
Metsamor	EBA	Armenia	1
Tsaghkasar	EBA	Armenia	1
Verin Naver	MBA	Armenia	1
Margahovit	EBA	Armenia	1
Aibasan	MBA?	Armenia	1
Velikent	EBA	Dagestan, Russia	1
Total			55

Table 6 List of obsidian artefacts originating from the Chikiani source (EBA = Early Bronze Age, MBA = Middle Bronze Age, LBA = Late Bronze Age)

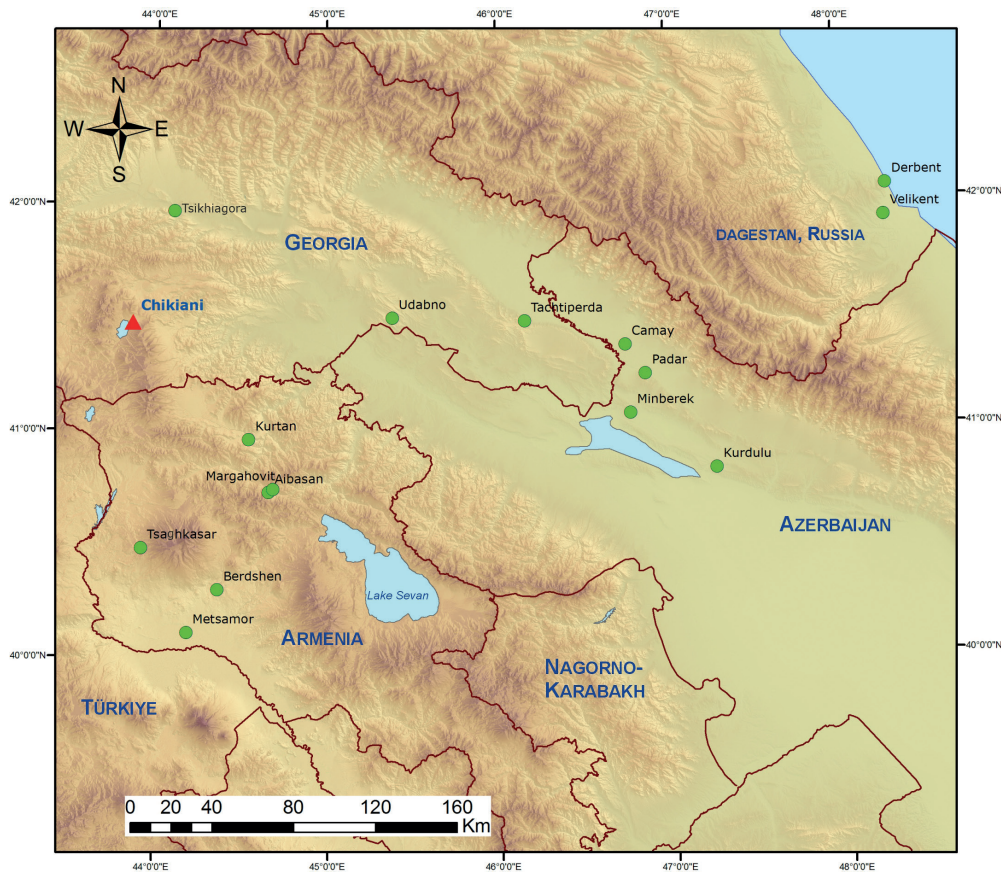


Fig. 48 Geographical distribution of archaeological sites (green circles) with obsidian artefacts deriving from the Chikiani source (red triangle) (graphics: K. Meliksetian)

is classified as Group I (Fig. 28) and is characterized by high Ba (800–1200 $\mu\text{g/g}$) and extremely low Ta (0.68–1.13 $\mu\text{g/g}$) and U (3.15–3.9 $\mu\text{g/g}$) contents. The only similarity to the neighbouring Chikiani source in southern Georgia is a high Ba content, but almost all other elemental

concentrations and geochemical indicators exhibit clear division of Chikiani and Kechut sources (see Fig. 29). The Kechut sources were not widely utilized in prehistory: only three artefacts have been identified as originating from Kechut, namely two artefacts from the neighbouring Ketu site in Armenia and one from Tachtiperda in Georgia.

Contrary to Kechut, the Chikiani source is one of the most widely utilized sources of obsidian in the prehistory of the entire region. Obsidian from Chikiani is found at dozens of archaeological sites in Georgia, Azerbaijan, Armenia¹²¹ and Velikent, Dagestan.¹²² The principal geochemical feature of Chikiani (Group I source), exactly as described before,¹²³ is its high Ba content (400–1050 µg/g). The set of samples analysed in this study confirms this feature, but it may be worth noting that obsidian from Kechut exhibits similar and even higher Ba concentrations. However, other geochemical indicators allow us to unequivocally distinguish between Chikiani and Kechut. Although the concentrations of Ta, Sc, Zr, Rb REE, and the La/Yb ratio of Chikiani obsidian exhibits some overlap with other Ba-rich sources such as Gutansar and Hatis, it can easily be distinguished by using Sc versus Ta and Hf versus Sc diagrams (Fig. 31). Table 6 lists a number of artefacts and archaeological sites where Chikiani artefacts have been recognized, and the map in Fig. 48 shows the geographical distribution of these archaeological sites.

Tsaghkunyats Ridge

The obsidian sources at the Damlik and Kamakar domes on the Tsaghkunyats ridge belong to Group I and are characterized by high Ba (714–1250 µg/g) and relatively high REE concentrations, but due to very high La/Yb ratios (30–55) they can clearly be separated from other sources high in Ba and REE such as Chikiani, Gutansar or Hatis. Other noteworthy geochemical fingerprints of these sources are the highest Th, slightly higher U and lowest Sc contents among Group I obsidians. Discrimination of the Tsaghkunyats sources from others is generally a very simple task, and after initial grouping, it can be achieved by using the diagrams Ta/Yb versus La/Yb (Fig. 29.a), La versus Th (Fig. 29.b), Var A versus La/Yb (Fig. 29.c) with sources of Group I.

Table 7 and Fig. 49 show the distribution and the number of artefacts analysed in this study and recognized as originating from the sources of Tsaghkunyats ridge.

Site	Dating	Country	Number of artefacts
Gegharot	EBA	Armenia	6
Fioletovo	EBA		4
Berdshen	MBA		3
Rya-Taza	Middle Palaeolithic		3
Harich	EBA		2
Apnagyugh-8 / Kmlo-2 Cave	Mesolithic/Early Neolithic		2
Kuchak	EBA		2
Gruzinskaya gorochka	LBA/EIA-MA?		2
Aratashen	Late Neolithic		1
Artashat	Chalcolithic		1
Norabats	EBA		1
Total			27

Table 7 List of obsidian artefacts originating from the Tsaghkunyats ridge (EBA = Early Bronze Age, MBA = Middle Bronze Age, LBA = Late Bronze Age, EIA = Early Iron Age, MA = Middle Ages)

¹²¹ Badalyan et al. 2004.

¹²² This study; Gadzhiev et al. 2000.

¹²³ Keller et al. 1996; Blackman et al. 1998.

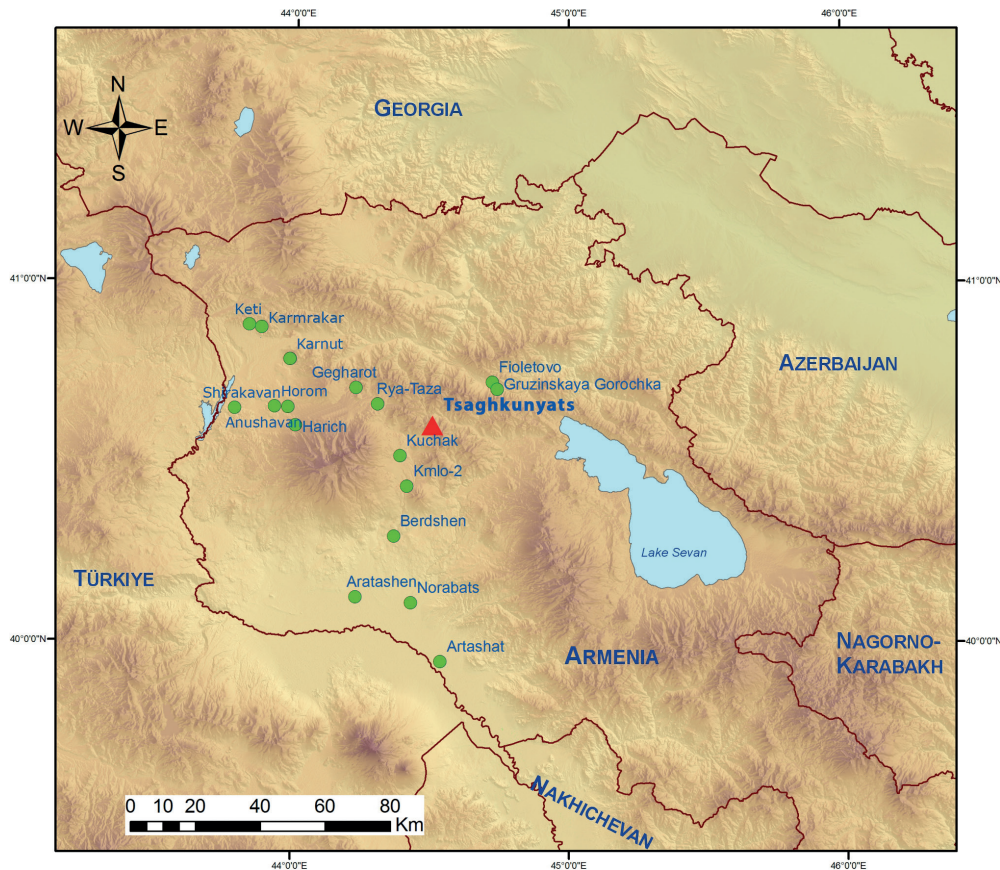


Fig. 49 Geographical distribution of archaeological sites (green circles) with obsidian artefacts deriving from the Tsaghkunyats source (red triangle) (graphics: K. Meliksetian)

Vardenis Volcanic Upland

On the Vardenis volcanic upland only a single source of obsidian is known, at Khorapor. It belongs to Group II with the following specific geochemical features: compared with Geghasar and Spitaksar, a relatively high enrichment of LREE over HREE ($La/Yb = 9.6-11.7$) as well as high U ($14.5-17.2\mu\text{g/g}$), comparable to Geghasar and Spitaksar, and high Th ($33.3-35.5\mu\text{g/g}$), comparable to obsidians from Syunik. The concentration of Ba is low, as for most Group II obsidians ($27-100\mu\text{g/g}$). The following diagrams allow us to differentiate Khorapor obsidian from other Group II sources: Ta/Yb versus La/Yb (Fig. 30.a), La versus Th (Fig. 30.c), Var A versus La/Yb (Fig. 30.b). The concentrations of some elements in obsidians from Khorapor are similar to those from Syunik, but Khorapor is characterized by lower LREE and higher HREE concentrations and consequentially by significantly lower La/Yb or La/Lu and Ce/Yb ratios.

So far, obsidian from this source was not identified among earlier analysed artefacts and thus, Khorapor was ruled out as a source of obsidian in prehistory.¹²⁴ Besides the absence of artefacts that match Khorapor geochemically, this conclusion was also based on the fact that obsidian from Khorapor contains abundant inclusions of plagioclase and is inferior in quality compared to other South Caucasian sources. But it is noteworthy that among obsidian artefacts and fragments collected during an archaeological survey within the framework of an Armenian-German geoarchaeological project, two samples from Tsovak 1 and Kol Par in the Sotk region were undoubtedly identified as material from the geographically closest Khorapor source (Table 8).¹²⁵

¹²⁴ Badalyan 2010; Blackman et al. 1998.

¹²⁵ Kunze et al. 2013.

Site	Dating	Country	Number of artefacts
Tsovak-1	EBA–HL	Armenia	1
Kol Par	EBA–HL		1
Total			2

Table 8 List of artefacts originating from the Khorapor volcano, Vardenis upland (EBA = Early Bronze Age, HL = Hellenistic)

Field observations assuming that artefacts with abundant plagioclase phenocrysts may originate from Khorapor have been securely confirmed by geochemical fingerprinting. It seems that the low-quality obsidian from Khorapor was nevertheless used in prehistoric times due to the proximity and easy access of the source. More recently, the presence of obsidian from Khorapor was reported in Mentesh Tepe, northwestern Azerbaijan¹²⁶ and Kultepe, Julfa, northwestern Iran.¹²⁷

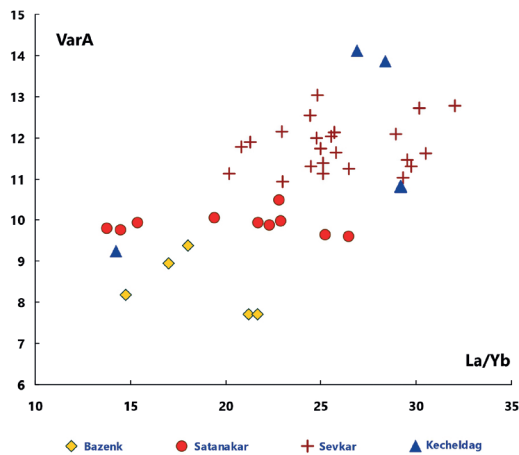
Syunik Volcanic Upland

Several sources of obsidian, namely Sevkar, Mets Satanakar, Pokr Satanakar, Michnek Satanakar, Kecheldag and Bazenk are known in the northern part of the Syunik volcanic upland and are located in geographical proximity to each other. All of them are located within a relatively small area of about 130km², while the distance between two outer sources does not exceed 20km. Samples analysed for this study originate from Sevkar, Mets Satanakar and Bazenk, some rare analyses from the Kecheldag source are available in the literature.¹²⁸ All sources in the Syunik highland cluster geochemically into Group II and plot together in all diagrams, forming an extended compositional field, but clearly separated from all other sources. The principal geochemical features of Syunik obsidian are: low Ba (15–121µg/g) and Sc (1.6–2.4µg/g) contents, high Rb (154–223µg/g) and relatively high LREE contents, high Ta/Yb and La/Yb ratios.

Artefacts originating from the Syunik highland can be easily distinguished from other Group II sources using the diagrams Ta/Yb versus La/Yb (Fig. 30.a), Th versus La (Fig. 30.c) and Var A versus La/Yb (Fig. 30.b), although some variability in La and other REE and in the La/Yb ratio is typical, but these differences cannot always be attributed to diverse sources.

We also attempted to adequately differentiate the Syunik sources from each other using the diagrams La versus Th, and La/Yb versus Var A using separate symbols for each Syunik source, as is shown in Fig. 50.

For sources with a large number of analyses, such as Mets Satanakar, Bazenk, and Sevkar, some clear differences can be observed and whenever possible, we can relate artefacts to these sources. But the geochemistry of the Kecheldag source is based on only a few analyses¹²⁹ that do not allow us to



Site	Dating	Country	Number of artefacts
Tehran, National Museum	unknown	Iran	7
Sisian I	MBA	Armenia	6
Leila-tepesi	Chalcolithic	Azerbaijan	6
Sotk-2	EBA	Armenia	3
Kültepe	Chalcolithic	Iran (NW)	2
Karkarer	EIA	Armenia	2
Ravaz	EBA	Iran (NW)	2
Sotk-1	EBA	Armenia	1
Paler	EBA–HL?	Armenia	1
Kol Par	EBA–HL?	Armenia	1
Norabak-1	EBA–MA?	Armenia	1
Norabak-3	EBA–MA?	Armenia	1
Azati Sar	unknown	Armenia	1
Kurdulu	MBA	Azerbaijan	1
Total			33

Table 9 List of artefacts originating from sources on the Syunik highland (EBA = Early Bronze Age, MBA = Middle Bronze Age, LBA = Late Bronze Age, EIA = Early Iron Age, MA = Middle Ages, HL = Hellenistic)

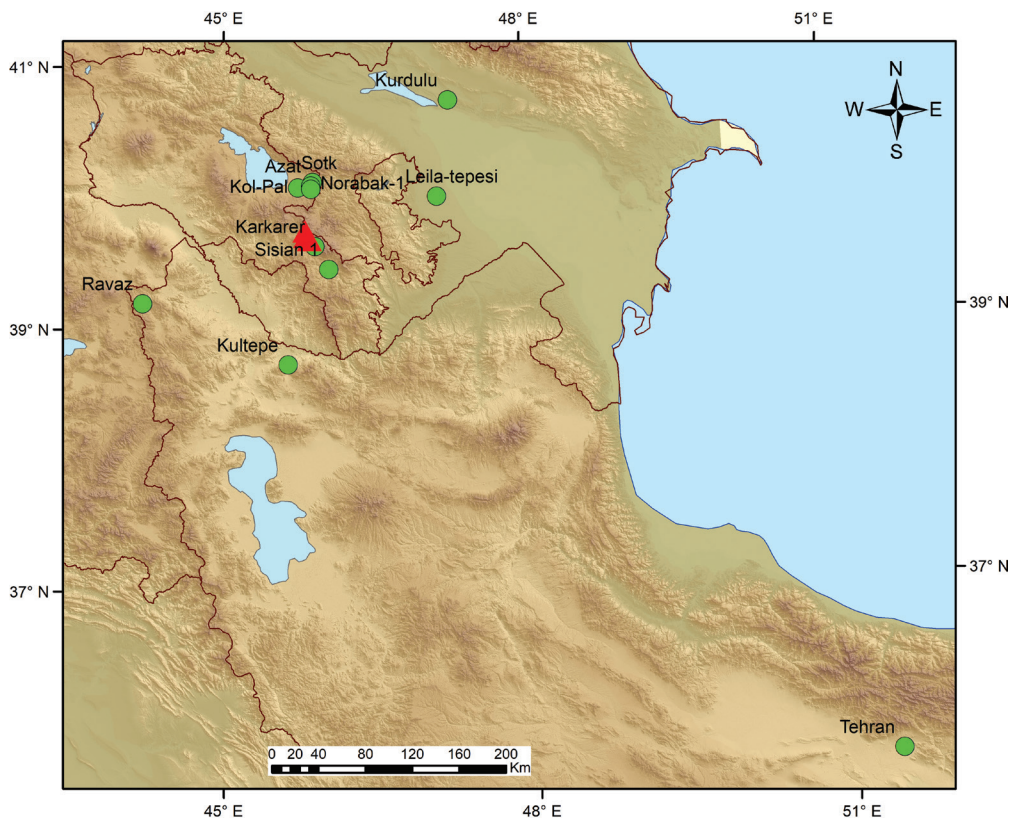


Fig. 51 Geographical distribution of archaeological sites (green circles) with obsidian artefacts deriving from sources of the Syunik volcanic upland (red triangles) (graphics: K. Meliksetian)

adequately distinguish it from other sources on the Syunik upland. With the current number of analyses from Kecheldag, we suggest considering the obsidians from the Syunik upland as a single source. This is also consistent with the geographical distribution of the obsidian sources. Obsidians from the Syunik highland have been recognized at some sites in the Lesser Caucasus

and also in Iran, as is shown on the map in Fig. 51 and in Table 9. It is worth noting that some Iranian artefacts marked as ‘Artefact group B’ with unknown provenance,¹³⁰ are related to sources in the Syunik upland. Somewhat surprisingly, obsidian from the Syunik highland was also found at Laodicea in Phrygia in four Chalcolithic samples and one dated to the Middle Bronze Age. It is further worth noting that Biagi et al.¹³¹ report obsidian originating from Syunik in the archaeological site of Lisaya Gora in the downstream of the Dnieper River, southeastern Ukraine.

Provenance of Iranian Artefacts

No quality sources of obsidian are known in the large territory of the Iranian Plateau. Recently two minor occurrences of obsidian in the Iranian province of East Azerbaijan have been reported in the form of small lenses in Miocene pyroclastics (Tajaraq) and in thin perlite layers (Ghizilja), but it is not known if they were at all usable for tools.¹³² The obsidian at the latter source in particular occurs only in small nodules and is quite friable. Therefore, the provenance of obsidian artefacts found in Iran may provide evidence of and information on long-distance distribution of obsidian. In the framework of this study, 45 archaeological obsidian samples from Iran have been

	Number of artefacts
Ravaz, NW Iran, EBA	
Syunik highland (Armenia)	2
Unknown	1
Tang-e-Bolaghi, SW Iran, Chalcolithic	
Nemrut peralkaline (SE Türkiye)	1
Pasargadae, SW Iran, EBA	
Nemrut peralkaline (SE Türkiye)	1
Kültepe, NW Iran, Chalcolithic	
Syunik highland (Armenia)	2
Samples from Tehran National Museum	
Syunik highland (Armenia)	7
Spitaksar and Geghasar (Armenia)	4
Nemrut peralkaline (SE Türkiye)	2
Tondrak/Tendürek (SE Türkiye)	1
G. Noushabad, Kashan, Late Neolithic/Early Chalcolithic	
Nemrut peralkaline (SE Türkiye)	4
Bingöl B calcalkaline (SE Türkiye)	4
Rahmatabad, Fars, Pre-Pottery Neolithic and Chalcolithic	
Nemrut peralkaline (SE Türkiye)	4
Bingöl B calcalkaline (SE Türkiye)	4
Tappeh Sialk, Kashan, Chalcolithic	
Nemrut peralkaline (SE Türkiye)	1
Sarab, Kermanshah, Neolithic	
Nemrut peralkaline (SE Türkiye)	1
Tappeh Guran, Kermanshah, Neolithic	
Nemrut peralkaline (SE Türkiye)	2
Nemrut peralkaline (SE Türkiye)	1

Table 10 Provenance of Iranian artefacts analysed in this study (EBA = Early Bronze Age)

¹³⁰ Blackman 1984.

¹³¹ Biagi et al. 2014.

¹³² Abedi et al. 2018.

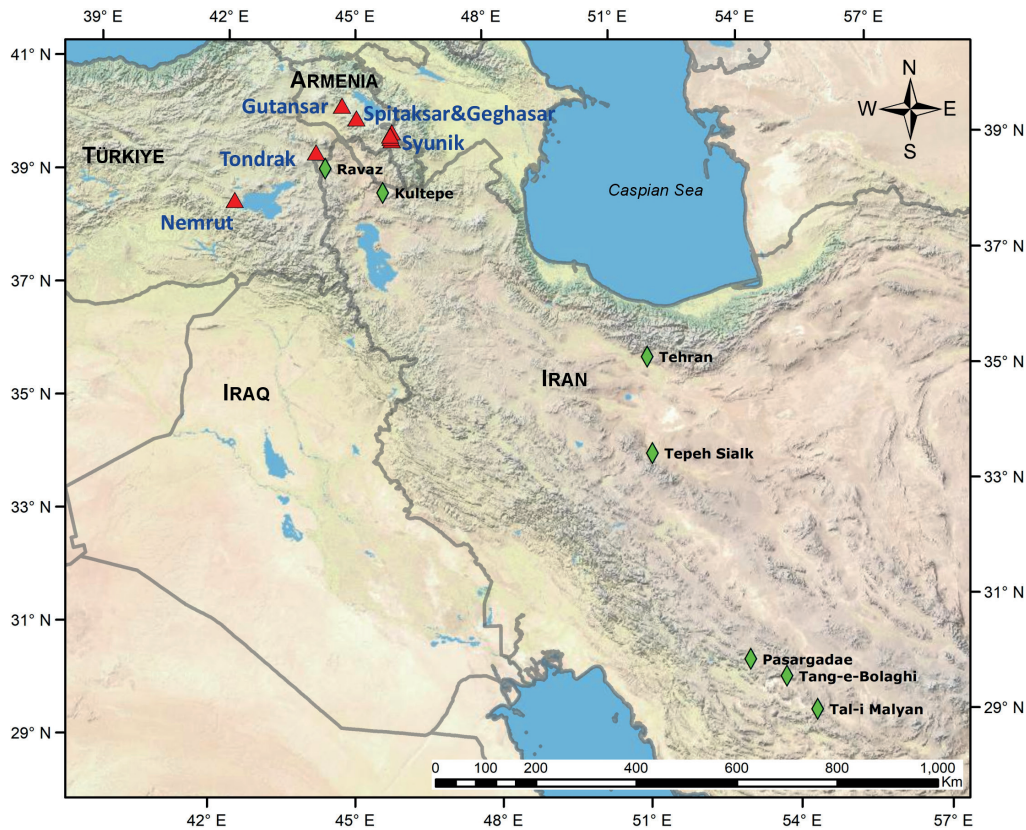


Fig. 52 Provenance of Iranian obsidian artefacts: evidence of long-distance distribution of obsidians from the southern Caucasus and southeastern Türkiye. Obsidian sources: red triangles; green diamonds: Iranian archaeological sites (graphics: K. Meliksetian)

analysed. These samples derive from five archaeological sites (Table 10). Sixteen archaeological Iranian artefacts were obtained from the National Museum of Iran in Tehran, but unfortunately the exact archaeological sources and dates of these artefacts are not known. While the specific archaeological sources of these obsidian samples are not known, it is worth noting that these Iranian archaeological obsidian samples definitely originate from archaeological sites located on the huge Iranian Plateau, with an area of 3,700,000km². This huge region is, in fact, one of the most important areas for prehistoric archaeology of Southwest Asia/the Middle East. But as was mentioned before, the Iranian Plateau is devoid of any obsidian occurrences, while the much smaller area of Armenia and Anatolia contains several dozens of known obsidian-bearing volcanoes and voluminous obsidian occurrences. Therefore, all archaeological obsidian from the Iranian Plateau is imported and thus provides important information on prehistoric obsidian trade and exchange on an interregional scale. The sources of most of the Iranian artefacts have been identified (Table 10). The map on Fig. 52 shows the locations of archaeological sites and sources of obsidian used in Iran.

Regarding the composition of Iranian artefacts analysed earlier, it should be mentioned that for two samples from Tal-i Malyan (Kaftari period, 2400–1800 BC) the artefacts were linked to the Lake Sevan I source.¹³³ However, they in fact derive from the Gutansar source, located on the Yerevan-Sevan highway. It is noteworthy that five artefacts from Tal-i Malyan, identified as ‘Artefact group B’ and marked as ‘provenance unknown’,¹³⁴ were later assumed to originate from

¹³³ Blackman 1984.

¹³⁴ Blackman 1984.

the Sevkar/Satanakar source by the same author.¹³⁵ With an increase in the number of analyses of obsidians from the Syunik highland, we are now able to securely confirm this assumption that the unknown ‘Artefact group B’ definitely relates to the sources on the Syunik upland.

Acknowledgements: The authors are thankful to Kirstin Kasper, who was involved as a PhD student in the initial stages of the project during sampling and analyses of obsidian. Special thanks go to Christine Chataigner, for providing geological and archaeological samples and to colleagues/archaeologists who contributed a number of samples for this study. We dedicate this work to the memory of Sergey Karapetyan (1932–2016), Armenian volcanologist, who enthusiastically studied the acid volcanism of Armenia for many decades and produced the first detailed geological maps of rhyolite volcanoes and obsidian occurrences in Armenia. We gratefully acknowledge the Armenian petrologist and volcanologist Alla Mnatsakanyan (1936–2013), who shared helpful ideas relating to the geochemical characterization and fingerprinting of obsidian. Part of this work was funded by the Deutsche Forschungsgemeinschaft by the grants PE 405/12-1 und PE 405/12-2 awarded to Ernst Pernicka with the title “Technologie und Handel von transkaukasischem Obsidian in prähistorischer Zeit”.

References

Abedi et al. 2018

A. Abedi – B. Vosough – M. Razani – M. Bagherzadeh Kasiri – D. Steiniger – G. Ebrahimi, Obsidian deposits from north-western Iran and first analytical results. Implications for prehistoric production and trade, *Mediterranean Archaeology and Archaeometry* 18, 2, 2018, 107–118.

Arutyunyan et al. 2007

E. V. Arutyunyan – V. A. Lebedev – I. V. Chernyshev – A. K. Sagatelyan, Geochronology of Neogene–Quaternary volcanism of the Geghama Highland (Lesser Caucasus, Armenia), *Doklady Earth Sciences* 416, 7, 2007, 1042–1046.

Aslanyan 1958

A. Т. Асланян, Региональная геология Армении (Yerevan 1958).

Aslanyan et al. 1980

A. Т. Асланян – К. Г. Ширинян – С. Г. Карапетян, Петрогенетические аспекты новейшего вулканизма Тавро-Кавказского орогена, in: *Международный геологический конгресс. XXVI сессия. Доклады советских геологов. Петрология (Moscow 1980)* 58–66.

Aspinall et al. 1972

A. Aspinall – S. W. Feather – C. Renfrew, Neutron activation analysis of Aegean obsidians, *Nature* 237, 1972, 333–334.

Badalian et al. 2001

R. Badalian – G. Bigazzi – M.-C. Cauvin – C. Chataigner – R. Jrbashyan – S. G. Karapetyan – M. Oddone – J.-L. Poidevin, An international research project on Armenian archaeological sites. Fission-track dating of obsidians, *Radiation Measurements* 34, 2001, 373–378.

Badalyan 2010

R. S. Badalyan, Obsidian of the South Caucasus. The use of raw materials in the Neolithic to Early Iron Age, in: S. Hansen – A. Hauptmann – I. Motzenbäcker – E. Pernicka (eds.), *Von Majkop bis Trialeti. Gewinnung und Verbreitung von Metallen und Obsidian in Kaukasien im 4.–2. Jt. v. Chr.*, *Kolloquien zur Vor- und Frühgeschichte* 13 (Bonn 2010) 27–38.

Badalyan et al. 1996

Р. С. Бадалян – З. К. Кикодзе – Ф. Л. Коль, Кавказский обсидиан. Источники и модели утилизации и снабжения (Результаты анализов нейтронной активации) [Caucasian obsidian. Sources and patterns of exchange and utilization (results of neutron activation analysis)], *Պատմա-բանասիրական հանդես / Patma-banasirakan handes* 1, 2, 1996, 245–264.

¹³⁵ Blackman et al. 1998.

Badalyan et al. 2004

R. Badalyan – C. Chataigner – P. L. Kohl, Trans-Caucasian obsidian. The exploitation of the sources and their distribution, in: A. Sagona (ed.), *A View from the Highlands. Archaeological Studies in Honour of Charles Burney, Ancient Near Eastern Studies Supplement 12* (Leuven 2004) 437–465.

Badalyan et al. in press

R. Badalyan – C. Chataigner – O. Barge – K. Meliksetian – E. Pernicka, The use of obsidian in the South Caucasus (Armenia). History and results of provenance studies, in: F.-X. Le Bourdonnec – M. Orange – M. S. Shackley (eds.), *Sourcing Obsidian. A State-of-the-Art in the Framework of Archaeological Research, Interdisciplinary Contributions to Archaeology series* (in press).

Baghdasaryan – Ghukasyan, 1985

Г. П. Багдасарян – Р. Х. Гукасян, Геохронология магматических, метаморфических и рудных формаций Армянской ССР (Yerevan 1985).

Balog et al. 1990

К. Балог – Г. П. Багдасарян – К. И. Карапетян – З. Печкай – Е. Арва-Шош – Р. Х. Гукасян, Первые К/Аг изотопные датировки верхнеплиоцен-четвертичных вулканических пород Республики Армения, *Известия АН Армении. Науки о Земле* 43, 2, 1990, 25–38.

Biagi et al. 2014

P. Biagi – B. Gratuze – D. V. Kiosak – O. V. Tubolzev – Z. H. Popandopulo, The Neolithic obsidians from southeastern Ukraine. First characterization and provenance determination, *Anatolia* 40, 2014, 1–20.

Blackman 1984

M. J. Blackman, Provenance studies of Middle Eastern obsidian from sites in highland Iran, in: J. B. Lambert (ed.), *Archaeological Chemistry III, Advances in Chemistry Series 205* (Washington DC 1984) 19–50.

Blackman et al. 1998

J. Blackman – R. Badaljan – Z. Kikodze – P. Kohl, Chemical characterization of Caucasian obsidian geological sources, in: M.-C. Cauvin – A. Gourgaud – B. Gratuze – N. Arnaud – G. Poupeau – J.-L. Poidevin – C. Chataigner (eds.), *L'obsidienne au Proche et Moyen Orient. Du volcan à l'outil*, *British Archaeological Reports International Series 738* (Oxford 1998) 205–31.

Bigazzi et al. 1994

G. Bigazzi – Z. Yeğingil – T. Ercan – M. Oddone – M. Özdoğan, The Pisa-Adana joint project on provenance studies of prehistoric obsidian artifacts. First results from an interdisciplinary research, *Mineralogica et Petrographica Acta* 37, 1994, 17–36.

Cann – Renfrew 1964

J. Cann – C. Renfrew, The characterization of obsidian and its application to the Mediterranean region, *Proceedings of the Prehistoric Society XXX*, 1964, 111–133.

Chataigner 1995

C. Chataigner, *La Transcaucasie au Néolithique et au Chalcolithique*, *British Archaeological Reports International Series 624* (Oxford 1995).

Chataigner – Gratuze 2014a

C. Chataigner – B. Gratuze, New data on the exploitation of obsidian in the southern Caucasus (Armenia, Georgia) and eastern Turkey. Part 1: source characterization, *Archaeometry* 56, 1, 2014, 25–47.

Chataigner – Gratuze 2014b

C. Chataigner – B. Gratuze, New data on the exploitation of obsidian in the southern Caucasus (Armenia, Georgia) and eastern Turkey. Part 2: obsidian procurement from the Upper Palaeolithic to the Late Bronze Age, *Archaeometry* 56, 1, 2014, 48–69.

Chataigner et al. 1998

C. Chataigner – J.-L. Poidevin – N. O. Arnaud, Turkish occurrences of obsidian and use by prehistoric peoples in the Near East from 14,000 to 6000 BP, *Journal of Volcanology and Geothermal Research* 85, 1998, 517–537.

Chataigner et al. 2003

C. Chataigner – R. Badalian – G. Bigazzi – M.-C. Cauvin – R. Jrbashian – S. G. Karapetian, – P. Norelli – M. Oddone – J.-L. Poidevin, Provenance studies of obsidian artefacts from Armenian archaeological sites using the fission-track dating method, *Journal of Non-Crystalline Solids* 323, 2003, 167–171.

Chataigner et al. 2014

C. Chataigner – M. Işikli – B. Gratuze – V. Çil, Obsidian sources in the regions of Erzurum and Kars (north-east Turkey). *New data, Archaeometry* 56, 3, 2014, 351–374.

Chernyshev et al. 2002

I. V. Chernyshev – V. A. Lebedev – M. M. Arakelyants – R. T. Jrbashyan – Y. G. Gukasyan, Quaternary Geochronology of the Aragats volcanic center, Armenia. Evidence from K-Ar dating, *Doklady Earth Sciences* 384, 4, 2002, 393–398.

Cherry et al. 2010

J. Cherry – E. Faro – L. Minc, Field exploration and instrumental neutron activation analysis of the obsidian sources in southern Armenia, *Journal of Field Archaeology* 35, 2, 2010, 147–163.

Dixon 1977

J.-E. Dixon, Obsidian characterization studies in the Mediterranean and Near East, in: R. E. Taylor (ed.), *Advances in Obsidian Glass Studies. Archaeological and Geochemical Perspectives* (Park Ridge, New Jersey 1977) 288–333.

Fornaseri et al. 1977

M. Fornaseri – L. Malpieri – A. M. Palmieri – A. Taddeucci, Analyses of obsidians from the Late Chalcolithic levels of Arslantepe (Malatya), *Paléorient* 3/1975–1977, 1977, 231–246.

Frahm – Feinberg 2013

E. Frahm – M.-J. Feinberg, Empires and resources. Central Anatolian obsidian at Urkesh (Tell Mozan, Syria) during the Akkadian period, *Journal of Archaeological Science* 40, 2013, 1122–1135.

Frahm et al. 2014

E. Frahm – B. A. Schmidt – B. Gasparyan – B. Yeritsyan – S. Karapetian – K. Meliksetian – D. S. Adler, Ten seconds in the field. Rapid Armenian obsidian sourcing with portable XRF to inform excavations and surveys, *Journal of Archaeological Science* 41, 2014, 333–348.

Frahm et al. 2016

E. Frahm – S. Campbell – E. Healey, Caucasus connections? New data and interpretations for Armenian obsidian in Northern Mesopotamia, *Journal of Archaeological Science: Reports* 9, 2016, 543–564.

Francaviglia 1994

V. M. Francaviglia, L'origine des outils en obsidienne de Tell Magzalia, Tell Sotto, Yarim Tepe et Kül Tepe, Iraq, *Paléorient* 20, 2, 1994, 18–31.

Gadzhiev et al. 2000

M. G. Gadzhiev – P. Kohl – R. Magomedov – D. Stronach – S. Gadzhiev, Daghestan-American archaeological investigations in Daghestan, Russia 1997–99, *Eurasia Antiqua* 6, 2000, 47–123.

Jrbashyan et al. 1996

Р. Т. Джрбашян – Г. А. Казарян – С. Г. Карапетян – Х. Б. Меликсетян – А. Х. Мнацаканян – К. Г. Ширинян, Мезокайнозойский базальтовый вулканизм северо-восточной части Армянского нагорья, *Известия НАН Республики Армения. Науки о Земле* 49, 1996, 19–32.

Juharyan 2018

A. Juharyan, Portable X-ray fluorescence analysis of Armenian obsidian sources, *Aramazd. Armenian Journal of Near Eastern Studies* XII, 1, 2018, 66–75.

Karakhonian et al. 2003

A. Karakhonian – R. Jrbashyan – V. Trifonov – H. Philip – S. Arakelian – A. Avagyan – H. Baghdassaryan – V. Davtian – Y. Ghoukassyan, Volcanic hazards in the region of the Armenian nuclear power plant, *Journal of Volcanology and Geothermal Research* 126, 2003, 31–62.

Karapetian 1972

С. Г. Карапетян, Особенности строения и состава новейших липаритовых вулканов Армянской ССР (Yerevan 1972).

Karapetian et al. 2001

S. G. Karapetian – R. T. Jrbashyan – A. K. Mnatsakanian, Late collision rhyolitic volcanism in the north-eastern part of the Armenian Highland, *Journal of Volcanology and Geothermal Research* 112, 2001, 189–220.

Keller et al. 1996

J. Keller – R. Djerbashian – S. G. Karapetian – E. Pernicka – V. Nasedkin, Armenian and Caucasian obsidian occurrences as sources for the Neolithic trade. Volcanological setting and chemical characteristics, in: Ş. Demirci – A. M. Özer – G. D. Summers (eds.), *Archaeometry 94. The Proceedings of the 29th International Symposium on Archaeometry*, Ankara 9–14 May 1994 (Ankara 1996) 69–86.

Keller – Seifried 1990

J. Keller – C. Seifried, The present status of obsidian source identification in Anatolia and the Near East, in: C. Albore Livadie – F. Widemann (eds.), *Volcanology and Archaeology. Proceedings of the European Workshops of Ravello*, November 19–27, 1987 and March 30–31, 1989, PACT. *Journal of the European Study Group on Physical, Chemical, Biological and Mathematical Techniques Applied to Archaeology* 25, 1990, 57–87.

Keskin 2003

M. Keskin, Magma generation by slab steepening and breakoff beneath a subduction-accretion complex. An alternative model for collision-related volcanism in Eastern Anatolia, Turkey, *Geophysical Research Letters* 30, 2003, 8046. doi: 10.1029/2003GL018019

Keskin et al. 1998

M. Keskin – J. A. Pearce – J. G. Mitchell, Volcano-stratigraphy and geochemistry of collision-related volcanism on the Erzurum-Kars Plateau, northeastern Turkey, *Journal of Volcanology and Geothermal Research* 85, 1998, 355–405.

Khademi Nadooshan et al. 2013

F. Khademi Nadooshan – A. Abedi – M. D. Glascock – N. Eskandari – M. Khazaei, Provenance of prehistoric obsidian artefacts from Kul Tepe, northwestern Iran using X-ray fluorescence (XRF) analysis, *Journal of Archaeological Science* 40, 2013, 1956–1965.

Kharazyan 1968

Э. Х. Харазян, Новейшие вулканические образования верховьев бассейна р. Ахурян (Арм. ССР), *Известия АН Армянской ССР. Науки о Земле* 21, 5, 1968, 3–17.

Kharazyan 1970

Э. Х. Харазян, Геология новейших вулканических образований северо-западной части территории Армянской ССР (басс. пр. Ахурян и Дзорагет). Автореферат дисс. (Yerevan 1970).

Komarov et al. 1972

A. Н. Комаров – Н. В. Сквородкин – С. Г. Карапетян, Определение возраста природных стекол по трекам осколков деления Урана, *Геохимия* 6, 1972, 693–698.

Kuleff – Djingova, 1999

I. Kuleff – R. Djingova, Activation analysis in archaeology, in: Z. Alfassi (ed.), *Activation Analysis. Volume 2* (Boca Raton 1990) 427–489.

Kunze et al. 2013

R. Kunze – A. Bobokhyan – E. Pernicka – K. Meliksetian, Projekt Ushkiani. Untersuchungen der Kulturlandschaft um das prähistorische Goldrevier von Sotk, in: H. Meller – P. Avetisyan (eds.), *Archäologie in Armenien II. Berichte zu den Kooperationsprojekten 2011 und 2012 sowie ausgewählten Einzelstudien*, Veröffentlichungen des Landesamtes für Denkmalpflege und Archäologie Sachsen-Anhalt – Landesmuseum für Vorgeschichte 67 (Halle/Saale 2013) 49–92.

Lebedev et al. 2008

V. A. Lebedev – S. N. Bubnov – O. Z. Dudaury – G. T. Vashakidze, Geochronology of Pliocene volcanism in the Dzhavakheti Highland (the Lesser Caucasus). Part 2: western part of the Dzhavakheti Highland, *Stratigraphy and Geological Correlation*, 16, 2, 2008, 204–224.

Lebedev et al. 2011

V. A. Lebedev – I. V. Chernyshev – A. I. Yakushev, Initial time and duration of Quaternary magmatism in the Aragats neovolcanic area (Lesser Caucasus, Armenia), *Doklady Earth Sciences* 437, 2011, 532–536.

Lebedev et al. 2013

V. A. Lebedev – I. V. Chernyshev – K. N. Shatagin – S. N. Bubnov – A. I. Yakushev, The Quaternary volcanic rocks of the Geghama Highland, Lesser Caucasus, Armenia. Geochronology, isotopic Sr–Nd characteristics, and origin, *Journal of Volcanology and Seismology* 7, 2013, 204–229.

Le Bourdonnec et al. 2012

F.-X. Le Bourdonnec – S. Nomade – G. Poupeau – H. Guillou – N. Tushabramishvili – M.-H. Moncel – D. Pleurdeau – T. Agapishvili – P. Voinchet – A. Mgeladze – D. Lordkipanidze, Multiple origins of Bondi Cave and Ortvale Klde (NW Georgia) obsidians and human mobility in Transcaucasia during the Middle and Upper Palaeolithic, *Journal of Archaeological Science* 39, 2012, 1317–1330.

Martirosyan-Olshansky 2018

K. Martirosyan-Olshansky, Sourcing of obsidian artifacts from Masis Blur, Armenia, Aramazd. *Armenian Journal of Near Eastern Studies* XII, 1, 2018, 19–34.

Meliksetian 2013

K. Meliksetian, Pliocene-Quaternary volcanism of the Syunik upland, in: H. Meller – P. Avetisyan (eds.), *Archäologie in Armenien II. Berichte zu den Kooperationsprojekten 2011 und 2012 sowie ausgewählten Einzelstudien, Veröffentlichungen des Landesamtes für Denkmalpflege und Archäologie Sachsen-Anhalt – Landesmuseum für Vorgeschichte* 67 (Halle/Saale 2013) 247–258.

Meliksetian – Karapetian 1981

Б. М. Меликсетян – С. Г. Карапетян, Геохимия редких и рудных элементов в новейших кислых вулканитах Армянской ССР, *Известия АН Армянской ССР. Науки о Земле* 34, 4, 1981, 28–48.

Nadareishvili et al. 2002

Г. Ш. Надареишвили – Т. В. Джанелидзе – Р. Т. Джрбашян – Г. В. Мустафаев – М. А. Мустафаев, Фанерозойский вулканизм южного Кавказа, in: *Сборник трудов, посвященный 90-летию со дня рождения Г.С.Дзоценидзе, Академия наук Грузии, Геологический институт им. А. И. Джанелидзе, Труды Новая серия* 117, 2002, 39–52.

Nasedkin 1981

В. В. Наседкин, Основные закономерности формирования месторождений водосодержащих стекол и пути их промышленного использования, in: *Перлиты (Moscow 1981)* 17–42.

Nedelcheva et al. this volume

P. Nedelcheva – E. Pernicka – I. Gatsov, Obsidian Tool Production and Exchange in the Southern Caucasus during Late Prehistory.

Neill et al. 2013

I. Neill – K. Meliksetian – M. Allen – G. Navarsadyan – S. Karapetyan, Pliocene-Quaternary volcanic rocks of NW-Armenia. Magmatism and lithospheric dynamics within an active orogenic plateau, *Lithos* 180–181, 2013, 200–215.

Neill et al. 2015

I. Neill – K. Meliksetian – M. B. Allen – G. Navarsadyan – K. Kuiper, Petrogenesis of mafic collision zone magmatism. The Armenian sector of the Turkish–Iranian plateau, *Chemical Geology* 403, 2015, 24–41.

Oddone et al. 2000

M. Oddone – G. Bigazzi – Y. Keheyan – S. Meloni, Characterisation of Armenian obsidians. Implications for raw material supply for prehistoric artifacts, *Journal of Radioanalytical and Nuclear Chemistry* 243, 3, 2000, 673–682.

Ovchinnikov – Grigoryan 1970

Л. Н. Овчинников – С. В. Григорян, Закономерности состава и строения первичных ореолов сульфидных месторождений, in: *Научные основы геохимических методов поисков глубокозалегающих рудных месторождений (Irkutsk 1970)* 3–36.

Palumbi et al. 2018

G. Palumbi – D. Guilbeau – L. Astruc – C. Chataigner – B. Gratuze – B. Lyonnet – G. Pulitani, Between cooking and knapping in the southern Caucasus. Obsidian-tempered ceramics from Aratashen (Armenia) and Mentesh Tepe (Azerbaijan), *Quaternary International* 468, 2018, 121–133.

Pearce et al. 1990

J. A. Pearce – J. F. Bender – S. E. Delong – W. S. F. Kidd – P. J. Low – Y. Güner – F. Saroglu – Y. Yilmaz – S. Moorbath – J. G. Mitchell, Genesis of collision volcanism in eastern Anatolia, Turkey, *Journal of Volcanology and Geothermal Research* 44, 1990, 189–229.

Perlman – Asaro 1969

I. Perlman – F. Asaro, Pottery analysis by neutron activation, *Archaeometry* 11, 1969, 21–52.

Pernicka et al. 1997

E. Pernicka – J. Keller – M.-C. Cauvin, Obsidian from Anatolian sources in the Neolithic of the Middle Euphrates region (Syria), *Paléorient* 23, 1997, 113–122.

Philip et al. 2001

H. Philip – A. Avagyan – A. Karakhanian – J. F. Ritz – S. Rebai, Estimating slip-rates and recurrence intervals for strong earthquakes along an intracontinental fault. Example of the Pambak-Sevan-Sunik Fault (Armenia), *Tectonophysics* 343, 2001, 205–232.

Renfrew et al. 1966

C. Renfrew – J. E. Dixon – J. R. Cann, Obsidian and early cultural contact in the Near East, *Proceedings of the Prehistoric Society* 32, 1966, 30–72.

Shirinyan 1975

К. Г. Ширинян, К вопросу о новейших (верхнеплиоцен-четвертичных) вулканических формациях Армении, *Известия АН Армянской ССР. Науки о Земле* 28, 1, 1975, 3–15.

Shirinyan – Zadoyan 1990

К. Г. Ширинян – В. А. Задоян, Петрогенетическая систематика позднеорогенных базальтоидов Армении, *Доклады Академии Наук Армянской ССР* 90, 3, 1990, 125–130.

Skhirtladze, 1958

Н. И. Схиртладзе, Постпалеогеновый эффузивный вулканизм Грузии (Tbilisi 1958).

Yilmaz et al. 2000

A. Yilmaz – S. Adamia – A. Chabukiani – T. Chkhotua – K. Erdoğan – S. Tuzcu – M. Karabiyikoğlu, Structural correlation of the southern Transcaucasus (Georgia)–eastern Pontides (Turkey), in: E. Bozkurt – J. A. Winchester – J. D. A. Piper (eds.), *Tectonics and Magmatism in Turkey and the Surrounding Area*, Geological Society Special Publication 173 (London 2000) 171–182.

Appendix

Chemical and trace element composition of geological obsidian samples. All concentrations are in $\mu\text{g/g}$, except for Na, K, Fe in weight percent.

	Tsaghkunyats ridge										
	Damlık		Tsaghkunyats								MA-090151
	1	2	3	4	5	6	7	8	9	10	
	FG-011911	FG-011912	FG-020573	FG-020574	FG-020575	FG-020576	FG-020577	FG-020578	FG-020579		
Na %	3.29	3.38	–	–	3.09	3.22	–	3.34	–	3.16	
K %	3.64	3.12	–	–	–	–	–	3.30	–	2.99	
Fe %	1.61	1.09	1.08	1.02	1.05	1.10	1.06	1.06	1.05	0.8	
Sc	1.59	1.28	1.46	1.55	1.51	1.62	1.46	1.41	1.57	1.4	
Cr	0.62	0.63	0.66	0.67	–	–	0.79	0.43	0.67	3.7	
Co	0.82	0.82	0.46	0.45	0.58	0.63	0.63	0.73	0.51	0.9	
Zn	27.4	21.1	–	–	–	–	–	–	–	35.5	
As	–	–	–	–	–	–	–	–	–	2.97	
Sb	0.31	0.25	0.22	0.33	0.29	0.34	0.14	0.26	–	0.2	
Rb	136	91	88	89	91	93	93	109	92	86	
Cs	3.78	2.89	2.99	2.46	2.98	3.27	3.42	3.67	3.16	3.23	
Ba	838	967	869	901	922	937	914	714	927	1236	
Zr	116	96	77	113	76	77	91	72	84	122	
Hf	–	–	3.29	3.11	2.95	3.18	3.31	2.85	3.12	3.89	
Ta	1.55	1.40	1.58	1.55	1.44	1.64	1.68	1.52	1.50	1.3	
Th	20.6	29.4	28.0	31.1	28.4	30.7	32.3	28.2	29.3	28.8	
U	8.73	8.22	9.92	9.66	10.43	11.40	10.08	9.19	9.75	8.73	
La	39.8	51.2	38.4	41.6	42.0	42.8	40.9	42.5	39.6	55.8	
Ce	51.7	78.4	69.3	60.2	56.8	62.3	69.6	51.6	70.0	74.3	
Nd	12.9	15.9	–	–	–	–	–	–	–	23.3	
Sm	3.74	3.44	2.68	3.23	3.31	3.46	3.86	2.72	3.39	3.07	
Eu	0.493	0.412	0.434	0.412	0.439	0.413	0.316	0.398	0.524	0.462	
Tb	–	0.64	0.62	0.42	0.48	0.69	0.45	0.66	0.56	0.66	
Yb	1.29	1.23	1.25	0.94	0.98	1.28	1.28	1.20	2.65	0.91	
Lu	0.200	0.176	0.178	0.188	0.199	0.195	0.220	0.195	0.468	0.145	

Gutansar volcanic complex, Gegham volcanic upland												
Jraber												Fontan
	21	22	23	24	25	26	27	28	29	30		
	FG-020544	FG-030835	FG-030836	FG-030837	FG-030838	FG-030839	FG-030868	FG-020535	FG-020536	FG-030834		
Na %	3.17	3.36	3.75	3.72	3.46	3.48	3.64	3.22	3.15	3.78		
K %	3.41	3.62	3.36	3.99	3.31	3.87	–	3.99	3.26	3.57		
Fe %	1.35	1.44	1.40	1.37	1.40	1.41	1.40	1.77	1.78	1.44		
Sc	3.05	3.27	3.16	3.11	3.12	3.15	2.97	2.97	2.84	3.26		
Cr	1.74	2.77	2.04	3.95	2.50	3.15	–	–	–	2.82		
Co	0.79	0.81	0.78	0.78	0.71	0.77	0.80	0.65	0.71	0.82		
Zn	–	43.4	40.5	39.7	42.1	42.6	–	49.2	49.3	41.7		
As	3.01	2.39	2.23	2.98	2.20	1.91	–	1.65	1.60	1.50		
Sb	0.46	0.44	0.43	0.41	0.49	0.40	0.54	0.36	0.42	0.49		
Rb	142	135	140	125	133	136	135	166	177	155		
Cs	4.30	5.64	5.41	5.21	5.21	5.28	5.18	5.81	5.99	5.63		
Ba	571	528	527	508	540	520	468	475	446	567		
Zr	153	153	107	176	100	154	112	149	162	125		
Hf	5.15	5.06	4.90	4.81	4.80	4.87	4.66	5.45	5.21	5.15		
Ta	3.24	2.95	2.80	2.86	2.73	2.86	2.62	2.28	2.38	2.97		
Th	15.8	18.8	18.2	18.1	17.2	17.8	17.0	21.0	17.0	18.5		
U	8.61	8.74	8.70	9.23	3.80	3.82	8.64	9.16	9.08	9.47		
La	32.0	33.0	35.1	36.2	32.8	34.3	28.2	31.9	31.7	35.3		
Ce	56.2	57.8	53.6	58.2	54.6	55.5	56.1	62.3	53.7	58.8		
Nd	–	–	–	–	–	–	–	–	–	–		
Sm	3.02	3.73	3.70	3.89	3.58	3.83	3.92	3.87	3.82	4.19		
Eu	0.494	0.535	0.533	0.534	0.537	0.543	0.588	0.514	0.578	0.580		
Tb	0.69	0.62	0.63	0.59	0.62	0.54	0.68	0.63	0.67	–		
Yb	2.21	2.52	2.62	2.88	2.39	2.61	2.44	2.46	2.50	2.43		
Lu	0.491	0.456	0.415	0.389	0.472	0.405	0.445	0.443	0.420	0.403		

Hatis volcano, Gegham volcanic upland										
Hatis										
	41	42	43	44	45	46	47	48	49	
	FG-030829	FG-030830	FG-030831	FG-030832	FG-030833	FG-011910	FG-020528	FG-020529	FG-020530	
Na %	3.23	3.45	3.48	3.38	3.42	3.30	3.05	3.12	3.13	
K %	3.40	3.75	3.61	3.58	3.29	–	3.52	3.50	3.36	
Fe %	1.08	1.07	1.18	1.01	1.20	1.09	1.06	1.15	1.08	
Sc	3.30	3.26	3.26	3.21	2.97	3.27	3.05	3.11	3.33	
Cr	2.26	1.42	1.26	2.20	2.27	1.82	2.54	1.87	1.80	
Co	0.65	0.63	0.62	0.67	0.64	0.58	0.61	0.64	0.70	
Zn	32.7	35.9	36.9	37.4	32.2	36.5	36.4	33.4	36.8	
As	–	–	–	–	–	2.87	2.71	2.41	2.72	
Sb	0.28	0.29	0.25	0.25	0.29	0.30	0.27	0.28	0.28	
Rb	116	110	135	124	124	135	118	122	124	
Cs	4.73	4.53	4.46	4.26	3.88	4.74	4.07	4.11	4.09	
Ba	725	766	719	710	781	551	473	516	494	
Zr	106	146	99	93	157	92	79	53	137	
Hf	3.18	3.77	3.73	3.59	4.18	3.59	3.81	2.94	3.34	
Ta	1.94	1.81	1.79	1.81	1.63	1.84	2.23	2.29	1.89	
Th	17.5	17.8	17.9	17.1	16.1	18.8	17.1	17.5	13.7	
U	9.37	8.74	8.76	8.71	7.53	9.15	9.16	9.26	9.73	
La	28.4	33.4	33.9	33.6	37.1	33.6	36.3	27.5	27.5	
Ce	45.8	53.5	55.1	55.1	58.1	56.3	43.1	44.6	49.3	
Nd	–	–	–	–	–	15.2	–	–	–	
Sm	2.71	2.90	2.92	2.75	3.08	3.43	3.01	3.09	3.40	
Eu	0.608	0.589	0.581	0.606	0.400	0.495	0.523	0.585	0.418	
Tb	0.39	0.43	0.45	0.41	0.58	0.37	0.40	0.35	0.39	
Yb	1.81	1.54	1.54	1.52	2.79	1.73	1.68	1.78	1.83	
Lu	0.426	0.403	0.388	0.475	0.467	0.373	0.377	0.386	0.376	

Gegham ridge												
Geghasar												
	50	51	52	53	54	55	56	57	58	59		
	FG-011913	FG-011914	FG-011915	FG-011916	FG-030502	FG-030503	FG-030810	FG-030812	FG-030813	FG-030814		
Na %	3.34	3.37	3.25	3.37	—	—	3.12	3.17	3.24	3.13		
K %	2.60	2.97	2.47	2.74	—	—	—	—	—	—		
Fe %	0.55	0.52	0.51	0.73	0.48	0.38	0.61	0.62	0.63	0.62		
Sc	3.12	3.03	3.01	3.14	3.20	3.05	3.06	3.09	3.18	3.05		
Cr	1.31	1.21	1.06	—	—	—	—	1.14	1.16	1.64		
Co	0.05	0.04	0.04	0.04	0.06	0.05	0.02	0.02	0.02	0.02		
Zn	—	31.1	35.2	31.2	33.9	29.3	—	—	—	—		
As	3.28	3.16	2.76	2.80	—	—	—	—	—	—		
Sb	0.54	0.56	0.52	0.58	0.59	0.58	0.58	0.54	0.64	0.63		
Rb	200	198	195	172	215	203	199	194	200	188		
Cs	7.38	7.22	7.07	7.44	7.31	7.23	7.78	8.06	8.31	7.83		
Ba	57	53	62	65	378	234	278	275	308	217		
Zr	65	62	46	49	65	52	55	47	54	59		
Hf	—	—	—	—	3.22	3.08	3.08	3.16	3.19	3.06		
Ta	5.06	4.91	4.91	5.47	5.09	5.01	4.36	4.32	5.22	4.55		
Th	28.8	28.3	27.8	25.2	26.0	28.2	26.9	27.3	28.1	26.8		
U	13.88	13.93	14.25	15.51	15.87	16.37	14.15	14.99	15.44	14.74		
La	16.4	16.2	15.9	15.7	18.6	19.0	17.3	17.7	18.2	17.5		
Ce	32.3	32.5	31.0	35.0	35.6	31.3	32.3	32.2	32.6	30.5		
Nd	14.2	14.1	14.6	11.2	—	—	—	—	—	—		
Sm	3.89	3.97	3.18	3.85	3.38	3.78	4.02	4.11	4.24	3.99		
Eu	0.236	0.226	0.185	0.191	0.236	0.247	0.262	0.254	0.264	0.254		
Tb	—	—	—	0.62	0.55	0.62	0.65	0.68	0.61	0.63		
Yb	2.47	2.36	3.28	2.93	2.04	2.50	2.38	2.50	2.43	2.34		
Lu	0.620	0.547	0.393	0.381	0.446	0.766	0.778	0.826	0.696	0.751		

Gegham ridge												
Geghasar												Spitaksar
	60	61	62	63	64	65	66	67	68	69		
	FG-030815	FG-030816	FG-030817	FG-030818	FG-030824	FG-030825	FG-030826	FG-030826	FG-011930	FG-030805		
Na %	3.10	3.17	3.16	2.95	3.05	2.98	3.18	3.20	4.11	3.92		
K %	–	–	–	–	4.01	4.28	–	3.20	–	–		
Fe %	0.60	0.62	0.62	0.75	0.58	0.57	0.72	0.73	0.52	0.60		
Sc	3.00	3.11	3.05	3.42	3.37	3.28	3.12	3.28	3.17	3.19		
Cr	–	–	1.62	0.08	4.35	3.75	–	–	2.54	–		
Co	0.02	0.01	0.02	0.01	0.15	0.15	0.20	0.02	0.39	0.25		
Zn	–	–	–	–	34.9	32.3	–	32.4	29.9	–		
As	–	–	–	–	3.92	3.56	–	–	–	–		
Sb	0.68	0.53	0.64	0.62	0.57	0.51	0.59	0.62	0.72	0.63		
Rb	182	195	195	207	201	199	203	166	179	180		
Cs	7.59	7.96	7.89	7.94	8.39	8.05	8.12	7.70	6.53	7.19		
Ba	256	273	361	257	60	57	80	105	26	171		
Zr	54	51	42	67	34	45	65	57	46	41		
Hf	3.09	3.16	3.12	3.02	3.27	3.09	3.12	2.96	2.84	2.90		
Ta	4.51	4.51	4.60	4.59	4.37	4.24	6.04	4.58	4.81	4.03		
Th	26.4	27.3	27.0	28.3	28.4	27.6	27.0	27.6	18.5	18.0		
U	14.62	14.94	14.57	13.69	17.65	16.25	12.37	14.19	16.19	13.73		
La	17.3	18.0	17.9	16.8	18.8	17.9	18.5	18.0	19.1	18.3		
Ce	30.6	32.3	31.1	30.2	28.4	31.6	33.2	34.6	28.4	28.7		
Nd	–	–	–	–	–	–	–	–	10.4	–		
Sm	3.96	4.14	4.10	3.28	4.56	4.50	5.19	3.28	4.12	4.33		
Eu	0.255	0.271	0.229	0.258	0.253	0.230	0.244	0.222	0.233	0.239		
Tb	0.67	0.65	0.68	0.88	0.86	0.68	0.59	0.62	0.64	0.64		
Yb	2.46	2.43	2.26	2.80	2.68	3.77	2.14	2.49	2.05	2.02		
Lu	0.681	0.703	0.727	0.813	0.783	1.065	0.815	0.462	0.393	0.422		

Arteni volcanic complex, Aragats volcanic province												
	Arteni C						Arteni A+B					
	80	81	82	83	84	85	86	87	88	89		
	FG-020551	FG-011926	FG-020541	FG-020545	FG-020552	FG-020553	FG-020556	FG-020557	FG-020546	FG-020547		
Na %	2.99	4.79	4.05	4.04	3.00	2.93	3.14	3.00	3.08	3.04		
K %	–	–	–	–	–	6.07	–	–	1.98	–		
Fe %	0.40	1.19	2.13	0.36	0.39	0.41	0.41	0.41	0.37	0.33		
Sc	2.35	2.99	2.87	2.90	2.49	2.42	2.54	2.48	2.72	2.86		
Cr	1.83	–	3.14	1.77	1.28	1.71	1.08	2.08	2.11	1.51		
Co	0.18	0.13	0.12	0.16	0.20	0.23	0.20	0.17	0.15	0.22		
Zn	–	43.2	–	44.2	–	–	–	–	19.9	–		
As	2.40	5.30	5.80	5.30	1.87	2.29	2.66	2.56	2.82	3.36		
Sb	0.43	0.48	0.39	0.54	0.45	0.40	0.40	0.45	0.44	0.48		
Rb	121	140	155	155	121	121	141	125	142	158		
Cs	3.52	4.95	4.45	4.06	3.71	3.71	3.66	3.36	3.64	4.00		
Ba	334	496	447	432	101	164	121	130	129	122		
Zr	40	63	57	51	49	60	38	51	29	42		
Hf	3.30	4.79	4.82	4.17	3.13	3.35	3.40	3.13	2.99	3.06		
Ta	2.54	3.08	2.75	2.96	2.60	2.55	2.58	2.46	2.80	2.77		
Th	14.9	18.1	17.9	15.3	13.6	14.9	16.2	15.9	14.2	15.6		
U	6.91	10.87	8.79	8.00	6.93	7.16	7.39	6.87	7.37	7.77		
La	17.4	31.8	30.3	31.8	16.1	17.4	16.4	16.5	13.3	12.2		
Ce	29.8	52.2	49.8	55.2	30.7	30.8	30.8	32.4	27.7	28.2		
Nd	–	–	–	–	–	–	–	–	–	–		
Sm	3.40	4.85	3.75	3.86	3.39	3.42	3.51	3.38	3.76	3.70		
Eu	0.515	0.440	0.490	0.957	0.356	0.311	0.321	0.283	0.283	0.295		
Tb	0.65	0.71	0.83	–	0.69	0.70	0.69	0.72	0.65	0.70		
Yb	3.64	3.51	3.28	1.98	3.02	2.95	2.74	3.01	3.08	2.56		
Lu	0.557	0.442	0.488	0.200	0.428	0.450	0.426	0.470	0.503	0.429		

		Chikiani/Javakheti ridge											
Kechut-Javakheti Sizavet	100	Chikiani										109	
		101	102	103	104	105	106	107	108	MA-121224			
	FG-011923	FG-011908	FG-011909	FG-041693	FG-041694	FG-041691	FG-041692	FG-041695	MA-121224	MA-121225			
Na %	3.63	3.37	3.40	3.13	3.15	3.02	3.11	3.20	2.97	2.97			
K %	2.97	1.98	2.68	—	—	—	—	—	4.40	4.30			
Fe %	1.74	0.77	0.84	0.92	0.92	0.90	0.93	0.96	0.53	0.55			
Sc	2.72	1.90	2.09	2.10	2.08	2.10	2.16	2.13	2.09	2.12			
Cr	1.38	2.23	4.04	2.62	4.50	3.27	3.42	5.24	2.40	3.20			
Co	1.35	0.42	0.46	—	0.21	0.19	0.20	0.24	0.18	0.25			
Zn	40.2	34.9	41.1	40.9	42.5	46.0	41.3	42.9	44.0	43.0			
As	3.58	1.33	1.55	—	—	—	—	—	2.70	2.70			
Sb	0.20	0.25	0.33	0.72	0.58	2.57	1.19	0.54	0.11	0.24			
Rb	95	112	133	135	126	123	134	122	120	120			
Cs	2.49	4.19	4.59	5.18	5.07	4.97	5.29	4.91	4.99	4.89			
Ba	814	674	726	746	389	810	891	412	650	650			
Zr	180	51	49	71	83	55	102	74	88	80			
Hf	—	2.90	3.19	3.06	3.08	2.92	2.92	3.27	3.04	3.16			
Ta	1.13	1.42	1.62	1.49	1.37	1.44	1.48	1.45	1.32	1.33			
Th	17.0	14.4	16.0	15.4	15.4	15.0	15.8	15.6	15.0	15.2			
U	3.44	5.67	6.51	5.93	5.24	5.45	5.66	5.52	5.10	5.10			
La	52.3	25.8	26.9	23.7	25.8	23.6	25.0	25.9	23.7	25.7			
Ce	77.3	42.2	46.7	40.5	44.4	42.9	43.0	45.3	43.2	45.7			
Nd	24.6	18.1	21.3	—	—	—	—	—	14.0	12.0			
Sm	3.39	3.14	3.23	3.48	3.49	3.42	3.53	3.41	3.07	3.11			
Eu	0.973	0.646	0.573	0.583	0.594	0.608	0.639	0.252	0.581	0.611			
Tb	0.56	0.51	0.53	0.52	0.51	0.54	0.53	—	0.40	0.43			
Yb	1.81	1.41	1.49	1.50	1.48	1.57	1.38	2.56	1.51	1.53			
Lu	0.210	0.227	0.244	0.274	0.252	0.277	0.250	0.621	0.158	0.161			

	Chikiani/Javakheti ridge						Syunik volcanic upland					
	Chikiani						Bazank			Mets Satanakar		
	110	111	112	113	114	115	116	117	118	119		
	MA-121226	MA-121227	FG-030857	FG-030858	FG-030859	FG-030840	FG-030841	FG-030842	FG-030842	FG-030843		
Na %	3.02	2.93	3.16	3.41	3.42	3.38	3.44	3.34	3.24	3.24		
K %	4.60	4.20	—	—	—	4.36	4.09	—	3.98	—		
Fe %	0.54	0.54	0.85	0.75	0.79	0.82	0.83	0.83	0.66	0.84		
Sc	2.12	2.08	2.19	2.41	2.33	2.13	2.14	2.03	2.13	2.05		
Cr	3.50	3.40	—	—	—	1.66	1.52	—	4.44	—		
Co	0.21	0.22	0.17	0.10	0.10	0.13	0.11	—	0.13	0.24		
Zn	45.0	43.0	—	39.4	36.0	33.5	33.1	—	31.0	—		
As	3.00	2.50	—	—	—	1.67	1.77	—	2.81	—		
Sb	0.10	0.23	0.43	0.29	0.26	0.31	0.37	0.11	0.38	0.14		
Rb	122	121	209	196	224	189	195	197	182	202		
Cs	5.01	4.77	6.35	4.89	4.51	5.50	5.68	5.73	5.55	5.66		
Ba	640	660	91	44	48	58	81	15	99	27		
Zr	87	86	56	95	121	32	39	92	76	83		
Hf	3.14	3.13	4.12	3.61	3.48	3.78	4.02	3.71	3.88	3.82		
Ta	1.35	1.27	2.56	2.50	2.43	2.21	2.30	2.59	2.22	1.80		
Th	15.2	15.0	29.5	30.7	30.9	36.1	37.8	35.1	37.3	34.6		
U	5.30	4.90	12.49	12.35	12.54	11.79	12.38	10.90	13.21	10.90		
La	24.5	25.9	26.8	26.7	26.2	28.3	29.3	30.5	30.3	29.8		
Ce	44.1	46.1	29.8	34.9	30.9	45.0	46.9	44.6	44.2	44.5		
Nd	12.0	20.0	—	—	—	—	—	—	—	—		
Sm	3.17	3.10	2.33	2.49	2.37	2.33	2.56	2.86	2.55	3.18		
Eu	0.609	0.609	0.120	0.115	0.133	0.130	0.147	0.144	0.164	0.147		
Tb	0.42	0.37	0.27	0.24	0.43	0.43	0.28	0.88	0.26	0.89		
Yb	1.69	1.58	1.26	1.21	1.12	1.28	1.33	2.09	1.37	2.15		
Lu	0.167	0.139	0.280	0.290	0.250	0.253	0.260	0.026	0.240	0.634		

		Syunik volcanic upland											
		Mets Satanakar						Sevkar					
		120	121	122	123	124	125	126	127	128	129		
		FG-030843	FG-030844	FG-030844	FG-030845	FG-030845	FG-011928	FG-011929	FG-030504	FG-030505	FG-030846		
Na %		3.22	3.22	3.23	3.04	3.16	3.28	3.23	–	3.39	3.07		
K %		4.32	–	3.88	–	3.87	–	3.67	–	3.82	–		
Fe %		0.70	0.82	0.66	0.82	0.70	0.56	0.49	0.56	0.63	0.87		
Sc		2.15	2.04	2.16	2.02	2.20	1.79	1.80	1.74	1.70	1.71		
Cr		5.18	–	5.33	–	5.39	2.89	2.44	3.37	–	–		
Co		0.14	–	0.14	–	0.15	0.12	0.13	0.12	0.11	0.07		
Zn		32.5	–	31.5	–	33.8	35.8	39.2	29.3	37.2	–		
As		2.13	–	1.02	–	1.54	0.43	0.51	–	0.42	–		
Sb		0.40	0.13	0.31	0.17	0.37	0.20	0.21	0.28	0.26	0.17		
Rb		184	198	191	191	198	205	200	170	154	195		
Cs		5.66	5.57	5.73	5.63	5.78	4.37	4.38	4.30	4.25	3.84		
Ba		116	15	121	22	76	55	78	68	–	86		
Zr		49	89	57	84	44	88	81	86	–	65		
Hf		3.99	3.81	3.96	3.84	4.10	3.23	3.14	3.61	3.90	3.42		
Ta		2.28	1.80	2.26	2.03	2.29	2.12	2.57	2.32	2.20	2.66		
Th		38.1	34.2	38.2	35.9	38.8	29.2	34.4	33.8	36.1	31.3		
U		13.86	10.40	13.96	9.40	12.86	10.20	9.27	10.37	8.14	9.09		
La		33.1	29.5	30.8	25.1	28.2	30.7	34.1	32.1	34.5	35.6		
Ce		44.5	44.2	43.3	45.8	43.4	53.8	57.6	55.4	56.0	41.6		
Nd		–	–	–	–	–	12.5	14.1	–	–	–		
Sm		2.87	3.38	2.49	2.86	0.45	2.36	2.37	2.09	3.05	2.47		
Eu		0.137	0.166	0.174	0.167	0.170	0.180	0.220	0.140	0.180	0.200		
Tb		0.23	1.01	0.23	0.96	0.22	0.23	0.22	0.21	0.20	0.21		
Yb		1.32	2.24	1.29	1.07	1.52	1.38	1.54	1.51	1.46	1.51		
Lu		0.210	0.495	0.290	0.130	0.253	0.259	0.275	0.348	0.247	0.259		

Syunik volcanic upland													
Sevkar													
	130	131	132	133	134	135	136	137	138	139			
	FG-030847	FG-030848	FG-030849	FG-030850	FG-030851	FG-030852	FG-030853	FG-030854	FG-030855	FG-030856			
Na %	3.10	3.23	3.23	3.20	3.20	3.24	3.29	3.08	3.20	3.24			
K %	–	–	–	–	–	–	–	–	–	–			
Fe %	0.85	0.67	0.92	0.82	0.89	0.89	0.88	0.84	0.83	0.96			
Sc	1.78	1.83	1.68	1.75	1.69	1.78	1.79	1.60	1.78	1.75			
Cr	–	–	–	–	–	–	–	–	–	–			
Co	0.08	0.12	0.15	0.07	0.14	0.14	0.14	0.12	0.15	0.07			
Zn	–	–	–	–	–	–	–	–	–	–			
As	–	–	–	–	–	–	–	–	–	–			
Sb	0.18	0.19	0.19	0.14	0.17	0.17	0.17	0.14	0.12	0.11			
Rb	204	174	183	169	184	200	223	189	176	180			
Cs	3.88	5.06	4.89	4.88	5.03	4.87	5.06	4.44	4.65	5.07			
Ba	75	81	83	88	87	98	61	91	82	82			
Zr	65	70	85	90	86	74	65	69	86	88			
Hf	3.52	3.76	3.62	3.71	3.81	3.73	3.78	3.58	3.73	3.70			
Ta	2.74	2.37	2.20	2.39	2.10	2.81	2.51	2.49	2.19	2.34			
Th	31.2	33.6	32.9	32.1	36.1	33.2	34.8	32.1	33.6	32.8			
U	9.20	9.50	9.39	10.15	10.54	9.62	9.96	10.41	10.36	10.48			
La	34.6	36.3	37.0	39.1	31.9	38.0	36.7	35.4	36.0	37.2			
Ce	41.8	46.1	60.5	42.8	43.3	48.0	45.6	44.4	43.0	43.8			
Nd	–	–	–	–	–	–	–	–	–	–			
Sm	2.43	2.37	2.58	2.55	2.58	2.66	2.57	2.48	2.53	2.65			
Eu	0.210	0.214	0.206	0.220	0.217	0.199	0.199	0.177	0.209	0.150			
Tb	0.21	0.15	0.19	0.17	0.21	0.16	0.17	0.22	0.17	0.23			
Yb	1.45	1.49	1.52	1.50	1.48	1.44	1.45	1.43	1.49	1.29			
Lu	0.237	0.228	0.240	0.240	0.228	0.212	0.226	0.211	0.213	0.240			

Vardenis volcanic upland					
Khorapor					
	150	151	152	153	
	FG-020569	FG-020570	FG-020571	FG-020572	
Na %	3.08	3.00	2.95	2.95	
K %	3.68	3.44	3.62	3.32	
Fe %	0.40	0.40	0.38	0.39	
Sc	2.00	1.95	1.91	1.92	
Cr	–	–	–	–	
Co	0.20	0.24	0.23	0.21	
Zn	29.6	26.4	27.2	28.9	
As	5.45	5.72	6.16	5.04	
Sb	0.57	0.58	0.40	0.36	
Rb	213	205	196	199	
Cs	7.68	7.54	7.48	7.59	
Ba	45	34	<100	27	
Zr	47	50	15	<50	
Hf	3.46	3.50	3.30	3.42	
Ta	2.41	2.38	2.45	2.58	
Th	35.1	35.3	32.9	32.9	
U	14.50	14.94	16.38	17.20	
La	20.7	20.3	20.0	20.4	
Ce	39.0	37.5	37.0	37.1	
Nd	19.8	16.1	22.4	19.1	
Sm	3.64	3.56	3.44	3.49	
Eu	0.199	0.179	0.180	0.144	
Tb	0.36	0.37	0.31	0.12	
Yb	1.91	1.91	1.96	1.58	
Lu	0.416	0.660	0.674	0.240	

Chemical and trace element composition of archaeological obsidian samples analysed in this study, originating from outside the territory of the Republic of Armenia. All concentrations are given in $\mu\text{g/g}$, except for Na, K, Fe in weight percent. Analyses of archaeological object samples from the territory of the Republic of Armenia are listed in another publication (Badalyan et al. in press).

Azerbaijan										
Camay										
EBA										
	1	2	3	4	5	6	7	8	9	10
	FG-011952	FG-020425	FG-020426	FG-020427	FG-020428	FG-020429	FG-020430	FG-020431	FG-020432	FG-020433
Na %	3.26	2.71	3.35	5.06	3.30	2.86	3.15	3.37	2.94	5.11
K %	–	–	4.43	5.98	2.52	3.08	2.97	4.28	3.62	8.10
Fe %	0.90	1.34	0.84	0.80	0.86	0.78	0.74	0.50	0.74	0.53
Sc	2.09	2.16	2.04	2.08	2.04	1.81	1.92	2.94	1.82	1.89
Cr	4.4	3.2	2.3	3.4	2.0	2.3	1.7	1.9	2.4	3.9
Co	0.60	0.74	0.52	1.24	0.54	0.56	0.40	0.35	0.50	0.86
Zn	–	–	39.9	34.8	36.2	32.6	35.2	27.0	36.1	37.6
As	4.51	–	1.78	4.12	1.73	1.21	1.35	3.86	1.92	6.58
Sb	0.27	0.31	0.25	1.29	0.26	0.25	0.25	0.58	0.26	–
Rb	119	101	121	97	123	102	119	189	114	118
Cs	4.05	3.51	4.27	3.15	4.10	3.50	4.30	6.88	3.92	4.10
Ba	853	1552	731	1185	846	767	625	38	626	656
Zr	67	125	53	43	79	70	39	32	61	24
Hf	3.60	3.95	3.17	3.92	3.37	3.00	2.87	2.89	2.72	2.90
Ta	1.45	2.20	1.55	1.13	1.43	1.20	1.45	4.79	1.38	1.43
Th	16.56	15.67	16.00	15.67	16.12	14.37	14.46	27.17	13.85	14.55
U	5.00	4.17	5.73	9.71	5.22	4.52	5.23	14.66	4.97	12.35
La	31.7	40.3	28.6	40.2	31.1	28.9	23.6	16.3	23.1	25.6
Ce	54.8	64.9	50.2	60.9	52.9	48.8	41.9	30.9	41.4	41.3
Nd	11.66	–	16.57	18.83	9.64	23.57	19.39	11.95	15.42	25.16
Sm	3.31	3.61	3.38	7.20	3.36	2.96	3.06	4.05	2.97	6.61
Eu	0.67	0.80	0.64	0.77	0.64	0.60	0.57	0.23	0.55	0.59
Tb	0.46	0.68	0.47	0.44	0.47	0.42	0.43	0.70	0.31	0.45
Yb	1.46	1.44	1.50	4.36	1.57	1.41	1.46	2.32	1.30	3.63
Lu	0.27	0.24	0.22	0.69	0.23	0.18	0.20	0.56	0.21	0.77

		Azerbaijan									
		Camay					Leyla Tepe				
		EBA					Chalcolithic				
	11	12	13	14	15	16	17	18	19	20	
	FG-020434	FG-020435	FG-020436	FG-020437	FG-020438	FG-030492	FG-030493	FG-030494	FG-030495	FG-030496	
Na %	3.93	4.62	4.09	2.44	2.57	3.07	3.09	3.16	3.03	3.01	
K %	5.15	7.21	5.32	—	3.43	2.59	—	5.54	—	—	
Fe %	0.72	0.58	2.09	1.09	0.54	0.80	0.39	0.38	0.38	0.37	
Sc	1.89	2.01	5.39	1.71	1.84	2.72	3.06	3.04	3.08	3.03	
Cr	3.6	3.1	5.6	3.5	3.6	2.5	4.7	3.3	2.3	2.1	
Co	1.16	0.74	4.07	0.64	0.68	1.13	0.88	0.74	0.61	0.63	
Zn	33.1	37.3	36.9	—	34.0	37.8	31.7	26.6	24.5	22.7	
As	4.25	5.57	5.01	—	1.15	3.20	4.21	3.35	4.00	4.27	
Sb	1.30	—	—	0.31	0.27	0.57	0.88	0.77	0.63	0.67	
Rb	92	119	150	81	113	125	195	201	198	191	
Cs	2.92	4.29	8.52	2.85	3.92	4.55	7.30	7.24	7.34	7.32	
Ba	993	680	1195	1181	666	273	35	36	53	43	
Zr	35	25	261	102	57	33	20	15	44	57	
Hf	3.60	3.23	9.00	3.19	2.98	4.55	2.97	3.05	2.94	3.06	
Ta	1.06	1.47	0.89	0.76	1.28	2.89	5.12	5.14	5.02	4.95	
Th	14.96	15.98	18.40	12.29	14.67	16.78	28.25	28.62	28.69	28.49	
U	7.86	10.66	8.20	3.41	4.81	14.54	15.25	15.72	15.07	15.39	
La	31.7	24.6	29.9	32.6	24.0	16.9	17.4	17.6	17.3	17.3	
Ce	57.5	46.3	72.3	51.1	44.9	49.7	31.4	31.1	31.3	31.2	
Nd	20.22	22.83	21.91	—	—	15.99	10.72	—	—	—	
Sm	5.74	6.05	5.82	2.77	3.03	4.10	4.15	1.23	4.20	4.18	
Eu	0.67	0.63	0.91	0.66	0.57	0.56	0.28	0.25	0.23	0.21	
Tb	0.55	0.45	0.81	0.41	0.44	0.59	0.66	0.66	0.73	0.70	
Yb	3.28	4.61	3.70	1.11	1.38	2.64	2.47	2.59	2.45	2.66	
Lu	0.56	0.70	0.57	0.21	0.24	0.51	0.56	0.51	0.55	0.55	

		Georgia													
		Udabno							Tsikhiagora, Level A						
		LBA							EBA III						
	61	62	63	64	65	66	67	68	69	70					
	Ma-061320	Ma-061321	Ma-061322	Ma-061323	Ma-061324	Ma-061325	FG-020592	FG-020593	FG-020594	FG-020595					
Na %	2.82	2.98	2.98	0.02	2.92	2.94	2.86	2.90	2.82	2.90					
K %	3.82	3.58	3.95	0.10	2.90	3.18	4.35	3.34	3.63	3.34					
Fe %	0.74	0.73	1.13	0.03	1.14	0.89	0.49	0.57	0.58	0.57					
Sc	1.99	2.06	2.23	0.13	2.26	2.17	1.83	1.91	1.97	1.91					
Cr	1.6	2.6	3.8	3.4	2.3	2.0	2.2	1.5	2.9	1.5					
Co	0.21	0.17	0.73	0.04	0.68	0.34	0.65	0.67	0.71	0.67					
Zn	38.6	42.1	39.5	0.9	42.3	41.5	35.9	37.9	40.6	37.9					
As	3.00	2.97	2.44	0.13	2.82	3.35	1.95	1.35	1.24	1.35					
Sb	0.25	0.29	0.38	0.02	0.24	0.28	0.32	0.22	0.30	0.22					
Rb	121	128	109	5	104	119	109	106	116	106					
Cs	4.51	4.79	3.58	0.06	3.62	4.61	4.09	3.74	4.06	3.74					
Ba	857	847	1428	84	1513	1151	664	859	778	859					
Zr	74	86	127	6	136	80	57	75	71	75					
Hf	3.01	2.97	4.32	0.12	4.17	3.70	2.64	3.10	3.03	3.10					
Ta	1.20	1.41	1.10	0.05	1.06	1.22	1.43	1.28	1.44	1.28					
Th	14.26	14.77	16.01	0.06	16.20	16.28	13.79	15.00	15.52	15.00					
U	4.91	5.36	4.20	0.27	4.25	4.98	5.49	5.04	5.21	5.04					
La	25.1	23.0	40.7	0.2	41.7	32.9	24.6	32.2	28.4	32.2					
Ce	43.7	41.3	67.2	0.2	67.1	56.3	39.4	48.3	48.5	48.3					
Nd	—	—	—	—	—	—	—	—	—	—					
Sm	2.92	2.96	3.41	0.04	3.43	3.24	3.23	3.50	3.32	3.50					
Eu	0.56	0.55	0.77	0.07	0.81	0.67	0.53	0.59	0.60	0.59					
Tb	0.54	0.54	0.59	0.03	0.57	0.61	0.43	0.44	0.43	0.44					
Yb	1.78	1.58	1.73	0.05	1.35	0.19	1.53	1.43	1.54	1.43					
Lu	0.17	0.20	0.16	0.01	0.30	0.21	0.25	0.24	0.21	0.24					

Iran											
National Museum of Iran, Tehran											
?											
	Ravaz	81	82	83	84	85	86	87	88	89	90
	EBA	FG-050200	FG-050621	FG-050622	FG-050899	FG-050900	FG-050901	FG-050902	FG-050903	FG-050904	FG-050905
Na %	4.15	3.79	3.92	3.81	3.21	4.28	4.31	3.03	3.20	3.92	3.13
K %	6.12	13.75	3.81	3.21	3.21	4.28	4.31	3.03	3.39	4.35	3.90
Fe %	1.50	0.70	1.48	0.70	0.70	0.58	0.76	0.77	0.77	3.12	0.68
Sc	2.19	4.15	2.11	1.82	1.82	3.29	1.83	1.93	1.93	0.35	2.03
Cr	11.2	43.4	4.7	2.8	2.8	4.2	3.6	3.1	3.0	3.6	2.7
Co	0.40	1.30	0.31	0.19	0.19	0.11	0.17	0.17	0.19	0.12	0.12
Zn	71.6	44.6	74.1	33.6	33.6	31.6	30.2	32.7	31.7	168.1	25.4
As	3.62	17.53	3.57	2.16	2.16	7.71	1.79	2.35	1.99	27.01	2.27
Sb	0.92	1.72	0.70	0.23	0.23	0.68	0.24	0.31	0.26	1.42	0.33
Rb	219	263	213	173	173	212	166	170	174	208	174
Cs	10.99	9.69	10.68	4.60	4.60	7.93	4.50	4.93	5.04	8.26	5.48
Ba	79	100	108	88	88	78	120	85	70	105	25
Zr	185	148	243	36	36	5	32	69	54	1037	21
Hf	9.46	4.29	9.26	3.79	3.79	3.10	3.85	3.98	3.89	29.30	3.96
Ta	2.49	6.50	2.31	1.76	1.76	3.72	1.81	1.95	2.03	3.82	2.09
Th	27.73	33.19	26.98	33.17	33.17	27.49	33.47	35.32	35.87	27.09	36.40
U	11.39	21.35	9.58	9.99	9.99	14.84	9.71	10.22	10.68	8.96	11.05
La	39.6	23.8	36.0	34.9	34.9	17.9	37.1	37.1	35.9	99.8	29.8
Ce	76.6	41.7	74.2	53.5	53.5	32.3	57.1	57.4	56.8	200.6	46.6
Nd	—	—	—	—	—	—	—	—	—	—	—
Sm	0.13	5.53	8.47	2.36	2.36	4.00	2.37	2.41	2.33	19.08	2.02
Eu	0.61	1.09	0.53	0.22	0.22	0.24	0.22	0.23	0.19	0.52	0.21
Tb	1.72	1.14	1.56	0.65	0.65	0.82	0.57	0.69	0.66	3.07	0.88
Yb	7.25	4.10	6.24	1.44	1.44	2.47	1.41	1.47	1.40	12.71	1.38
Lu	1.35	0.68	1.08	0.22	0.22	0.33	0.22	0.16	0.16	1.93	0.15

		Türkiye														Nemrut Dağ	
Yenibademli Höyük, Gökçeada		Kuntepe														EBA	
EBA		Chalcolithic														EBA	
		99	100	101	102	103	104	105	106								
FG-041971		FG-990818	FG-990821	FG-990827	FG-990828	FG-990829	FG-990830	FG-990831	FG-050121								
Na %	3.37	2.97	3.13	3.09	3.13	3.09	2.98	2.98	2.98								
K %	–	3.34	3.57	3.24	3.64	4.15	2.66	3.55	3.68								
Fe %	1.15	1.15	1.22	1.23	1.54	1.19	1.47	1.18	7.18								
Sc	3.12	1.62	1.72	1.69	2.29	1.73	2.21	1.66	0.58								
Cr	2.4	2.8	5.2	10.6	4.0	9.2	3.0	5.9	5.7								
Co	0.76	0.63	0.72	0.83	1.24	0.89	1.11	0.82	0.22								
Zn	40.0	31.5	33.3	35.2	38.1	32.8	34.1	30.6	222.9								
As	4.52	3.01	3.72	4.22	3.44	3.16	2.84	3.28	23.24								
Sb	0.62	0.26	0.30	0.32	0.28	0.26	0.25	0.32	1.29								
Rb	135	118	128	130	121	138	110	125	254								
Cs	5.32	4.01	4.15	4.40	3.99	4.30	3.65	4.20	12.03								
Ba	619	687	729	722	720	674	663	689	73								
Zr	193	118	137	129	179	120	160	69	1294								
Hf	4.88	3.62	3.93	3.85	4.01	3.94	3.84	3.57	33.54								
Ta	2.80	0.90	0.87	1.08	0.83	0.95	0.74	0.86	5.28								
Th	17.44	14.48	15.38	14.97	13.87	15.13	13.42	14.52	33.84								
U	10.22	4.03	4.29	4.19	3.72	4.73	3.77	3.98	10.37								
La	34.3	26.9	29.4	29.0	27.4	28.8	26.2	26.7	118.2								
Ce	55.8	45.7	49.7	48.6	46.3	49.2	44.8	47.8	241.6								
Nd	–	–	–	–	–	–	–	–	–								
Sm	4.04	2.73	2.98	2.95	2.84	2.95	2.70	2.76	22.40								
Eu	0.57	0.58	0.57	0.54	0.62	0.66	0.52	0.62	1.79								
Tb	0.67	0.62	0.64	0.69	0.63	0.65	0.59	0.64	4.03								
Yb	3.15	2.57	2.43	2.77	2.45	2.34	2.22	2.41	15.72								
Lu	0.47	0.40	0.38	0.45	0.43	0.44	0.40	0.46	2.45								

Türkiye												
Troy												
EBA												
	108	109	110	111	112	113	114	115				
	FG-990890	FG-990892	FG-990893	FG-990894	FG-990895	FG-990896	FG-990898	FG-990899				
Na %	3.23	3.26	2.92	3.23	3.13	3.43	3.11	3.45				
K %	4.85	3.65	5.48	3.83	2.61	5.52	4.67	5.14				
Fe %	1.28	0.92	1.35	0.93	1.55	0.97	1.55	0.98				
Sc	1.74	2.05	2.16	1.94	2.29	2.06	2.35	2.11				
Cr	23.4	18.8	24.1	7.4	6.0	8.7	16.6	32.4				
Co	1.58	0.79	1.81	0.40	1.31	0.54	1.53	1.34				
Zn	36.2	24.9	35.6	24.6	36.2	26.7	26.4	22.1				
As	5.20	8.02	4.12	8.01	3.12	10.10	3.86	10.00				
Sb	0.55	1.29	0.39	0.92	0.31	1.14	0.42	1.19				
Rb	129	193	129	201	115	205	129	225				
Cs	4.59	9.09	4.41	8.73	4.08	9.13	3.87	9.34				
Ba	984	315	719	272	673	329	668	548				
Zr	165	101	180	56	146	42	200	42				
Hf	4.06	3.31	3.95	3.25	3.90	3.43	3.68	3.35				
Ta	1.10	2.12	0.78	2.06	0.72	2.16	0.96	2.25				
Th	15.01	24.40	14.75	25.05	13.78	26.31	13.86	26.23				
U	4.92	9.54	4.65	9.11	4.35	9.61	4.07	10.86				
La	28.6	27.9	27.6	26.6	27.5	27.8	27.5	28.6				
Ce	48.9	46.1	47.3	47.5	47.2	49.6	47.6	55.1				
Nd	—	—	—	—	—	—	—	—				
Sm	2.96	3.49	2.91	3.48	2.80	3.63	2.82	3.72				
Eu	0.81	0.42	0.77	0.29	0.57	0.19	0.91	0.69				
Tb	0.61	1.05	0.68	0.91	0.63	1.01	0.67	1.03				
Yb	2.63	2.64	2.33	2.46	2.47	2.75	2.35	2.78				
Lu	0.47	0.59	0.47	0.33	0.42	0.34	0.43	0.38				